University of Stavanger

FACULTY OF SCIENCE AND TECHNOLOGY

MASTER'S THESIS

Study program/Specialization: Petroleum Engineering / Natural Gas Technology	Spring semester, 2018 Open
Author: Andrew Mburu	…………………………………………… (signature of author)
Internal supervisor: Dag Chun Standnes External supervisors: Knut Kristian Meisingset (Equinor) Ingun Skjevrak (Equinor)	
Title of master's thesis: Well Modelling of H_2S Production on a Field in the North Sea	
Credits (ECTS): 30	
Key words: *Microbiological reservoir souring* *Waterflooding* *Sulphate reducing bacteria (SRB)* *Reservoir simulation* *Mathematical models* *History matching* *Prediction*	Number of Pages: 107 + supplemental material/other None Stavanger, June 15th 2018

Foreword

I would first like to thank my thesis supervisors Dag Chun Standnes, Knut Kristian Meisingset and Ingun Skjevrak for their advice and support throughout the writing of this thesis. Their patience and dedication to excellence has been vital in keeping me engaged. I would also like to extend my gratitude to Equinor and particularly the whole Department of Remaining Reservoir Resources at Stavanger (ST-RRR) for the opportunity to participate in this research project. Your expertise and guidance has been second to none. I would additionally like to thank fellow MSc student, Alisher Narzullaev for his input and advice along the way.

I must also express my utmost appreciation for all support, encouragement and inspiration throughout my years of study and research that I have received from my family, friends and the extended UIS community.

Stavanger, June 2018
Andrew Mburu

Abstract

Hydrogen sulphide production can prove to be a very costly affair for exploration and production companies. Failure to implement efficient H_2S control and mediation strategies can lead to a decrease in production assets, increase in operational costs and lost production as a result of shut-in wells. Developing a model to predict H_2S production can therefore be very useful.

The aim of this thesis was to develop a model that could be used to predict the amount of H_2S produced in seawater on a wellbore basis. A synthetic reservoir model was created using ECLIPSE100 simulator tracer tracking option to obtain a cumulative H_2S production profile by plotting cumulative H_2S against cumulative produced seawater. The results from this 2D homogenous reservoir model were used to form a basis upon which the mathematical models could be tested.

Two models were tested, a piecewise linear model and an exponential model. Having tested the mathematical expressions and optimized the parameters, the models were then applied to wellbore plots of H_2S data from a souring field on the North Sea. The historical cumulative production data from the field was plotted in order to observe the production profiles of the different wellbores. Of the three distinct profiles that were observed, only two were used for analysis in this thesis, type 1 and type 2. The models were then compared based on how well they fit the historical data of two types of curves. Finally, the prediction of H_2S production rate in g/m^3 of produced seawater for each of the models is presented.

Based on the model fit to the historical data and the assumption that conditions in the reservoir will remain constant during the period of prediction then the models developed in this work allow a fairly reasonable prediction of the rate of H_2S production. These predictions can be very useful for planning H_2S control strategies and production management of producing wells and new infill wellbores.

Table of Contents

List of figures

List of tables

Chapter 1 : Introduction

Reservoir souring is the process whereby a previously sweet reservoir (containing low concentrations of hydrogen sulphide (H_2S)), starts to produce sour fluids with increasing H_2S concentrations. H_2S in petroleum reservoir systems has three main sources of generation:

- Microbiological sulphate reduction at temperatures below 60°C. Believed to be the biggest contributor to reservoir souring.
- Thermal cracking of kerogen and petroleum. The rate of thermal cracking increases with increasing depth of burial after reaching a certain threshold temperature.
- Thermochemical sulphate reduction at temperatures between 80-120°C depending on the amount of H_2S already present in the reservoir to catalyse the process.

Detecting H_2S on oil and gas fields is important for health, safety and economic reasons. H_2S is severely toxic and highly flammable thus frequent measurements are carried out to ensure safety during field operations. Additionally, H_2S is corrosive (microbial induced corrosion) damaging steel piping which may lead to equipment failure.

The concentration of H_2S produced depends on several factors such as, reservoir structure, geology, water-oil composition, GOR (Gas-Oil ratio), WOR (Water-Oil Ratio) and microbial activity. However, changes in the relative mass of the produced water and production gas may also give an increased H_2S concentration despite no microbial activity [63].

Whilst reservoirs can be naturally sour, a large portion of reservoir souring in a large portion of fields is due to the action of microbial activity after the initiation is secondary recovery by waterflooding. It can be described in three stages: 1) Initial stage of production, almost no H_2S in the produced oil and gas; 2) water breakthrough is experienced; 3) increasing H_2S concentration is observed in the produced fluids. This occurrence of H_2S is caused by microbiological activity and should be distinguished from reservoirs that already contain significant amounts of H_2S upon discovery.

Oil reservoirs constitute deep geological environments with diverse physiochemical in situ conditions where indigenous microbial communities are supposed to grow. Sulphate reducing bacteria (SRB) is an example of a bacteria species that can found in oil reservoirs. SRB is widespread in nature, virtually found to thrive in every anaerobic environment investigated. They play a vital role in the global sulphur cycle, and in marine sediments they account for up

to 50% of the total carbon mineralization process. SRB have a remarkable catabolic diversity using, lactate, ethanol, acetate, propionate and higher volatile fatty acids (VFAs) as sources of energy.

In order to deal with the implications of H_2S production, certain methods have been applied to inhibit H_2S production once water injection is initiated. Once reservoir souring is noted, chemical scavengers and corrosion inhibitors are deployed to shield vulnerable production facilities. These measures are important to consider since they influence the chemical and operational costs. Additionally, the sales value of the retrieved hydrocarbons is reduced when contaminated with H_2S. To reduce the H_2S contamination and bring it down to export line levels (<0.5 ppm on the Norwegian Continental Shelf), chemical sweetening systems need to be installed.

Accurately modelling and predicting the onset and severity of H_2S production is therefore very valuable. If underestimated, reservoir souring may prompt unexpected installation of equipment such as sweetening units, chemical injectors and pipes. In deep water fields where equipment replacement may prove difficult, shutting-in producers with high H_2S concentrations is inevitable. However, modelling and predicting reservoir souring is a significant challenge. Not only does it demand an understanding of H_2S generation in reservoirs, but it also requires knowledge and understanding of fluid flow, mineral scavenging and fluid phase partitioning of H_2S between water, oil and gas [31].

The conventional method for determining the total amount of H_2S is by measuring the H_2S concentration in the gas phase. This amount depends on the pH, pressure, temperature, ionic strength and the ratio of produced fluids [5]. Increasing H_2S concentration in the produced gas is not necessarily an indicator that microbial souring is occurring, increasing water-cut will cause an increase in gas H_2S concentration as the gas makes up a reduced proportion of the production. Determination of whether H_2S production is increasing is done by summing the amount in each phase to get the total mass of H_2S produced (kg/day).

Effective and accurate prediction of biogenic reservoir souring is essential when undertaking major technical and economic decisions regarding field development and material selection. Several mathematical souring models have been developed to help predict oilfield souring potential. These models include old modelling tools, 1D or 2D single well pair simulations

which can be done in ECLIPSE using tracer track option and the newer 3D transient multi-well souring simulators such as SourSim®RL. A good souring model should incorporate the generation and transport of H2S in the oil reservoir since the ability to recreate the essential environment necessary for generation and transportation of hydrogen sulphide in a souring model affects the prediction accuracy. Empirical correlations can then be developed to estimate H2S production based on the cumulative H2S production profiles.

Thesis aim and objectives

Thesis aim: Develop a mathematical model for H2S prediction to optimize production of producing wells that are producing sour fluids in addition to evaluating new infill wellbores.

Thesis objectives carried out to achieve this goal are listed below:

- ➢ Develop 2D homogenous synthetic reservoir model using ECLIPSE tracer tracking option to simulate H2S production profile that will be used as a basis for curve fitting and parameter optimization.
- ➢ Test mathematical expression on the H2S production profile of the synthetic model, determine optimal parameters for best possible match (model fit).
- ➢ Apply the optimized mathematical expressions to match the historical cumulative production of H2S and seawater on 6 wellbores from a souring field in the North Sea. This stage includes:
  - ○ Gathering H2S data: measured H2S in gas phase (ppm), amount of H2S in the produced fluids (kg/d), total amount of H2S produced (kg) and H2S souring index [45] in produced seawater (g/m^3)
  - ○ Well history
  - ○ Ion analysis of produced water to obtain seawater cut (SWC)
  - ○ Allocated and test separator production data for all produced phases (oil, gas and water)
- ➢ Obtain prediction for rate of H2S production (g/m^3 of seawater) for each of the wellbores.

Chapter 2 : Literature Review

The generation of hydrogen sulphide can be problematic during production of a field. It is highly toxic, detrimental to equipment through corrosion and reduces the quality of sales oil and gas. It is important to differentiate between geochemically produced H_2S and reservoir souring. Geochemically produced H_2S refers to H_2S that is already present in the reservoir, produced during deposition of the sedimentary rock and maturation of oil. While both abiotic and biotic mechanisms have been proposed as responsible for reservoir souring, sulphate reduction by microorganisms is believed to be the most significant in oil reservoirs as a result of waterflooding [63]. It occurs in reservoirs with very low concentrations of H_2S at the beginning of production. After the start of secondary recovery using seawater injection, the concentration of H_2S increases in the producing fluids. In this chapter, the basics of reservoir souring process and its remediation methods are discussed. The extent of the work done on prediction and modelling of reservoir souring is also reviewed.

2.1 Improved Oil Recovery: Waterflooding

Engineered waterflooding is the principal method of secondary recovery practised by the oil and gas industry. As early as 1865, waterflooding occurred as a result of accidental injection of water in the Pithole City area in Pennsylvania, U.S. Leaks from shallow water sands and surface water entered drilled holes, resulting in much of the early waterflooding [55]. From 1924, where the first 5-spot pattern flood was implemented in Pennsylvania, waterflooding found widespread applications in the oil and gas industry [55]. It is applied in order to energise the system by maintaining the reservoir pressure and displacing hydrocarbons towards the producer well. Its use is advantageous over other forms of secondary recovery because of its availability, low cost and high specific gravity which facilitates injection.

The North Sea is one of the major provinces in which this technique has been applied extensively. Due to the demanding responsibilities and constraints faced by engineers when dealing with offshore projects, waterflooding was considered the main recovery mechanism from the outset. The decision to use waterdrive must be made from the initiation of the project since it affects the design and development of the infrastructure. It was important to have a mitigating 'insurance' in place in case the pressure support of the field was depleted too

quickly. Additionally, water injection is used by operators to gain a degree of engineering control on the flood despite the presence of a strong natural pressure support.

Over its extended history of use, waterflooding has been successful in increasing the hydrocarbon recovery and consequently increased value for shareholders. However, the use of water injection has resulted in some problems. These complicating factors should be considered when deciding the technical and economic feasibility of the applying waterflood technology. One major consideration is the water quality of the injected water. Inadequate water treatment leads to corrosion, scale formation and reservoir souring, all of which increase overall costs.

An important consideration with regards to injection water is to prevent the inoculation of the reservoir with SRB that can cause an in-situ H_2S concentration in the reservoir during the water injection. For this paper, reservoir souring because of seawater injection will be the central focus.

Table 2.1: Typical formation water and seawater ion composition

Ion	Formation water, FW [mg/l]	Seawater, SW [mg/l]
Na^+	8640	11150
K^+	190	420
Mg^{2+}	70	1410
Ca^{2+}	300	435
Ba^{2+}	60	0
Sr^{2+}	50	7
Cl^-	14300	20310
SO_4^{2-}	0	2800
HCO_3^-	1100	150
HA_c (organic acids)	397	0
TDS (total dissolved solids)	25107	36682

2.2 Microbiological Reservoir Souring

The main method used to increase oil recovery (secondary) is waterflooding with seawater. Water is injected to maintain pressure and to sweep the oil toward the producers. Despite the increased oil recovery, in many of these reservoirs, H₂S production started after the onset of water injection. The process of determining the source of sulphide production came after a long process of research and elimination. The conclusion was that sulphate reducing prokaryotes (SRP) i.e. SRB and sulphate reducing archaea (SRA), were responsible.

SRB can already be present in the reservoir in a dormant state or introduced into the reservoir through water injection during waterflooding or during drilling operations. 14 species of SRB have been isolated from oil fields over the years have individual growth temperatures spanning from 4 to 85°C. SRB is categorized based on their active temperature range i.e., thermophilic and mesophilic bacteria (t-SRB and m-SRB). T-SRB can thrive at high temperatures whereas m-SRB are active at more moderate temperatures.

The microbial reservoir souring is mediated by SRB. This takes place because of anaerobic respiration where the bacteria "respire" sulphate instead of oxygen thus producing H₂S as a by-product. In many cases, the reservoir at the primary production stage is a hostile environment to microbial activities. Growth and development of the bacteria in question depends on favourable reservoir conditions and availability of nutrients.

As represented in equation 2.1, bacteria use volatile fatty acids from formation water as a carbon source (electron donor) and sulphate (electron acceptor) from the injected seawater.

$$CH_3COO^- + SO_4^{2-} \rightarrow 2HCO_3^- + HS^- \qquad \text{[2.1]}$$

In some cases, rather than organic compounds, some SRB use hydrogen as electron donors.

$$4H_2 + SO_4^{2-} + H^+ \rightarrow 4H_2O + HS^- \qquad \text{[2.2]}$$
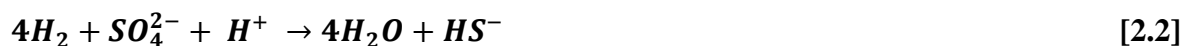
Looking at the equations, it can be noted that the mixing between formation water and injected sea water is key for growth and reproduction of SRB [43]. These mixing zones are in turn affected by the reservoir rock permeability and porosity variations within the reservoir. One common practice in water injection operations is to re-inject the produced water. In this case, the injection water contains fatty acids that normally exist in the formation water and provides all the required compounds for SRB activity. Therefore, bacteria grow in an area around the

wellbore and form a microbial biofilm. In this situation, the reaction zone for production of H2S is near the injectors.

2.2.1 Factors affecting microbiological reservoir souring (Population growth, limiting Factors and transport)

Sulphidogenesis does not commence until some critical conditions for the growth and development of the SRB have been met. Understanding these factors is essential with regards to predicting the amount of H2S generated as well as remediation implementation.

i. Sulphate, carbon source and nutrients: SRB need necessary components for biomass building and respiration. These include, carbon, sulphate, nitrogen and phosphorous. Carbon, mainly volatile fatty acids, is essential for both respiration and biomass building. Sulphate, present as SO_4^{2-} is required as an electron acceptor for anaerobic respiration where it is reduced to sulphide. The main source of sulphate in most souring scenarios is injection water. However, it is also available in formation water in low concentrations. Nitrogen (N) and Phosphorous (P) also occur in trace amounts and are vital for biomass building since they form essential compounds of various cellular protein and nucleic acids [31].

ii. Temperature: Thermophilic SRB can grow and thrive at temperatures up to 80°C whereas m-SRB have growth optima in the 20-45°C. On the other hand, SRA may tolerate temperatures >100°C but will not grow at temperatures <65°C. Initial research on reservoir souring in the 1980s and 1990s placed emphasis on temperature profile of the reservoir thus resulting in the development of thermal viability models and mixing models.

iii. Salinity: Sulphate reducing microorganisms, depending on the species, have reduced activity and become inactive at very high total dissolved solids concentrations (TDS). High salt concentration reduces microbial activity by stunting growth. SRP metabolism is known to occur in salinities of fresh water to approximately 150,000 mg/l TDS [31].

iv. pH: pH is essential in controlling the partitioning behaviour of H2S between the different phases at the reservoir and surface conditions in the souring model [31]. SRB is very sensitive to changes in pH due to effects on their trans-membrane proton. SRB can survive in a wide range of pH conditions but for optimum growth the pH should be

  between 5-9, [33]. HS$^-$ and S^{2-} are more prevalent at neutral to high pH whereas H$_2$S is the predominant form at low pH.

  v. Pressure: Tolerance to pressure depends on the micro-organism in question. SRA tolerate higher pressures than SRB, making them highly adaptable to deep oil reservoirs. Laboratory studies have shown that pressures in excess of 15,000 psi greatly inhibit the activity of sulphate reducing organisms thus reducing the production of H$_2$S. Like pH, pressure is important in controlling the partitioning behaviour of H$_2$S [31].

  vi. Sulphide concentration: As discussed, the produced sulphide is highly toxic. As a result, there is a limit to how much the SRB can be exposed to highly concentrated H$_2$S before it begins to inhibit sulphate, sulphur and thiosulphate reducing metabolism. Concentrations (undissociated sulphide) >250 mg/l reduce the activity of the SRB. Toxicity increases at low pH since the more toxic H$_2$S species predominates [62].

Once the H$_2$S is generated, interactions of H$_2$S with the oil phase and the solid surfaces of the porous media as well as partitioning between phases, control to the overall amount of H$_2$S that is produced at the producer well. Due to the equilibrium with minerals, the initial concentration of H$_2$S in reservoirs on the Norwegian continental shelf is strongly correlated with reservoir temperature [27]. Reservoirs rich in iron-containing minerals and metal ions, scavenge the generated H$_2$S. These scavenging minerals, siderite (FeCO$_3$), hematite (Fe$_2$O$_3$) and magnetite (Fe$_3$O$_4$) [41] react with the sulphide and reduce the overall level of reservoir souring. It is worth mentioning, that the solubility of the iron-rich minerals is determined by the temperature, pH and pressure. Another geological factor is the permeability and porosity of the reservoir rock. According to [65] the species and abundance of the SRB in high permeability porous media is higher than those in low permeability porous media. As the waterflood is transported to the producer, it has been proposed [43] that a significant amount of H$_2$S is partitioned into the immobile oil, effectively acting as a sulphide sink.

At the wellbore and surface facilities, H$_2$S concentration is measured in the gas phase since the concentration of H$_2$S in gas is highest due to temperature and pressure changes. Despite this, H$_2$S concentration evaluation in produced water and oil is done for a more comprehensive and accurate measurement.

2.2.2 Transportation of H2S

Once the H2S has been generated, it is transported in direction of the waterflood towards the producers where it will eventually be produced at the surface. The time it takes to experience H2S breakthrough and the amount of H2S depends on the physiochemical conditions of the reservoir. The two main processes that control the amount of the H2S that reaches the producer wells during transportation are mineral scavenging and partitioning.

Presence of iron-rich minerals in the reservoir rock are responsible for adsorbing the generated H2S from the liquid phase, effectively acting as a significant sink. This takes place in the reactions 2.3, 2.4 and 2.5 below:

$$FeCO_3 + H_2S \rightarrow H_2O + CO_2 + FeS \qquad [2.3]$$

$$Fe_2CO_3 + 3H_2S \rightarrow 3H_2O + FeS_2 + FeS \qquad [2.4]$$

$$Fe_3CO_4 + 4H_2S \rightarrow 4H_2O + FeS_2 + 2FeS \qquad [2.5]$$

The efficacy of these minerals in the scavenging reactions is reliant on their solubility in the water phase. The solubility on the other hand is dependent on the predominating temperature, pressure and pH. It is important to be able to predict the degree of souring since it has a great effect on the time it takes for H2S to appear at the producers. However, determining the composition of minerals within the reservoir may be a challenge owing to the heterogeneity of the formation.

In practice, the H2S scavenging mechanism is a surface mechanism. Essentially, though the iron minerals may exist within the reservoir in large quantities, their scavenging capacity is limited by the surface area available for interaction with H2S present in the advancing waterflood. Other water-rock interactions affecting scavenging capacity include, ion exchange, oxidation-reduction and other physical adsorption processes. After a period of time, the scavenging surfaces get exhausted and the H2S dissolved in the water phase approaches the producers in high concentrations [63].

H2S partitioning into residual hydrocarbons behind the flood front may also contribute to delaying of H2S breakthrough. The partition coefficients of H2S between the water and oil

phases is significantly impacted by pressure, temperature and pH. As absolute pressure decreases, the H₂S concentration in the gas phase increases. Furthermore, changes in pH affect the resultant speciation of the H₂S. Lower pH correspond to dissolved H₂S occurring as H₂S whereas at high pH values the speciation changes to HS⁻ and S⁻².

The H₂S partition coefficient, K_H^{OW} , between a simulated North Sea oil and seawater under a range of conditions matching actual reservoirs in the North Sea was measured by Ligthelm et al. (1991) [41]. The result was a coefficient value within the range of 18-19.5 for conditions of 25°C at 350 bar to 100°C at 150 bar. The concentration of partitioned H₂S into residual oil was about 400ppmw which is 4-5 times that in injected seawater.

Apart from the minerology and partitioning, the distance between the producers and injectors also affects the timing and extent of H₂S appearance in produced fluids. Production wells placed near the injection wells have notably faster H₂S breakthroughs than those located at further distances. High injection rates also have the same undesirable effect, especially in reservoirs with high permeability since the scavenging capacity of the minerology will be quickly exhausted. Ideally, longer path lengths coupled with low injection rates would be the preferred method of implementation.

2.2.3 Control and Remediation of Reservoir Souring

First measure of control is the preventive approach. This entails using a combination of reservoir geology and appropriate chemical control from the onset of water injection to keep the reservoir sweet. The other measures come into play once souring in the reservoir has been noted and the factors influencing the souring have been considered. These approaches are, remedial reservoir approach and remedial scavenging approach. The former involves direct interaction with the bacteria through implementation of a biocide or nitrate treatment programme to sweeten the souring reservoir. The latter involves the use of chemical scavengers to remove the produced H₂S.

2.2.3.1 Biocides

Biocide can be introduced into the well periodically at constant concentration to modify the growth rate of the bacteria. Essentially, the biocide concentration should be enough to effectively reduce the microbe number to an acceptable level by killing off a large portion of

the population. Biocides are essential in counteracting the effects microbiologically induced corrosion (MIC). This corrosion is detrimental to downhole tubulars, topside equipment and pipelines and this results in high overall costs. With many oil and gas megaprojects exceeding USD 1 billion, these costs can be significant. Corrosion is estimated to cost the upstream oil and gas industry USD 1.4 billion annually in the US alone [37].

Traditionally, Tetrakishydroxymethylphosphonium sulphate (THPS) or glutaraldehyde, mixed with surfactants have been used as a preventive and remedial reservoir approach to control souring. A dose of X mg/l of TPHS is injected for Y hours up to twice weekly [32]. Other active agents such as biguanides and isothiazolones, may be more suitable for specific systems where hydrocarbons or unusual water sources are treated.

High biocide concentration is needed to effectively control SRB activity when a biofilm is formed around the injection well. Other factors that could aid the intensity of the biocide are increase in pressure and temperature. For low permeability, mature reservoirs, with a large zone of microbial activity, a continuous dosage of TPHS at relatively low concentrations is effective. For high permeability reservoirs, an optimal schedule of discreet slugs (squeeze treatment) of high concentration TPHS is necessary for effective souring control.

Whereas biocide treatment is full proof at surface facilities, this is not the case in the reservoir. This is because not all the biocide comes into contact with all the bacteria. This shortcoming coupled with the high dosage leads to high operational costs and severe effects on the environment. To cut down on costs related to produced water disposal, companies have opted to reinject the produced water though recent studies have shown that this may accelerate the reservoir souring [17]. One option is to use a combination of biocide at low concentration to slow H₂S generation (lowering cost and toxicity) and chemical scavengers to eliminate the souring [35].

2.2.3.2 Membrane filtration

This method involves controlling the activity of the SRB by controlling the biological factors that favour the growth and development of the SRB. As mentioned, one components required for respiration of the bacteria is the sulphate in the injected sea water. Thus, membrane filtration is applied to reduce the amount of sulphate in the seawater, limiting the ability of the SRB to

grow and spread in the reservoir. Membrane filtration can be categorized based on the size of particles retained by the membrane; reverse osmosis, nano-filtration, ultrafiltration and microfiltration.

The amount of sulphate required for SRB growth is relatively small. Small concentrations can stimulate large colonies of bacteria. Assuming 100% conversion, injecting 100 mg/l of sulphate results in the generation of 40 mg/l of dissolved sulphide. Removal of sulphate from seawater can therefore prove vital. Application of this technique dates to the late 1980s by Marathon Oil on the Brae platform in the North Sea. Current sulphate removal systems are able to reduce sulphate content from 2,500 ppm to 40-50 ppm. If the souring removal units are configured in series, the sulphate content may be even lower. Reducing the sulphate content to 20 mg/l in the injected seawater would only lead to generation of 6.7 mg/l sulphide, this is considerably low (93% less) than detected in souring sandstone reservoirs [43].

Despite the promising results, the main complication with regards to implementation of this technique is the cost of the sulphate reducing units.

2.2.3.3 Nitrate Treatment

Presently, the most technically and economically sound method of remediation for reduction of SRB activity (reservoir and oilfield water treatment systems) and MIC is the injection of nitrate into the injected seawater stream. Seawater and reservoir formations contain a multitude of microbe species. Nitrate reducing bacteria (NRB) is one such specie and just like SRB it can grow and thrive depending on whether or not it is supplied with the necessary nutrients, vitamins and energy (Equation 2.6). NRB populations supress the growth of SRB in the reservoir and thus decrease the produced H₂S.

$$2NO_3^- + 10_e^- + 12H^+ \rightarrow N_2 + 6H_2O + Energy \hspace{2cm} [2.6]$$

Nitrate is introduced to the injection water in the form of calcium nitrate [Ca(NO₃)₂]. Where nitrate is used to control microbial souring, continuous dosing at 40-100 mg/l of nitrate is used. In anaerobic conditions, introduction of nitrate into the reservoir favours NRB growth over SRB. This is because SRB and NRB are competing for limited carbon and nutrient sources within the reservoir. Nitrate is a stronger oxidant than sulphate thus benefiting growth and

development of NRB. NRB reduces the nitrate present in the injected seawater to intermediate quantities of intermediate species of nitrite that act as an inhibitor to SRB growth.

The mechanism by which nitrate inhibits microbial souring is not only limited to competitive exclusion of SRB, it also includes the following:

- Shift in redox potential: As a consequence of nitrate respiration the redox potential in the system will increase, which means favourable conditions for sulphate reduction. The shift towards a more positive redox potential will be enhanced by the chemical oxidation of sulphide by nitrite. [60].

- Production of Nitrite: Prior to the conversion to ammonia or nitrogen, nitrite is produced because of nitrate reduction. Nitrite is highly toxic to most micro-organisms, both NRB and SRB. Additionally, small quantities of nitrite directly inhibit the functioning of the dissimilatory (bi) sulphite reductase enzyme that is vital for sulphate reduction.

- Oxidation of sulphide: Oxidation of sulphide takes place by either, direct oxidation or through interaction between nitrate and sulphide [23]. Existence of a special group of NRB known as the nitrate-reducing sulphide-oxidizing bacteria that are supported by both nitrate and sulphide thus reducing microbial souring significantly.

- Metabolism alteration: Large proportion of total population of SRB have been found to be also capable of reducing nitrate. *Disulfovibrio* is one such sulphate reducing micro-organism capable of switching metabolism when exposed to nitrate in the occurrence of dwindling sulphate supply.

Glutaraldehyde is highly toxic and poses significant HSE concerns. Nitrate used, $[Ca(NO_3)_2]$, poses little or no risk to the marine environment coupled with the fact that it is user friendly to personnel. Another advantage of using nitrate is the fact that it has no known compatibility issues with other oilfield chemicals, these include; biocides, scale control formulations, oxygen scavengers and drag reducing agents [34]. In Bonga field in Nigeria, both nitrate and biocides are used to prevent bacterial growth in the reservoir and the surface facilities.

As mentioned earlier, this remedial technique has been used globally to counter the effects of reservoir souring owing to its many merits. Use of NRB to inhibit H2S generation dates back as early as 1943 where it was used in wastewater treatment. Laboratory research done by Jenneman et al (1997) [30] which showed the efficacy of nitrate in oil field waters was the breakthrough needed to encourage further investigations within the oil and gas community. Various field tests have been carried out over the years with varying measures of success.

In Saskatchewan, Canada use of nitrate resulted in a reduction in sulphide levels at injectors from 100 to 42% and producers from 50-60%. Concentration of indigenous NRB also increased at both ends [30]. In later years, the method was implemented in the Norwegian continental shelf on Veslefrikk, Skjold and Gullfaks fields. Studies showed a decline in H2S production in highly fractured zones as well as an increase in NRB numbers [60] [39]. In Gullfaks field which shall be looked at in detail later in this paper, there was an observed bonus in the form of reduced corrosion within the pipelines [58].

As reserves in conventional reservoirs around the world continue to dwindle, engineers are looking to improved oil recovery methods to increase recovery and delay abandonment. Waterflooding has proved to be one such effective method. However, remedial strategies should be implemented to prevent microbial reservoir souring. For unconventional resources such as shale that need to undergo hydrofracking, a microbiological control program may prove necessary [9]. To effectively design and take full advantage of remediation strategies, several models have been developed to explain the development of H2S generation within the reservoir.

2.3 Existing Microbial Reservoir Souring Models

During the planning and development phases of an oil field, crucial decisions must be made based on the expectations regarding the evolution of H2S in produced fields. This is especially important in challenging cases such as deep-water fields, subsea completions and fragile eco-systems. For an exploration and production (E&P) company, wrong assessment of H2S generation can lead to major losses. Overestimation of H2S can lead to millions of dollars in wasted resources while underestimation can result in catastrophic HSE related issues, replacement of existing equipment or shutting-in of wells where equipment installation is

technically and economically unfeasible [12]. Moreover, high H$_2$S concentrations produced culminate in high refining costs.

Mathematical models have been developed to predict microbial souring and aid operators prepare the necessary mitigation strategies. Modelling the reservoir souring as a result of water injection is fairly complex. One must consider, conditions under which the sulphide bio-generation takes, quantification in the specific subsurface environment and interaction of H$_2$S with the various phases during transport. Though the models are different, relevant parameters for modelling microbial souring comprehend:

- SRB metabolism: Quantification of SRB potential to generate H$_2$S when necessary components (carbon source and sulphate) are available. This depends on reservoir conditions, temperature, pressure and salinity as well as distribution of specific bacterial populations in the reservoir
- Minimum and maximum temperatures for bacterial activity
- Duplication rate of SRB population
- Minimum and maximum concentrations of SRB: Minimum amount of biomass needed for bacterial H$_2$S generation and maximum biomass available in the formation rock under local environmental conditions
- Water composition: Sulphate, dissolved carbon sources, nitrogen & phosphorous concentrations, salinity and pH

A review of some of the existing models and simulators shall be carried out below.

2.3.1 Mixing model

The mixing model developed by Ligthelm et al. (1991) was the first microbiological reservoir souring model. According to this model, the growth of SRB takes place in the zone where injected seawater mixes with the formation water. In this model, the injected seawater is seen primarily as a source of sulphate and the formation water is the source of VFA and other organic compounds due to contact with the oil phase. The biotic generation of H$_2$S in this model is independent of the chemical and physical constraint in the reservoir. The effects of nutrient concentrations and temperature profile of the reservoir are not accounted for. After generation, H$_2$S is transported to the producer. During transportation, the H$_2$S interacts with the oil and the iron-containing minerals within the reservoir rock. This interaction affects the development of

H2S at the producer. Iron-containing minerals (siderite, hematite and/or magnetite) contained in the porous reservoir rock coupled with partitioning between the residual oil and water phases, delays produced H2S breakthrough at surface facilities despite SRB growth in formation.
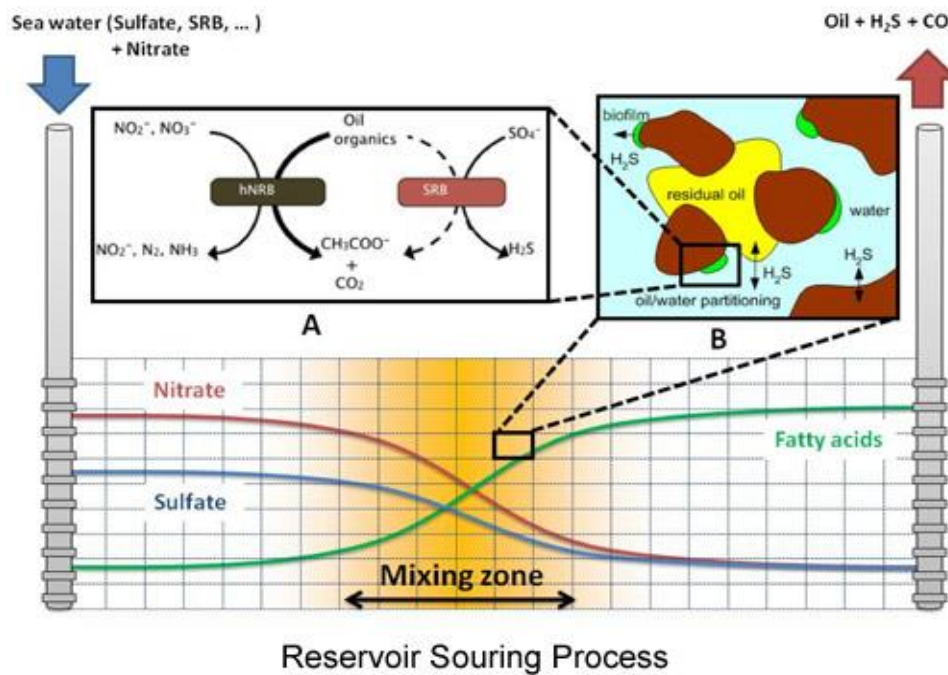
Figure 2.1: Mixing model illustration. Source of H₂S within mixing zone.

2.3.2 Biofilm model

The biofilm model developed by Sunde and Thorstenson (1993) was developed to address the shortcomings of the mixing model. The biofilm model shifted focus from thermophilic to m-SRB. This shift was supported by generated data from backflowing injection wells that showed a thriving H2S production environment near the injection well area. In addition, the biofilm model also considered the fact that the injection water was much cooler (20-30°C) than the hot formation, forming a cool zone around the injection well in areas where the injection water flowed.

The biofilm model proposes that majority of the H2S is produced by m-SRB at a site close to the injection well. It is based on the growth characteristics of SRB and the nutritional concentrations of injection water and the reservoir water. Thus, the model can be used to simulate the effects of adding nutrients to injected water. However, caution must be taken when applying the model to high permeability formations, >100 md. Lastly, the model also considers

the capacity for the reservoir to adsorb H2S which in turn determines the pore volumes injected before the reservoir sours
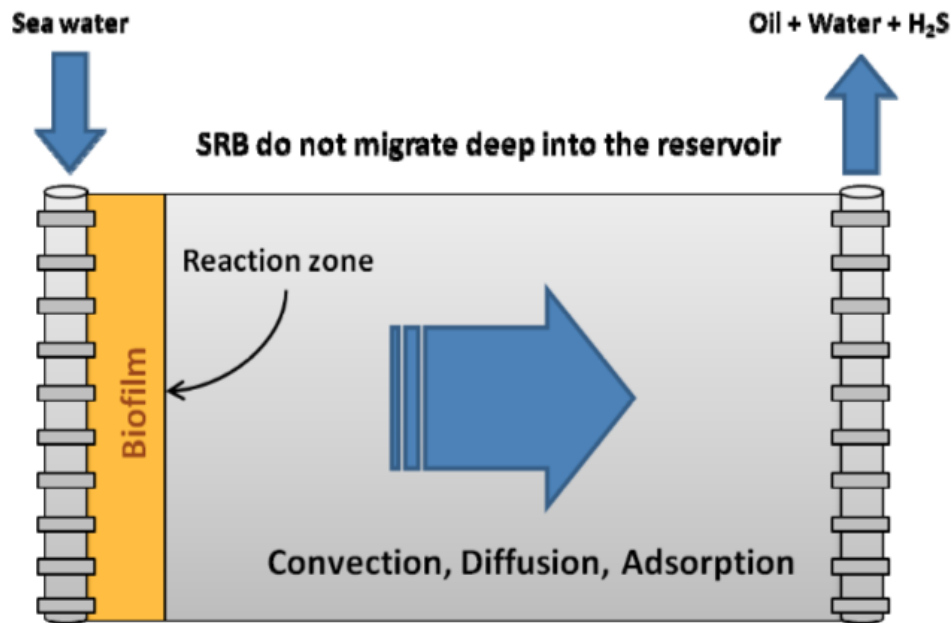
Figure 2.2: Biofilm model illustration. Biofilm formed near injection well.

2.3.3 Thermal Viability Shell Model (TVS)

The TVS model developed by Eden et al. (1991) focuses on temperature and pressure effects on microbiological activity. This model is based on the correlation of experimental data. The correlation includes the sulphate consumption rate of m-SRB, active at low temperatures (20-50°C). A "thermal viability shell" is formed when thermal equilibrium is established between the low temperature injection water and the high temperature formation water and the volume of the shell is dependent on the resulting temperature.

Unlike the biofilm model, the TVS model does not consider the nutrient effect on H2S generation. Moreover, the effects of adsorption and partitioning is also ignored. The calculation of the rate of H2S generated depends on the environmental temperature and pressure. As such, TVS model is limited for field application in that it cannot be used in system conditions other than those specified in the correlation. Based on simulated results, the TVS and mixing models are similar with the express differences in temperature profile and SRB type.
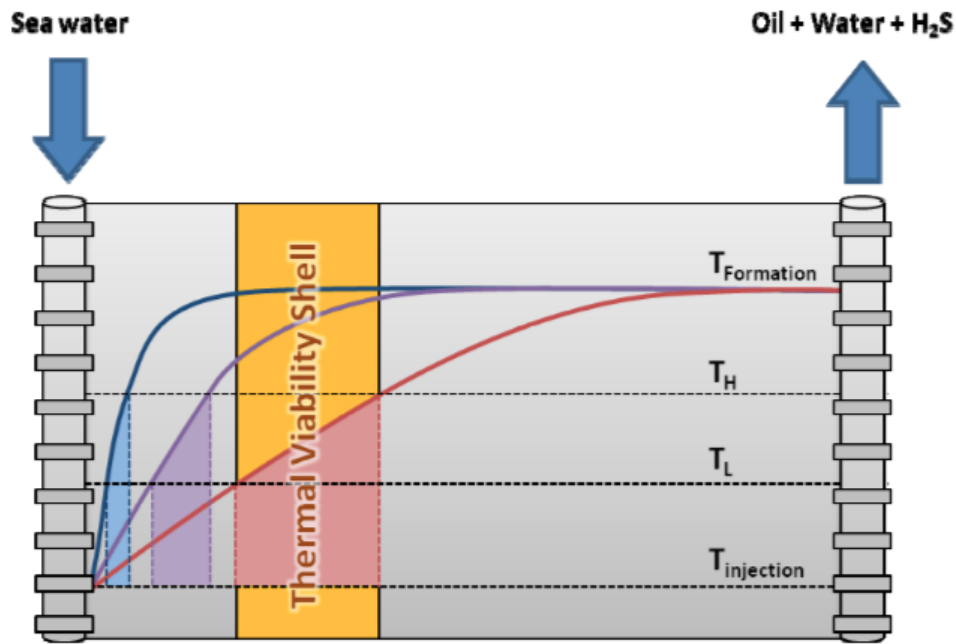
Figure 2.3: TVS model illustration. TVS is formed between the upper limit T_H and the lower limit T_L. The temperature profiles showing progress of the TVS at different stages of production (Early to late life).

2.3.4 Algorithm for history-matching of reservoir souring

This mechanistic model was developed by Burger et al. (2005) to simulate reservoir souring in the Ekofisk field. Ekofisk field contains a naturally-fractured chalk reservoir that is discretized in the model using equal size volume elements. These volume elements contain a fracture, chalk matrix, oil and connate water. Henry's Law and the Peng-Robinson equation are used to estimate the partitioning of H₂S in the different phases. It is assumed that the SRB is only active at temperatures below 80°C (m-SRB and t-SRB) thus the model constrains SRB mobility via permeability and the growth via temperature gradient.

The algorithm uses field data to estimate sulphate production in order to arrive at coefficients of maximum sulphate reduction and effective nutrient supply. Furthermore, results from experiments can be used to estimate the third coefficient that describes the effect of temperature on the sulphate reduction efficiency. During application at Ekofisk, the model assumed a limited sulphate concentration in the early volumetric elements due to the precipitation of $CaSO_4$. Additionally, the model was used to predict microbiological souring in the presence of siderite, scavenging some of the generated H₂S [4]. The model has also been utilized to assist the bio-competition between SRB and NRB based on potential substrates and simple stoichiometric relationships [5].

2.3.5 SourSim®RL

The SourSim®RL model was developed during several Joint Industry Projects. The approach to SourSim®RL is a 1-way coupling of the souring model to existing reservoir simulators such as ECLIPSE 100 and CHEARS (a Chevron in-house reservoir simulator). This means that the souring solution is solved by coupling with the reservoir simulator to incorporate the full 3D transient, based on the reservoir simulation. The benefit of this approach is that it is not necessary to rebuild the reservoir simulation and keeps the run times for SourSim®RL shorter as pressure and flow equations are not solved. SourSim®RL applies both mixing zone and biofilm in the same run during modelling [31].

The H₂S generation criteria used in the model is based on laboratory and field measurements of SRB at different conditions and the model includes criteria to predict the generation of biomass in different regions of the reservoir in terms of a "biomass potential". These criteria are implemented such that they can replicate the various stages of biomass development (lag, exponential growth, stationary and death phases). The advantage of biomass modelling is that it considers the impact of the consumption of nutrients in biomass building and thus H₂S generation. Another advantage of using SourSim®RL is the ability to include multiple nutrient sources in the model as well as the inclusion of a surface design feature.

Other simulators with full 3D transient capability include SourMax, Dynamic TVS, H₂S Model and REVEAL [31] [17].

2.4 Experimental Methods Used to Characterize Microbial Properties.

The growth phases of the microorganisms within the reservoir can be categorized into the following: Lag, exponential (log), stationary and decline phases. The first phase, lag phase, occurs at the period when the microorganism concentrations are at minimum levels when introduced by the seawater into the formation around the injector. The exponential phase takes place next, during this stage, the microorganisms adapt to their new environment and begin to multiply and increase in their concentrations.

After a period of time, the available nutrients needed for growth and development are depleted and this hinders further growth of the biomass. This stage is known as the stationary phase. Finally, increase in toxicity by bio-products and changes in acidity level lead to bacterial decay.

The result is the final stage, decline phase, where the decay rate of the organism exceeds that of generation.
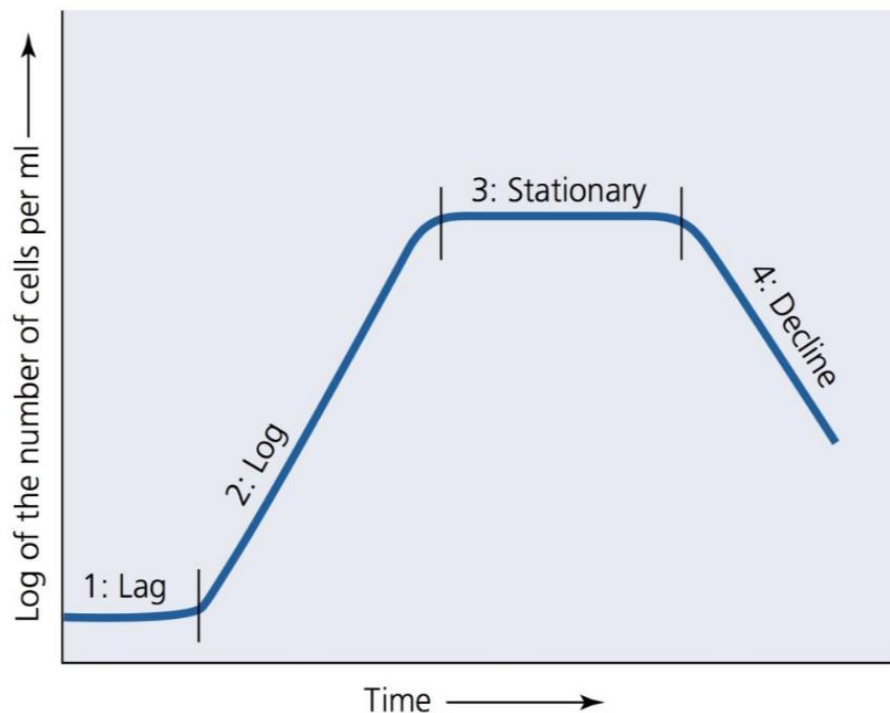
Figure 2.4: Phases of microbiological growth as per laboratory experiments.

Over the years, various experimental methods have been utilized to characterize microbial growth and yield, uptake of nutrients, generation of bio-products and the limiting factors of microbiological metabolism. The following sub-chapters will be dedicated to explaining the biofilm reactor experiments conducted to study microbiological souring.

2.4.1 Biofilm reactor experiments

Biofilm reactors can be used to assist in understanding microbial growth in natural systems, where microorganisms adhere and attach themselves to surfaces to form biofilms. A typical setup of an up-flow biofilm reactor consists of a vertical column/tube that is filled with sand grains or glass beads to form a porous medium. Sampling ports can be placed along the length of the column such shown in Figure 2.5. The biofilm reactors are used to characterize microbial growth and thermodynamics similar to basic reactors, as well as understand microbial transport and attachment in porous media.

Once the experiment is carried out, biomass attachment is estimated by retrieving the porous media. One approach is to slice the porous medium into several sections and then dry them at

75°C for 4 hours followed by another heating interval at higher temperatures, between 400-500°C, for 4 hours to remove organic materials [6]. The total weight of biomass is calculated by getting the difference between the weight before and after the removal of organic materials in the column. This method however lacks accuracy due to loss of water in the biofilms themselves, possible decomposition of biomass at high temperatures and loss of volatile suspended solids within the biofilms [54]. Furthermore, in the case of SRB, the measured mass may be the result of abiotic precipitates including carbonates and iron sulphides.

Biofilm reactors have also been utilized to evaluate mitigation methods of microbiological souring. Injection of biocides and stimulation of competitive microbes such as NRB are examples of mitigation methods that have been tested. The approach involves continuous injection of potential substrates that are affiliated with oil reservoirs into the reactors [7, 6, 54, 22, 2, 14, 64]. Few experiments have utilized residual oil as a substrate source for SRB, with or without the presence of oil-degrading microbes [46]. This underlines the importance of oil-degrading microbes for SRB to supply the VFAs required for their growth as SRB is unable to efficiently use oil components. SRB reduces the VFAs (acetate, butyrate and propionate). Thus, an increase in the acetate concentration would be an indication of microbiological souring in oil fields.

After injecting several pore volumes, a delay in H2S breakthrough has been commonly experienced in souring experiments. This delay has been attributed to reaction with aqueous iron in the medium and potential iron-bearing minerals. However, the compositions of the used sands in those experiments were not extensively characterized for iron content and so the impact of iron-scavenging was not considered in the analysis of the results of those experiments. Instead, the delay was assumed to be through entrapment of H2S gas inside the reactor [7]. Various experiments have been carried out to evaluate microbial iron reduction in iron-rich natural systems. Li et al. (2009) [40] conducted an experiment to evaluate microbial reduction of sulphate and iron at a uranium-contaminated site near Rifle, Colorado. Myoung-Soo et al. (2016) [47] studied the reduction of iron-bearing minerals in a managed aquifer recharge process.
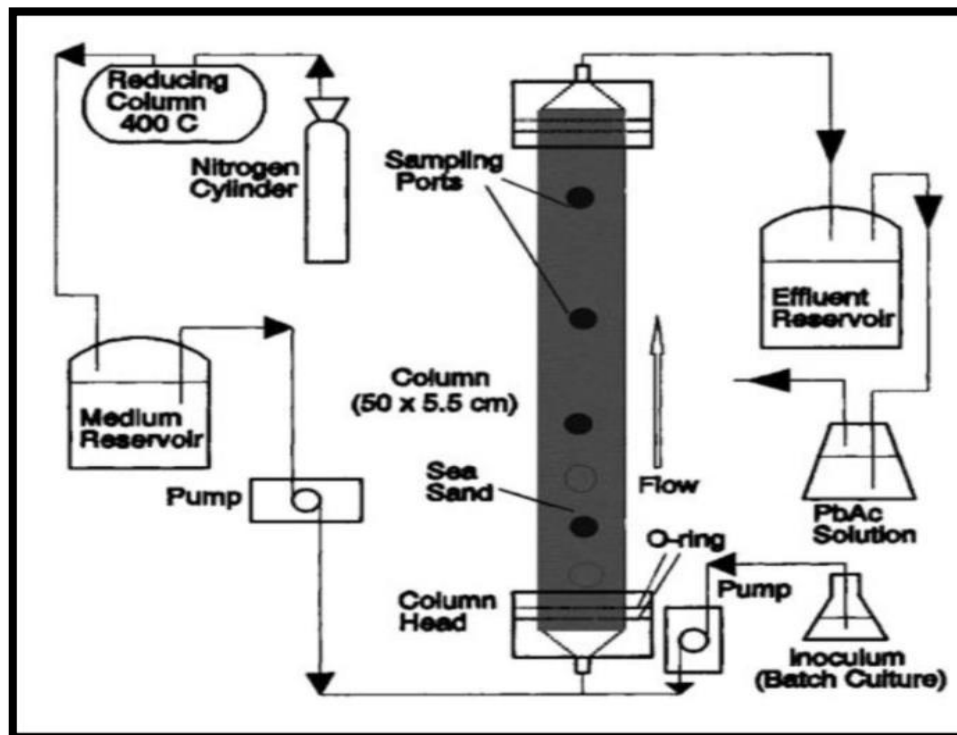
Figure 2.5: Typical up-flow biofilm reactor setup [6].

2.4.1.1 Model Verification with Experimental Data

Chen et al. (1991) [6] investigated microbial souring in a biofilm reactor. The experiment utilized an isolated SRB strain common to environmental studies. The study was carried out in a 50cm long up-flow porous column. The reactor was filled with sea sand with an average porosity of 37%. An isolated strain of SRB was cultured in the biofilm reactor and microbes were inoculated into the reactor when they reached their log (exponential) phase. The experiment was conducted three times using varying rates and concentrations. Sulphate and lactate were injected at concentrations of 130-900 mg/l respectively while the pore velocity was maintained at 2.74 cm/h. The microbes were expected to oxidize lactate to acetate as demonstrated by chemostat experiments. The results of the experiment are displayed in Figure 2.6
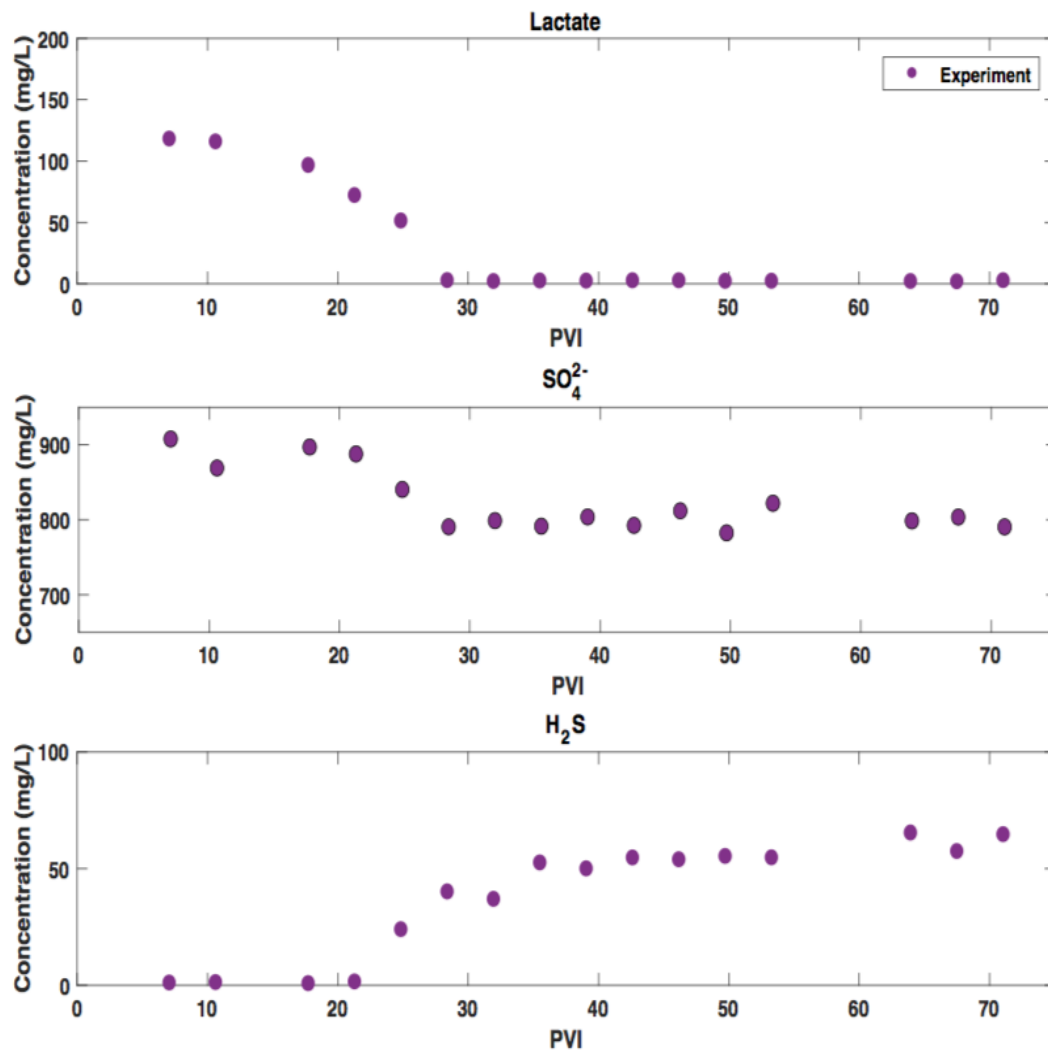
Figure 2.6: Outlet concentrations of lactate, acetate, sulphate and H₂S in a microbial column experiment [6].

The results showed a significant delay before H2S was observed in the outflow from the reactor. H2S production took place after 20 pore volumes had been injected. During this period the SRB grows to an amount that is large enough to facilitate oxidation-reduction reactions. After the initial indication of souring, H2S concentration in the effluent increases steadily until it becomes relatively constant at about 40 pore volumes injected. Additionally, the presence of iron in the medium was confirmed by the formation of black precipitates of FeS observed early in the experiment. Despite this, concentrations of the iron species were not quantified, and the geochemical composition of the sand was not characterized in the experiment.

During the estimation of biomass attachment at the end of the experiment, the column was divided into 14 regions and it was observed that most of the biomass has attached near the inlet.

2.5 Field Case Study: Gullfaks

Gullfaks field is located in the Tampen area in the Norwegian sector of the North Sea, Block 34/10. Discovery took place in 1978 and thenceforth the field has been developed with three processing, drilling and accommodation facilities with concrete bases and steel topsides, Gullfaks A (GFA), Gullfaks B (GFB) and Gullfaks C (GFC). Production started in 1986, 1988 and 1989 at GFA, GFB and GFC respectively. The Norwegian Petroleum Directorate (NPD) current reserve estimates for Gullfaks are 391 mill. Sm^3 oil equivalents (o.e) for oil and 23.1 mill. Sm^3 o.e for gas. The reservoirs lie at a depth of about 2000 m and the water depth is 135-217 m.

The geology of Gullfaks is complex. The reservoirs are located in rotated fault blocks in the west and a structural horst in the east with a highly faulted region in between. The main reservoirs consist of Jurassic of the Brent Group, Cook and Statfjord sandstone formations and the upper Triassic Lunde sandstone formation. The drive mechanism for the principal reservoirs is primarily water injection with water/alternating gas (WAG) injection used in some areas. In the first 20 years, 750 million m^3 of seawater had been injected into the field. Like other North Sea fields, Gullfaks was initially classified as a sweet reservoir, with a very low concentration of H₂S in the reservoir fluids.

2.5.1 Monitoring and mitigation methods implemented

Various mitigation methods discussed in the previous chapters have been implemented at Gullfaks. In 1986 at field start up, biocide treatment in the form of batch treatment of glutaraldehyde in injection water was used. The dosing regimen constituted 500ppm of glutaraldehyde injected 1hr/week. The injected water is pumped into the formation at 20 Mpa [2900 psi] at rates varying between 30,000 m^3/d and 70,000 m^3/d. Oxygen is the removed using a vacuum deaerator and the final water temperature downstream of the deaerator is 25°C.

Microbial monitoring of the water injection was carried out to ensure that the measures of control were effective. The total number of bacteria was determined with epifluorescence microscopy after filtering samples onto a $0.2\mu m$ nuclepore filter and staining the DNA specific fluorescent dye DAPI [51]. SRB was determined using the fluorescent antibody (FA) technique [46]. At the beginning of the monitoring period in 1989 and 1992 for GFB and GFC respectively, SRB dominated the bacterial community in the biofilm.

Despite stringent filtration and biocide treatment to control injection water quality, Gullfaks A experienced high levels of H₂S in the produced fluids in the early 1990s (35 mg/l of H₂S in produced water). The biofilm and water samples at GFB and GFC were collected downstream of the deaeration tower and additional water samples at wellhead for selected wells [58]. At GFB, SRB were regularly detected with viable counts from April 1994. Over the next two years a significant increase in viable SRB counts was noted, finally stabilizing at $1*10^6$ to $6*10^6$ SRB/cm³. The increase in viable counts was followed by an increase in sulphate reducing capacity in the biofilm to an average of 4.6 μg H₂S /cm²/day and an increase in corrosion. GFC showed a similar SRB count of $1*10^6$ SRB/cm³. The sulphate reducing capacity of GFC was higher, 11.9 μg H₂S /cm²/day. A new method of implementation was needed to reduce sulphate reduction and mitigate H₂S production.

Following success on Veslefrikk platform, Statoil implemented the use of nitrate treatment at Gullfaks in 1999 at B and C platforms. Nitrate salt is continuously added at a dosing rate of 30-40 ppm of a 45% Ca(NO₃)₂ solution [60]. A decrease in viable SRB counts on both platforms was observed approximately one month into the treatment. Reduction in SRB reduced sulphate reduction capabilities and thus there was a noted decrease of H₂S levels in produced water.
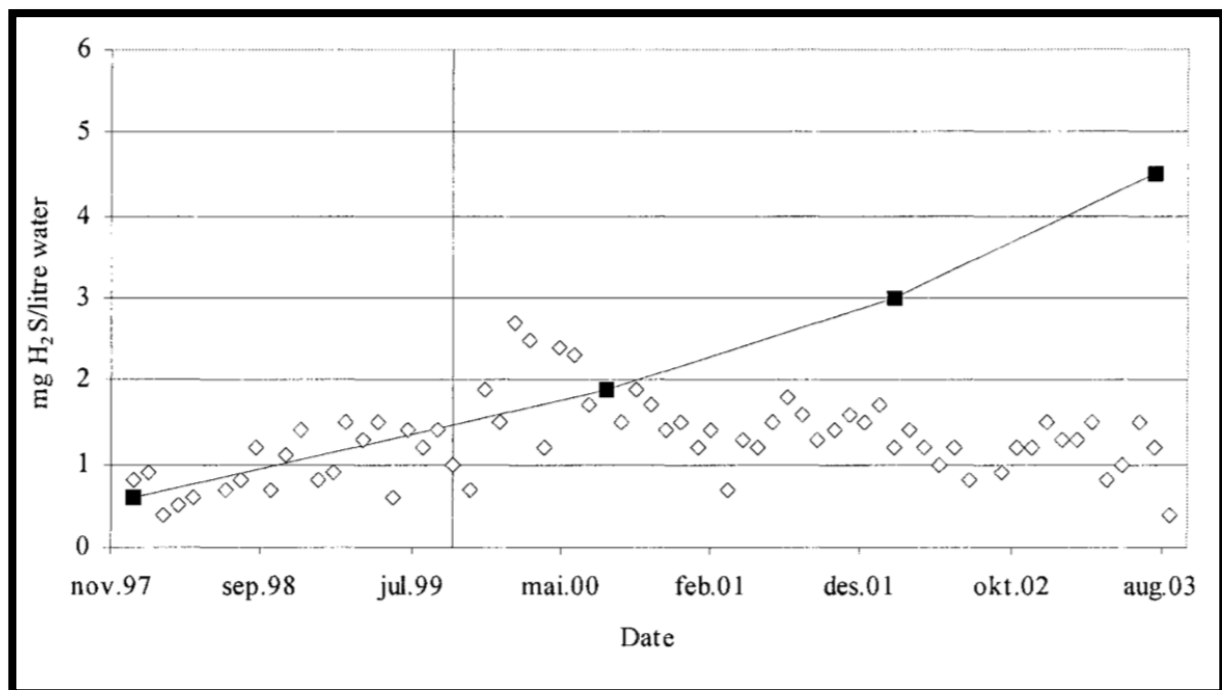
Figure 2.7: Illustrates the mean H₂S concentration for 14 producers and theoretical H₂S development of GFB. The scatter plot represents the measured H₂S produced water and the line represents the theoretical H₂S development [58].
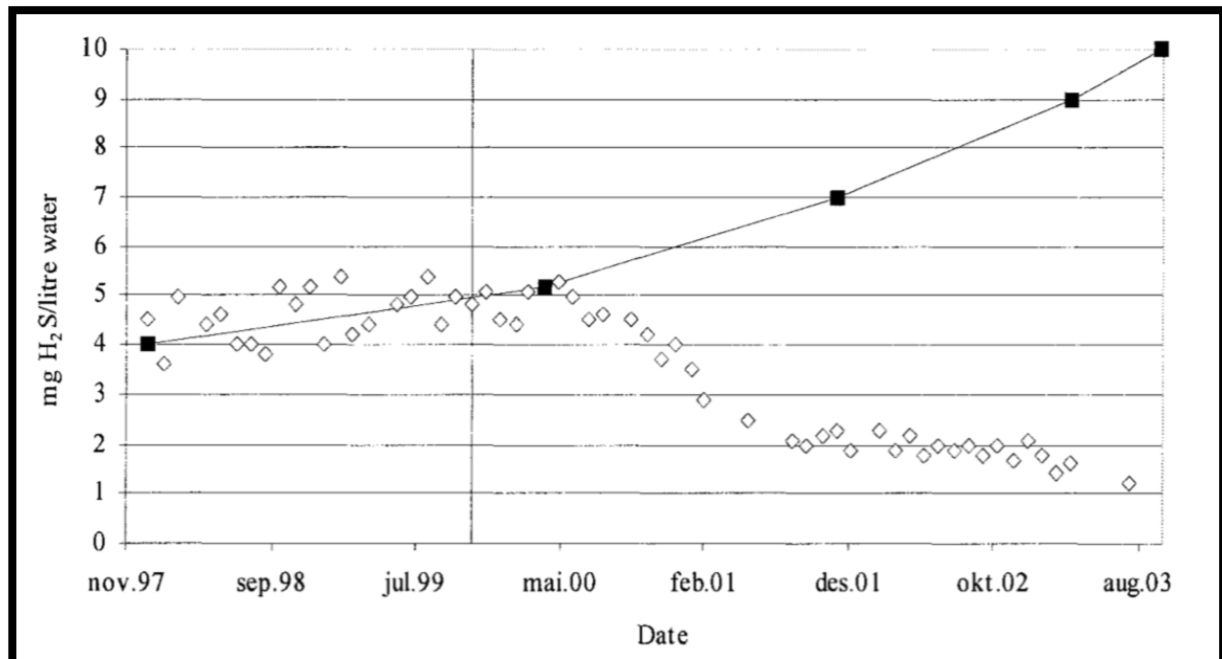
Figure 2.8: Illustrates the mean H₂S concentration for 14 producers and theoretical H₂S development of GFC. The scatter plot represents the measured H₂S in produced water and the line represents the theoretical H₂S development [58].

2.5.2 Modelling application and discussion

The mixing model which was initially put forward did not sufficiently explain the development of H₂S at Gullfaks. This is because one of the main observations was the fact that H₂S production was delayed by up to 3-4 pore volumes. This seemed to disagree with the mixing model, where H₂S production would be expected shortly after water breakthrough. Alternatively, SRB growth was assumed to take place in a biofilm near the sea water injection well. The parameters determined to affect the H₂S production profile include flow rate, porosity of the formation and the distance between the producer and the injector.

The basic shape of the H₂S production profile is as illustrated in Figure 2.4 but is susceptible to changes as a result of the different mechanisms taking hold in the reservoir after the H₂S generation. One such mechanism is the adsorption of H₂S by the surrounding reservoir rock. This explains the time lag between the water breakthrough and the initial rise in the H₂S production. The rate and extent of reservoir souring on Gullfaks based on the biofilm model was essentially determined by three parameters. The availability of nutrients which control the amount of biomass in the biofilm. The scavenging capacity of the reservoir rock which controls the amount of pore volumes injected before the H₂S is detected in the production fluids. Finally,

the flow regime which determines the time it takes to flow a pore volume was also considered in the model in order to simulate Gullfaks field data.

Another important consideration of accepting the Biofilm model was the quality of the injected water. Addition of N or P would lead to an increase in biomass which would translate to an increase in H$_2$S production.

Chapter 3 : Theory and Methods

Appearance of biogenic souring is dependent on both the initiation of a biofilm and the injected seawater breakthrough carrying the biologically produced H2S to the producer. This section goes through the theory that describes: the dispersion of the injected water in the reservoir as it moves from the injection well to the production well; generation of H2S from the inoculated SRB; and partitioning of H2S in the different phases as it is transported by the injected water flood towards the producer well. This chapter shall set a foundation for the results section of this paper.

3.1 Displacement Mechanics

The Buckley-Leverett displacement theory is the basic theory of waterdrive governing all calculations in the subject whether performed using analytical or numerical simulation techniques. It is used to estimate the advance of a fluid displacement front in an immiscible displacement process. The theory uses fractional flow theory and is based on the following assumptions [19]:

- Displacement is one dimensional
- Pressure is maintained
- Fluids are immiscible
- Gravity and capillary pressure effects are negligible

The Buckley-Leverett equation 3.1, states that the velocity plane of constant water saturation is directly proportional to the derivative of the fractional flow evaluated for the same saturation. Essentially, the fractional flow equation is a function of the increasing water saturation through its dependency on rock relative permeabilities.

$$v = \frac{q_t}{A} \, \varphi \, \frac{df_w}{ds_w} \qquad\qquad\qquad \textbf{[3.1]}$$

Where:

v: velocity of the moving plane

q_t: constant injection rate

A: Area of the cross section

φ : porosity

$\frac{df_w}{ds_w}$: slope of the fractional flow curve.

It is necessary to first examine some fundamental concepts that are essential in Buckley-Leverett displacement mechanics. The Buckley-Leverett equation and its application in simulators is revisited in more detail in chapter 4.

3.1.1 Miscibility [10]

Two phases are said to be miscible if they can mix and form a homogenous mixture. Miscible fluids are soluble in oil so there will be no interfacial force between the oil and the solvent, resulting in no interfacial tensions and capillarity existing between the two fluids. Therefore, the residual oil saturation can theoretically become zero in the case of miscible displacement. On the other hand, immiscible fluids are fluids that do not mix physically or chemically. Two phases that do not mix cannot form a homogenous mixture. In water flood or an immiscible gas flood, the displacing fluid is not soluble in the displaced oil. The displacement results in a residual oil saturation due to the inter-facial forces between the displacing fluid and the displaced oil.

Reservoir temperature and pressure, the composition of the injected fluid and composition of the oil are the major factors that influence the degree of miscibility. To achieve miscible conditions between the oil and the injected fluid (gas), a certain pressure for a given temperature must prevail. This pressure is defined as the minimum miscibility pressure (MMP). Both pressure control of the reservoir and control over the intermediate composition of the injected gas must be performed to achieve controlled miscible drive operations.

The manner in which water displaces oil is illustrated in Figure 3.1 for both an ideal and non-ideal linear horizontal waterflood.
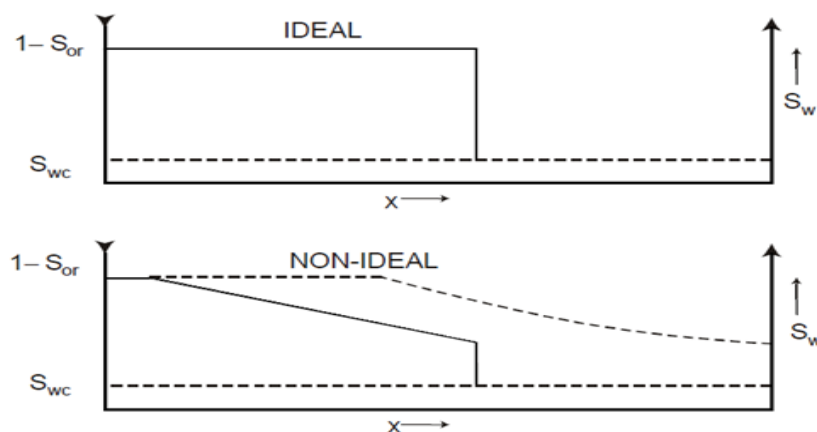
Figure 3.1: Water saturation distribution as a function of distance between injection and producing well for ideal (piston like) displacement and non- ideal displacement [36].

3.1.2 Relative permeability

Relative permeability relates the effective permeability with the absolute permeability. When a fluid occupies only a fraction of the total pore volume, effective permeability must be used. Relative permeability is defined as the ratio between effective permeability and absolute permeability.

$$k_{rl} = \frac{k_l}{k} , l = o, g, w \qquad\qquad\qquad\qquad \textbf{[3.2]}$$

Where:

k_{rl}: Relative permeability

k_l: Effective permeability

k: Absolute permeability

Even though relative permeability depends on the structure of the porous medium it is common to assume that relative permeability only is a function of the increasing displacing phase saturation. With this assumption it becomes simpler to determine the relative permeability with the experimental work. In an oil/water system the relative permeability of water and of oil are measured as functions of water saturation. Figure 3.2 illustrates the phase relative permeability dependence on saturation in two-phase oil/water systems. The end points S_{wir} and S_{or} are very important. S_{wir} is the critical water saturation. S_{or} is the critical oil saturation in the oil/water system.

During an immiscible flood, water saturation increases from its irreducible value, S_{wir} at which it is immobile to the maximum or flood-out saturation, $S_w = 1-S_{or}$, at which the oil ceases to flow. S_{or} represents the unconnected oil droplets trapped in each pore space by the surface tension forces at the end of the waterflood. The two curves in Figure 3.2 will be the relative permeability input to a simulator, k_{ro} and k_{rw}. The shape of the curves is dependent on rock and wetting characteristics.
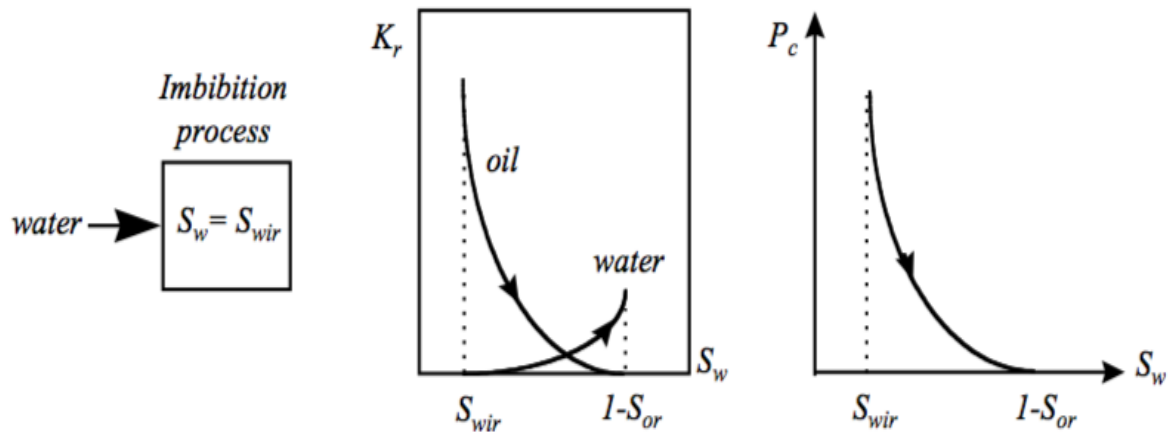
Figure 3.2: Water-oil rock relative permeability curves [36]

3.1.3 Mobility

Mobility, λ, is a measure of the ability of a fluid to flow through interconnected pore space. It can be calculated as the ratio between permeability, k and viscosity, μ.

$$\lambda_l = \frac{k_l}{\mu_l} = \frac{k k_{rl}}{\mu_l} \ , \ l = o, g, w \qquad \text{[3.3]}$$

The mobility ratio is calculated by dividing the displacing phase mobility by the displaced fluid mobility:

$$M = \frac{\lambda_{displacing\ phase}}{\lambda_{displaced\ phase}} \qquad \text{[3.4]}$$

If M=1 the two phases flow at equal velocities resulting in a piston like displacement. M < 1 indicates that there is stable displacement whereas M > 1 is an unfavourable mobility ratio and will make the displacement unstable. When describing a miscible displacement process, mobility and mobility ratio are some of the most important parameters. Waterflooding performance in multi-layered composite linear reservoirs is mainly controlled by the mobility ratio [1].
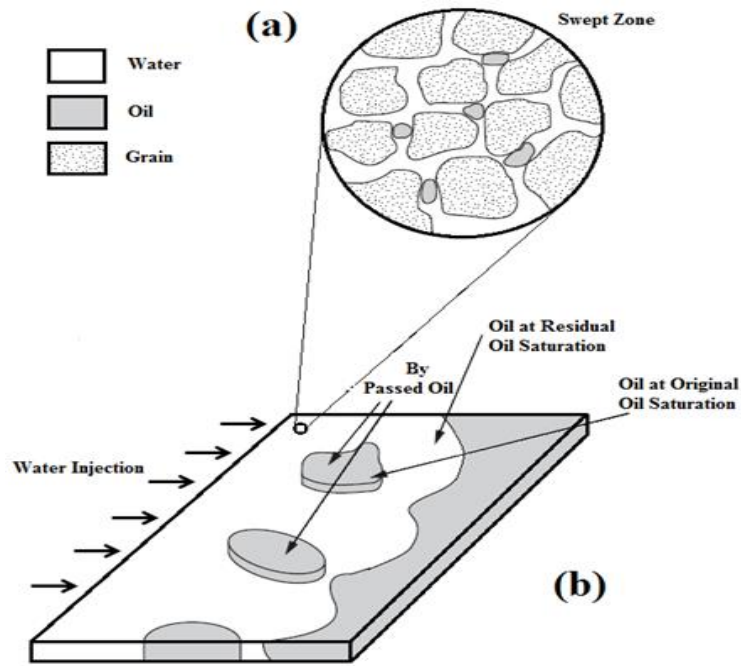
Figure 3.3: (a) Microscopic displacement (b) Residual oil remaining after waterflood

3.1.4 Transmissibility

Having a fluid flow through porous media, transmissibility, T, is defined as [15]:

$$T = \frac{\beta_c kA}{\mu \Delta L}$$

[3.5]

The transmissibility may be included in Darcy's law for horizontal flow through porous media:

$$q = \frac{\beta_c kA}{\mu} \frac{\Delta P}{\Delta L} = T\Delta P$$

[3.6]

Where:

q: flow rate

β_c: transmissibility conversion factor

k: permeability

A: cross-sectional area

μ : viscosity

ΔP: pressure difference

ΔL: segment length

The reservoir is segmented into grid blocks where each block is assigned given values such as permeability, porosity and saturation. The block permeability gives no insight into how easily the fluid will flow between the blocks, therefore transmissibility is introduced to describe the communication between the grid blocks. Transmissibility is a function of permeability and is defined so that $T_x(I)$ is between block (I) and (I + 1) as shown in Figure 3.4
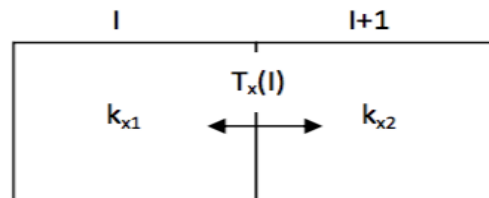
Figure 3.4: Transmissibility in the x-direction between two grid blocks

3.1.5 Viscous fingering

Viscous fingering is a phenomenon caused when a more viscous fluid is unstably displaced by a less viscous fluid. As the low viscosity fluid flows through the more viscous fluid it will begin to form "fingers". This can have a negative impact on recovery. Having a homogenous medium may result in formation of a symmetric pattern. However, this symmetry may be lost in heterogeneous mediums as is the case in many reservoirs. As a result, oil displacement will be inefficient and may lead to early water breakthrough. Most reservoir simulators do not accurately model fingering effects. The model accuracy can be marginally improved by use of a very fine grid to cover the area of interest.

3.1.6 Fractional flow

The fractional flow of water, f_w, at any point in a reservoir is defined as [10]:

$$f_w = \frac{q_w}{q_w + q_o} \qquad [3.7]$$

and is synonymous with the term water cut which refers to the water produced from a well. Substituting the rates using Darcy's law gives:

$$f_w = \frac{\frac{kk_{rw}}{\mu_w} A \frac{\Delta P_w}{\Delta L}}{\frac{kk_{rw}}{\mu_w} A \frac{\Delta P_w}{\Delta L} + \frac{kk_{ro}}{\mu_o} A \frac{\Delta P_o}{\Delta L}} \qquad [3.8]$$

Assuming that the pressure gradients in the water and oil are similar, therefore ignoring capillary pressure effects, cancelling the terms and dividing the numerator and denominator by K_{rw}/μ_w gives equation 3.9 which is the fractional equation for horizontal displacement.

$$f_w = \frac{1}{1 + \frac{\mu_w k_{ro}}{\mu_o k_{rw}}}$$
[3.9]

Waterflooding for field application entails maintaining the pressure such that the viscosity ratio μ_w/μ_o is constant. This further implies that the fractional flow is strictly a function of the water saturation upon which the ratio K_{ro}/K_{rw} depends. For a typical set of relative permeabilities, the fractional flow equation 3.9 usually has the shape indicated in Figure 3.5 with saturation limits S_{wc} and $1 - S_{or}$ between which the fractional flow increases from zero to unity.
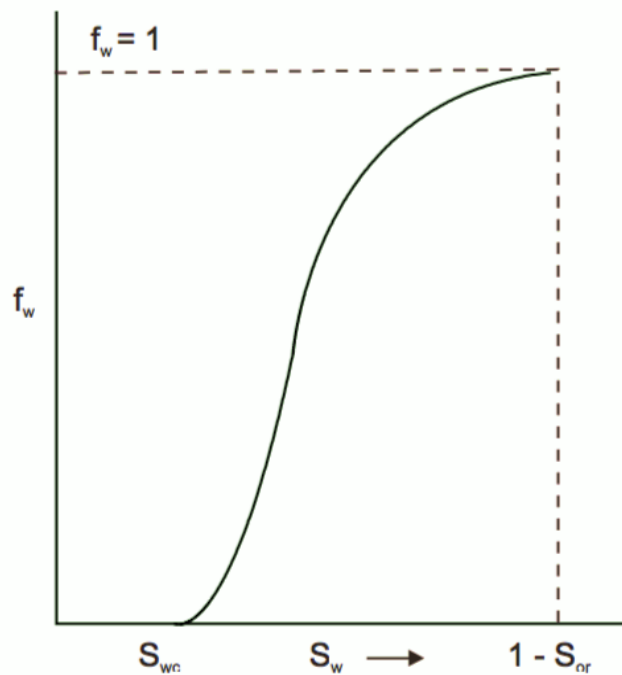
Figure 3.5: Typical fractional flow curve as a function of water saturation, equation 3.9

Fractional flow is fundamental in the concept of waterdrive because:
- The shape of the f_w function gives insight into the efficiency of the flood.
- When applied it incorporates the correct, in situ oil and water viscosities unlike most relative permeability measurements.

The fractional flow equation is used to calculate the fraction of the total flow which is water, at any point in the reservoir, assuming the water saturation at that point is known.

3.2 Colony Establishment and Transport of H$_2$S

As the injected seawater displaces the oil in the direction of the producer, the injected water cools the region around the injection well. At temperatures below 60°C, the larger percentage of H$_2$S is formed by microbial sulphate reduction. Vital elements for microbiological reservoir souring can be provided by the injection of deaerated cold seawater into a formation. This is because seawater is an excellent medium for bacterial growth with regards to salinity, pH (6-9) and redox potential (<-100 mV) [13].

It is suggested that the first sulphate-reducing organisms to colonize the formation are the m-SRB [13]. They are introduced into the reservoir via the injected seawater stream where they are detectable in low numbers, below 10 organisms per ml. These numbers are lowered even further through biocidal treatments. However, the large volumes of water needed for injection ensure that sufficient numbers of SRB needed to establish stable colonies overcome the effects of the biocide treatment. Owing to the temperature at which they thrive (20-45°C), the m-SRB are restricted to a region close to the injector.

Assuming that all H$_2$S is produced by microbial sulphate reduction where SRB is the catalyst, the reaction of the energy generating process is as follows:

$$\textbf{Organic carbon (C)} + \textbf{SO}_4 \longrightarrow \textbf{CO}_2 + \textbf{H}_2\textbf{S}$$

For biomass production, m-SRB is dependent on the availability of C, N and P whereas for energy, C and SO$_4$ are need. The bacterial biomass ratio for C, N and P is considered to be constant, 82% C, 14% N and 4% P by mass. It is further assumed that 90% of C is used for respiration and 10% contained in the biomass. In the absence of N or P, bacterial growth stops. In this case due to remineralization and resting cell metabolism, it is assumed that the sulphate reduction proceeds at a constant rate proportional to the amount of SRB biomass present. Therefore, it can be concluded that the reservoir souring is controlled by C, SO$_4$ and biomass. The H$_2$S production profile is shown in Figure 3.6.
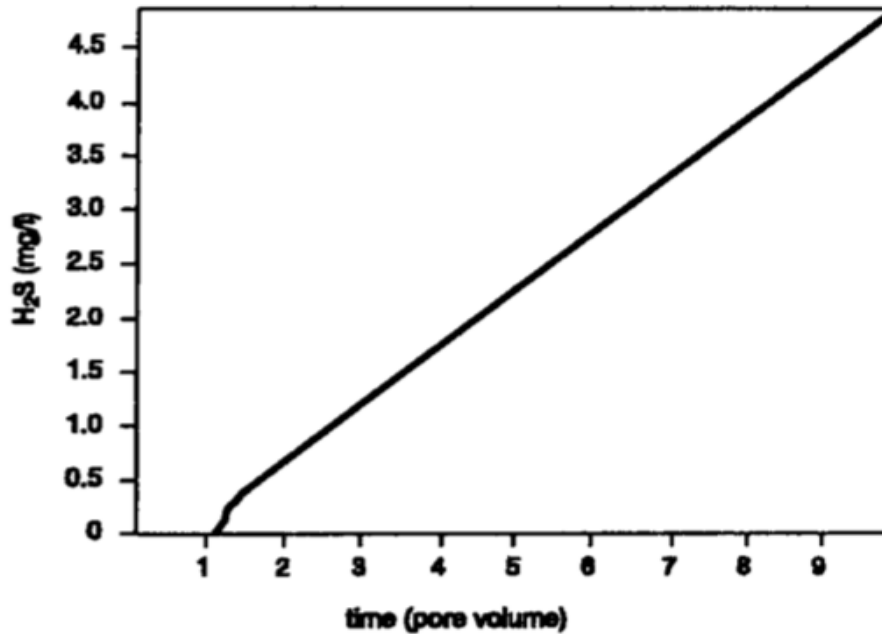
Figure 3.6: H₂S in produced water without adsorption [59].

The quality of injection water is crucial when accepting the biofilm model since it influences the rate of H_2S production. Addition of nutrients, e.g. N or P would lead to an increase in biomass which will inadvertently lead to an increase in H_2S production [59].

3.2.1 Adsorption

Once H_2S is generated it is transported by the water towards the producer. However, H_2S production does not increase at seawater breakthrough but starts increasing several pore-volumes after seawater breakthrough. This delay can be explained by adsorption of the initial volumes of H_2S produced in the reservoir. The higher the permeability of the formation rock, the lower the adsorption capacity whereas low permeability formations have higher adsorption capacity. According to [59] sandstones have a scavenging capacity of $5 - 19600$ mg/kg. The scavenging capacity of the reservoir rocks is a highly variable parameter and should be determined on a field by field basis.

3.2.1.1 Langmuir isotherm

Consider the following reaction adsorption of S^{-2} of a mineral surface

$$S^{-2}_{(in\ solution)} + Surface\ sites = S^{-2}_{adsorbed} \qquad\qquad [3.10]$$

The equilibrium constant for the reaction is

$$K = \frac{[S^{-2}_{(adsorbed)}]}{[S^{-2}_{(in\ solution)}]\,[Surface\ sites]} \qquad\qquad [3.11]$$

Where

K: Numerical constant of equilibrium (l/mg)

[]: Represents concentration.

The maximum scavenging capacity, [S^{-2} (adsorbed max)] is the sum of [surface sites] and [S^{-2}(adsorbed)]. The amount of S-2 adsorbed can be calculated using the Langmuir equation [3.12]

$$[S^{-2}_{(adsorbed)}] = \frac{[S^{-2}_{(adsorbed\ max)}][S^{-2}_{(in\ solution)}]\,K}{1 + [S^{-2}_{(in\ solution)}]\,K} \qquad\qquad [3.12]$$

At low concentrations of the adsorbing species $[S^{-2}_{(in\ solution)}]$ the denominator in the above equation is close to unit, $1 + [S^{-2}_{(in\ solution)}]\,K = 1$, so the amount of adsorption increases linearly with increasing concentration of $[S^{-2}_{(in\ solution)}]$. For high concentrations of the adsorbing species, where $1 + [S^{-2}_{(in\ solution)}]\,K = [S^{-2}_{(in\ solution)}]\,K$, the amount adsorbed equals the constant $[S^{-2}_{(adsorbed\ max)}]$.

After the calculation for the total amount of H₂S or the overall generation of H₂S in a cell, part of it will be adsorbed by the rock and can be given the following equation:

$$H_2S = H_2S_{gen} - H_2S_{ad} \qquad\qquad [3.13]$$

Where

$$H_2S_{ad} = \left[\frac{A_C * H_2S_w * K}{1 + H_2S_w * K}\right]\rho_r\,V_r \qquad\qquad [3.14]$$

And H_2S_w is the concentration in the water phase [59]. The H₂S profile with adsorption is illustrated in Figure 3.7.
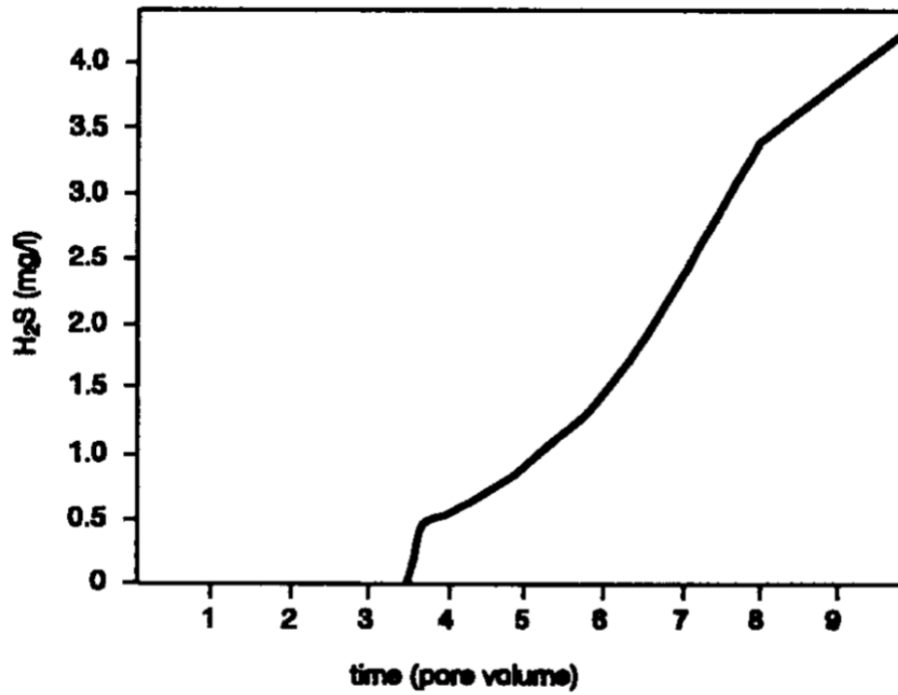
Figure 3.7: H₂S in produced water with adsorption [59].

3.2.1.2 Iron Scavenging

In the biofilm model, the presence of high dissolved iron concentration, $140 - 280$ ppm can represent a significant H₂S sink by precipitation as iron sulphide. The hydrogen sulphide reacts with the iron to precipitate iron sulphide as described in equation 3.15

$$FeS + H^+ = Fe^{+2} + HS^- \qquad\qquad [3.15]$$

The reaction product, FeS, solubility is dependent on several factors such as pH and temperature. Evans. (2001) [18] studied the iron sulphide stability at various pH values and H₂S concentrations, Figure 3.8. Przybylinski. (2001) [52] also studied the iron scale formation and presented a comparison of the solubility products of certain oil field scales.

The iron sulphide solubility product (K_{sp}), measured in fresh water at 20°C, is given by equation 3.16

$$K_{sp} = [Fe^{+2}][HS^-] = 3 * 10^{-(3+pH)} \qquad \qquad \textbf{[3.16]}$$

After a period of time, the scavenging capacity of the rock surfaces is depleted and the remaining H2S dissolved in the water phase approaches the producers in increasingly higher concentrations.
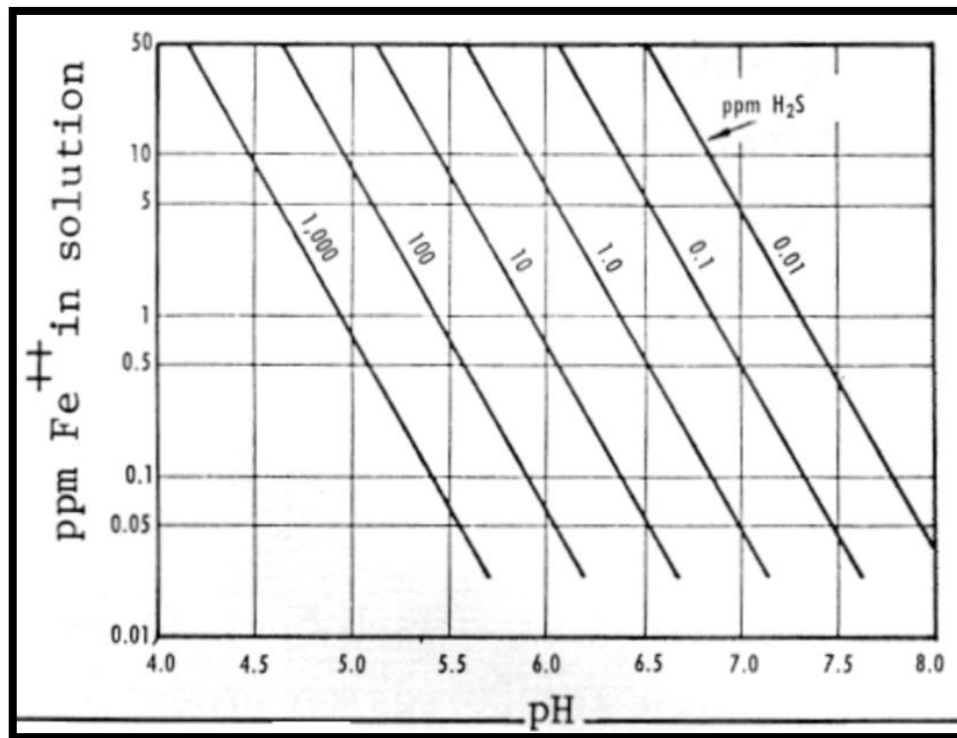
Figure 3.8: Iron sulphide stability diagram.

3.2.2 Partitioning

Due to equilibrium, H2S dissolved in the water phase might migrate into the oil and gas phases. The H2S partitioning coefficients are functions of pH, temperature and pressure. Absolute pressure controls the H2S partial pressure and hence the H2S concentration in the gas phase increases as the absolute pressure decreases to give the same partial pressure. Temperature changes the Henry's Law coefficients for H2S. The solubility of H2S in water is calculated using Henry's law:

$$X_w^g = \frac{X_o^g \, p_o}{K_H \, (T)} \qquad \qquad \textbf{[3.17]}$$

Where:

X_w^g : Solubility of H₂S (gas) in water.

X_o^g : Solubility of H₂S (gas) in oil.

p_o : Pressure in oil phase.

$K_H\ (T)$: Henry constant which is a function of temperature.

This phenomenon can be represented using partitioning coefficients expressed as the ratio of the concentrations of given phases.

$$\boldsymbol{k_{ow}} = \frac{H_2S_{oil}}{H_2S_{water}} \left[\frac{mg/l}{mg/l}\right] \qquad \text{[3.18]}$$

$$\boldsymbol{k_{og}} = \frac{H_2S_{gas}}{H_2S_{oil}} \left[\frac{ppmv}{mg/l}\right] \qquad \text{[3.19]}$$

Changes in pH result in a change in the speciation of the H₂S. Dissolved H₂S is produced at lower pH values whereas at higher pH values, HS⁻ and S⁻² are produced. Only the dissolved H₂S species is applied in Henry's Law.

Chapter 4 : Reservoir Simulation with a Tracer Representing H₂S

Modern reservoir simulators are computer programs designed to model fluid flow in porous media. The reservoir engineer then uses the results of these models to develop and optimize reservoir management strategies. The review of reservoir simulation is included in appendix A.

4.1 Tracer Technology

Tracer tests are used to determine the preferred flow paths between injectors and producers. It is done by adding a traceable substance to the injected fluid and measuring the tracer effluent concentration profile when it reaches the producing well. Tracers available for waterflooding include non-radioactive isotopes, radioactive molecules (e.g. titrated water (HTO), 14C labelled thiocyanate (514CN)) and non-radioactive chemicals (e.g. thiocyanate (SCN), fluorinated benzoic acids). Application of tracer tests is a unique and relatively cheap way of gaining information regarding information of fluid flow in the reservoir. Tracer tests are used for the following purposes:

- To clarify connectivity between wells
- To identify offending injectors
- To characterize the flood pattern and directional flow trends
- To delineate the features of reservoir architecture (faults, fractures, permeability variations etc.) that may cause poor sweep efficiency

There are different types of tracers that can be classified as either passive or active tracers. A passive tracer follows the fluid phase in which it is injected without reacting with the fluids or rocks in the reservoir. A passive tracer must have the following characteristics:

- Low detection limits
- Stable under reservoir conditions
- Follow the phase that is being tagged and have minimal partitioning into other phases
- No adsorption to rock material
- Environmentally friendly

Active tracers interact with other fluids in the system and/or with the formation rock. An aqueous tracer that is not reactive or soluble in gas or water in the reservoir, is an example of a passive tracer. To model the aqueous tracer, the Buckley-Leverett equation (1942) that describes immiscible displacement in one direction for water displacing oil is used. The

equation determines the velocity of a plane constant water saturation travelling through a linear system [3].

The mass conservation of water flowing through volume element A*dx, Figure 4.1, while gravity effects are neglected, water and oil are immiscible and incompressible, and temperature is constant, can be expressed as:

$$\begin{pmatrix} \textbf{\textit{Mass into the}} \\ \textbf{\textit{element at x}} \end{pmatrix} - \begin{pmatrix} \textbf{\textit{Mass out of the}} \\ \textbf{\textit{element at x}} + \Delta x \end{pmatrix} = \begin{matrix} \textbf{\textit{Rate of change of mass}} \\ \textbf{\textit{inside the volume element}} \end{matrix} \qquad \textbf{[4.1]}$$

This can be formulated as:

$$\frac{dq}{dx} = A\, \varphi\, \frac{dS_w}{dt} \qquad \textbf{[4.2]}$$

When the equation is rewritten by introducing the fractional flow, the following Buckley-Leverett equation can be obtained, which implies that the velocity of the plane of constant water saturation is directly proportional to the derivative of the fractional flow evaluated for that saturation under a constant rate of water injection [24].

$$\frac{dx}{dt} = \frac{q}{A}\, \varphi\, \frac{df_w}{ds_w} \qquad \textbf{[4.3]}$$

When an ideal tracer is added to the injected water, the equation for the tracer's is expressed as:

$$\frac{d}{dt}\left[\varphi\, S_w\, C + (1 - \varphi)C\right] + \frac{q}{A}\, \frac{df_w}{dx}\, C = 0 \qquad \textbf{[4.4]}$$

Where C is the Tracer concentration.

Assuming that the tracer concentration does not affect the water flow rate and that the tracer does not adsorb onto subsurface solids, equation 4.4 can be simplified to equation 4.5:

$$\frac{\partial C}{\partial t} + \frac{q}{A}\, \frac{f_w}{A\, \varphi\, S_w}\, \frac{\partial C}{\partial x} = 0 \qquad \textbf{[4.5]}$$

It can be found that injecting water with a velocity equal to $qdf_w/A\varphi S_w$ and the aqueous tracer will move with velocity of $qf_w/A\varphi S_w$, which means that the velocity of water is proportional to df_w/dS_w while the velocity of the tracer is proportional to f_w/s_w.
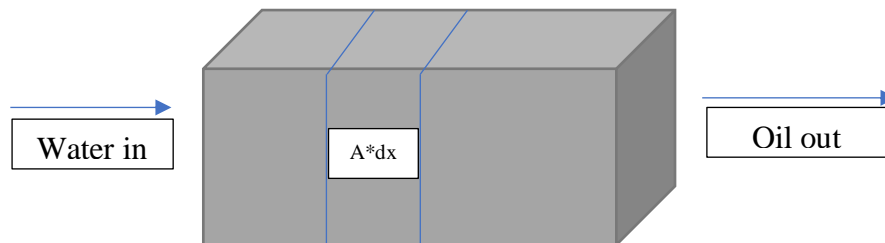
Figure 4.1: Mass flow rate through a linear system

4.1.1 Tracer tracking in the simulation model

The Eclipse Tracer Tracing option is a general facility implemented to follow the movement of "marked" fluid or fluid elements during a simulation run. Any fluid element can be considered as a tracer in the simulator, compared to external tracers that are added to the injected phase. Tracers defined to exist in the water phase can be used to determine the movement within the reservoir of water injected into any number of injection wells or to predict the variations in salinity or concentration of other chemical species in the water produced from the reservoir. The tracers in the simulator are considered to be passive. The tracer concentrations are updated fully-implicitly at the end of each time step after the oil, water and gas flows have been computed. In this study, a water and H₂S tracer have been implemented into the simulation. The tracers are set to:

- Monitor the injected seawater in the formation
- Monitor the efficiency of H₂S production around the injector

Tracer control is achieved by means of the WTRACER keyword in the SCHEDULE section. This keyword allows the specification of the concentration of a particular tracer in the injection stream for each well. The keyword optionally allows the injected tracer concentration to be a function of the total cumulative fluid injected which is useful for modelling H₂S generating process.

4.2 Cumulative H$_2$S Production Model Development

The Tracer Tracking option in Eclipse was used to trace the movement of injected sea water and H$_2$S in order to study the production profile in the reservoir formation. To do this a synthetic model simulation was carried out.

4.2.1 Model assumptions

The assumptions for the simulation model are listed below:

- Homogenous media
- Constant porosity
- Two-dimensional flow
- Constant production rate
- Single phase flow
- Specific set of rock-fluid and PVT data.

4.2.2 Model description

The model is a single-phase model, containing only water. Two wells, one injector and one producer, were added to the model and placed diagonally with respect to each other. The wells are set to be controlled by the surface flow rate target of 800 m^3/day. A constant injection and production rate is used in the model to capture the seawater cut trend and the cumulative H$_2$S production profile. Other properties used in the simulation are summarised below. The simulation initiation date is 1/1/1986.

The dimensions of the hypothetical reservoir and the position of the wells are defined in the input data file in ECLIPSE100. The reservoir is divided into 10,000 control volumes; 100 in the x-direction, 100 in the y-direction and 1 in the z-direction. The simulated reservoir is 1000 m in the x-direction, 1,000 m in the y-direction and 10m in the z-direction. The grid sizes are 10 m in the x and y-directions.

A normal well in the North Sea consists of pipe sections of 12.19 m. Each pipe section is equipped with a sand screen and one or more inflow controllers.
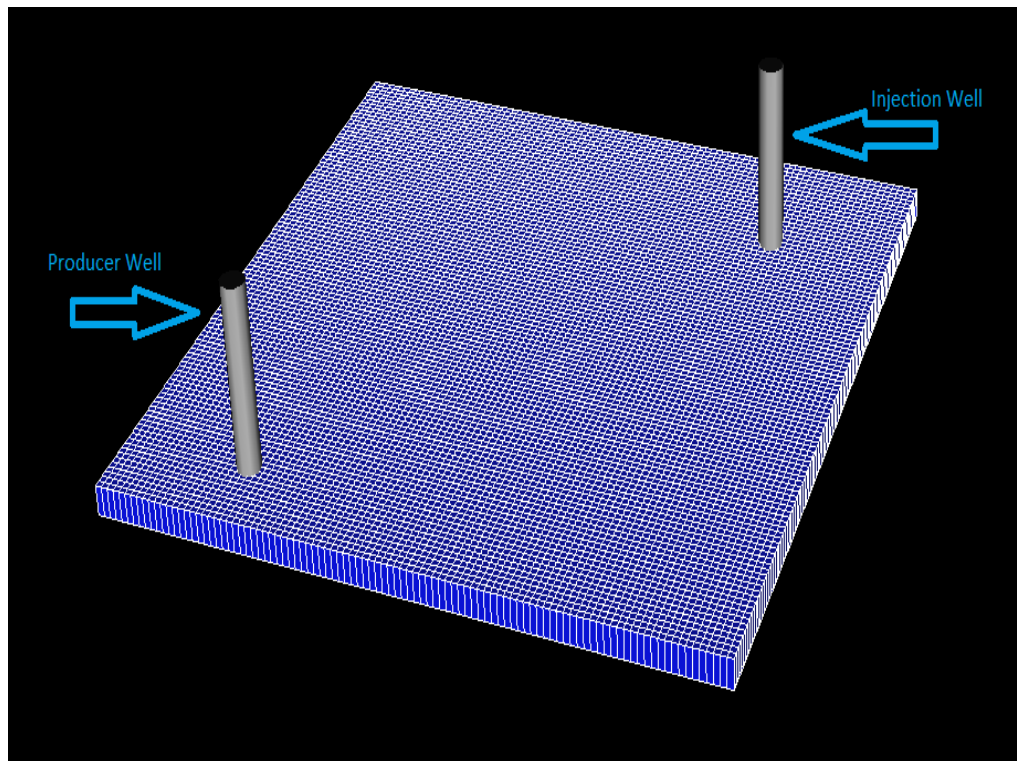
Figure 4.2: Grid section for synthetic reservoir model

The horizontal (x-y) permeability of the grid is 1,000 mD and the vertical (z) permeability is 0.01 mD corresponding to 0.00001 of the horizontal permeability. The relative permeability is the ratio of the effective permeability to the absolute permeability and is highly dependent on the type of reservoir.

An aquifer is also implemented in the model to supply additional energy in the form of water influx. The aquifer model used is a Carter-Tracy aquifer model. The initial aquifer pressure is 380 bar such that it is in initial equilibrium with the reservoir.

Table 4.1: Model input fluid and reservoir properties

Fluid Properties	
Water viscosity	0.5 cP
Water Density	1,000 kg/m^3
Water PVT model	Black oil
Reservoir Properties	
Porosity	0.2
Permeability (x-y direction)	1,000 mD
Initial conditions	
Pressure	380 bar

When seawater injection is initiated at the injection well, the keyword WTRACER is used to define the that all the water injected from the well is to be traced in the simulation. The concentration is therefore set to 1. This tracer is defined as INJ in the data file. The concentration of the H_2S generation tracer is set to 0. This tracer is defined as H2S in the data file.

```
WCONINJE
'I' 'WAT' 'OPEN' 'RATE' 800.0    /
/

WTRACER
'I' 'INJ' 1.0 /
'I' 'H2S' 0.0 /
/
```

The keyword TBLK is used in the SOLUTION section, which specifies the initial concentration of the tracer in each grid block. The keyword TBLK must be followed by the letter F (free state) or S (solution state) and then the name of the tracer which is being initialized. All the tracers in the water phase are in free state and therefore the keywords become, TBLKFINJ, TBLKFH2S and TBLFKAQ for the injected seawater, injected H_2S and aquifer water respectively. At initial conditions the concentrations are set to 0 for injected seawater and H_2S since they are not present in the reservoir. The concentration of the aquifer water is set to 1 in all 10,000 grid blocks.

```
SOLUTION
================================================================

TBLKFINJ
10000*0.0 /

TBLKFH2S
10000*0.0 /

TBLKFAQ
10000*1.0 /
```

The SUMMARY section contains the variables that are to be written to the summary file. Different keywords are added to in this section to include data outputs on field and well tracer production rates, cumulative tracer production, tracer production concentrations and tracer volume in the reservoir.

SUMMARY

===

FWPT -- Field Water Production Total

FTPTINJ -- Field Tracer Production Total for tracer named INJ
FTPTH2S -- Field Tracer Production Total for tracer named H2S

The last part of the SCHEDULE section contains the defined concentrations of each tracer in the injection stream. The concentration inputs for each the two cases are described below. The production profile for cumulative H_2S production is visualized by plotting field tracer production total for H_2S (FTPTH2S) against production total for injected seawater (FTPTINJ).

4.2.3 Simulation results and evaluation

The H_2S tracer concentration was increased from 0.005 kg/m^3/d after 200 days of seawater injection to 0.2 kg/m^3/d at the end of the simulation run. The resulting cumulative H_2S production profile is shown in Figure 4.3:
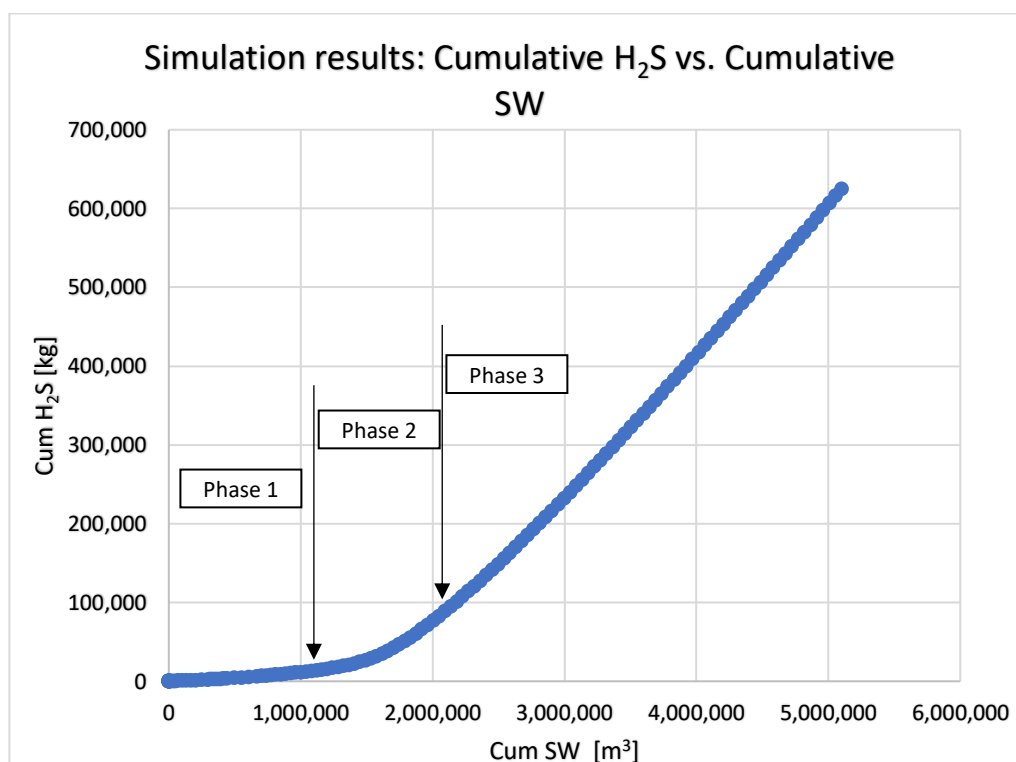
Figure 4.3: Cumulative H₂S vs. Cumulative SW for synthetic model

- Phase 1: The cumulative H_2S production gradually increases linearly from 0 to approximately $1.34*10^4$ kg after the production of $1.12*10^6$ m^3 of produced SW.

- Phase 2: The production profile then enters an exponential phase where the cumulative H₂S production increases from $1.34*10^4$ kg to $8.82*10^4$ kg after production of $2.10*10^6$ m³ of produced SW.

- Phase 3: For the final section of the production profile, the cumulative H₂S production increases linearly from $8.82*10^4$ kg to $6.25*10^5$ kg after production of $5.10*10^6$ m³ of produced seawater. The slope of this linear curve is higher than the initial linear slope of phase 1.

The cumulative H₂S production profile for case 1 in the synthetic model can be described using the phases of microbiological growth described in Figure 2.4.

Phase 1 represents the lag phase where the efficiency of H₂S production in the injector is low. This represents the period when the microorganism concentrations are at minimum levels when introduced by the seawater into the formation around the injector.

Phase 2 represents the log (exponential) phase where the efficiency of H₂S production in the injector are high. This represents the period where microorganisms round the injector adapt to their new environment and begin to multiply and increase their concentrations and biomass growth reaches its maximum.

Phase 3 represents the stationary phase where the efficiency of H₂S production in the injector has reached its maximum. In this period, available nutrients needed for growth and development are maintained (not increasing) thus hindering further growth of biomass.

4.3 Mathematical Models

Construction of a model from data involves three parts; a data set, a model structure and a rule to assess the quality of the models. Before choosing the model structure, one should look at the data and familiarize oneself with it. The choice of the model structure should be based on prior knowledge from this data.

Models can either be linear or nonlinear. Nonlinear structures are much more complicated than linear ones therefore it is prudent to describe a nonlinear system with a simple linear model when possible. The two models investigated in this thesis are:

1. Nonlinear: Exponential model. Two exponential models were tested on the simulation results from the simulation model. However, only one was chosen for history matching and prediction on the field data.
2. Linear: Piecewise linear model

4.3.1 Exponential model

A mathematical expression for the relationship between cumulative production of H₂S (Cum H₂S) and seawater (Cum SW) has been investigated. The mathematical expression, equation 4.6, is similar to the expression for relative permeability of water with the LET equation.

$$F(CumL) = \frac{m * (K2 + (1-K2) * F1(CumL)^{K3})}{F1(CumL)^{K3} + (1-F1(CumL))^{K4}} \qquad [4.6]$$

The slope of the plot of Cum H₂S against Cum SW is modelled as a function of cumulative liquid production (CumL):

$$F(CumL) = \frac{d(Cum\ H2S)}{d(Cum\ SW)} \qquad [4.7]$$

Where F(CumL) increases with time from 0 to '*m*' kg H₂S per m³ of produced SW. *m* represents the maximum amount of H₂S produced in the seawater.

Combining equations 4.6 and 4.7:

$$d(CumH2S) = d(CumSW) * \frac{m * (K2 + (1-K2) * F1(CumL)^{K3})}{F1(CumL)^{K3} + (1-F1(CumL))^{K4}} \qquad [4.8]$$

Where:
- m: This is the maximum slope for the Cum H₂S against Cum SW curve. In the synthetic model, this value is 4kg of H₂S per m³ of seawater. This value may vary from field to field.
- F1(CumL): Calculated in equation 4.9 where cumulative liquid production (CumL) is normalized by dividing it by a 'reference volume' (V_{ref}) which can be described as the cumulative liquid production in the well up to the time at which the first observation of H₂S in the well stream is observed, (CumL_first_H2S)

$$F1(Cum\ L) = 1 - K1^{\left(1 - \frac{CumL}{Vref}\right)} \qquad [4.9]$$

- K2: Represents the initial slope (represented by phase 1 in Figure 4.3) of the Cum H₂S versus Cum SW curve.

- K3 and K4: Control the severity of the exponential section of the curve (represented by phase 2 in Figure 4.3).

In an attempt to simplify the exponential model, a second function with fewer parameters was tested. In this model, F(CumL) is expressed as:

$$F(CumL) = \frac{m * (K1 + (1-K1)*(PV-1))}{(PV-1) + K2 * PV^{K3}} \qquad [4.10]$$

Combining equations 4.7 and 4.10:

$$d(Cum\ H2S) = d(Cum\ SW) * \frac{m * (K1 + (1-K1)*(PV-1))}{(PV-1) + K2 * PV^{K3}} \qquad [4.11]$$

Where
- K1: Represents the initial slope (represented by phase 1 in Figure 4.3) of the Cum H₂S versus Cum SW curve.
- K2 and K3: Control the severity of the exponential section of the curve (represented by phase 2 in Figure 4.3) and the maximum cumulative H₂S production.
- PV: This term represents the pore volume and is calculated by dividing CumL by V_{ref}.

4.3.1.1 Exponential models' verification and evaluation

Table 4.3 summarizes the list of coefficients and the corresponding values used in the mathematical expressions, equations 4.8 and 4.11, to model cumulative H₂S production in the synthetic model. The V_{ref} in the synthetic model is the value of the field water production total (FWPT), injected SW and aquifer water, at the time H₂S breakthrough is observed.

Table 4.2: Identification of V_{ref}

FTPTH2S [m³]	FWPT [m³]
0.00E+00	0.00E+00
0.00E+00	8.00E+02
0.00E+00	3.20E+03
0.00E+00	1.04E+04
0.00E+00	3.20E+04
0.00E+00	9.60E+04
0.00E+00	1.60E+05
2.72E-05	2.40E+05
5.07E-04	3.20E+05
9.47E-02	4.00E+05

Table 4.3: Exponential model input parameters

Parameter	**Exponential model (1):** Eq.4.8 **Value**	**Exponential model (2):** Eq.4.11 **Value**
m	0.2 [kg/m^3]	0.2 [kg/m^3]
V_{ref}	160,000 [m^3]	160,000 [m^3]
K1	1.13	0.001
K2	0.03	7.46E+08
K3	29	-5.51
K4	0.89	N/A
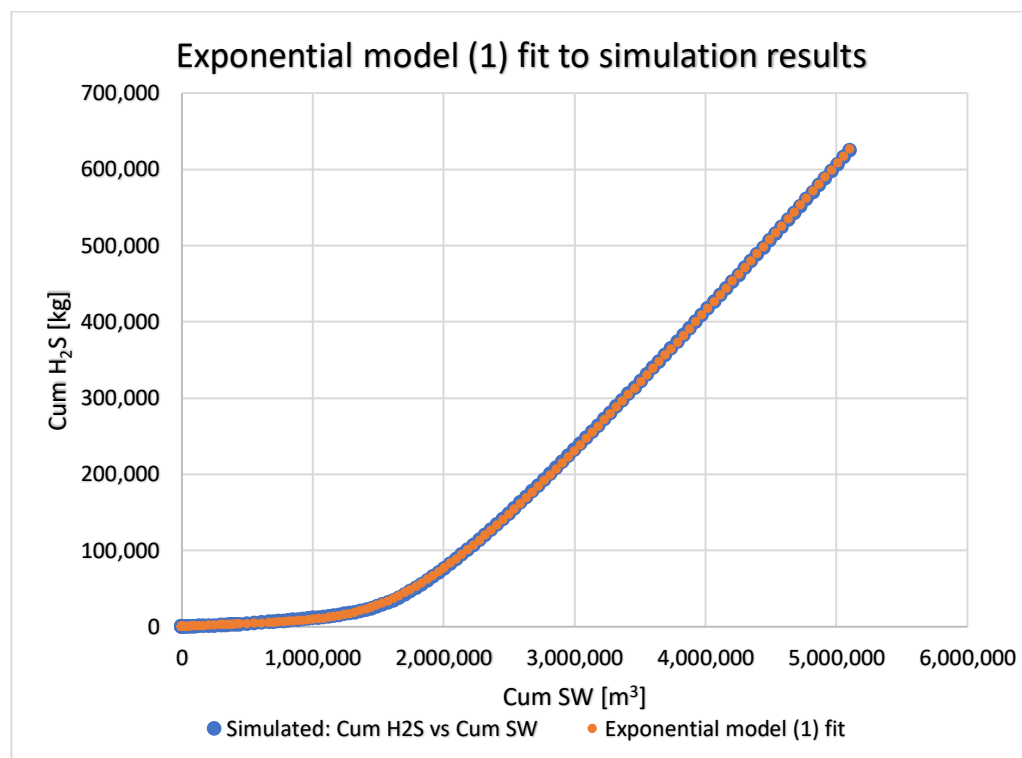
Figure 4.4: Exponential model (1) fit

Having fitted the model to the observed data it could be noted that the mathematical expression used in the model, equation 4.8, gave a reasonably good fit. The squared correlation coefficient R^2 of this correlation was 0.9999. The R^2-value indicates how much of a linear variation of observed values (simulated) is explained by the variation of predicted values (model). The value of R^2 can range between 0 and 1, and the higher its value the more accurate the regression model is [50].
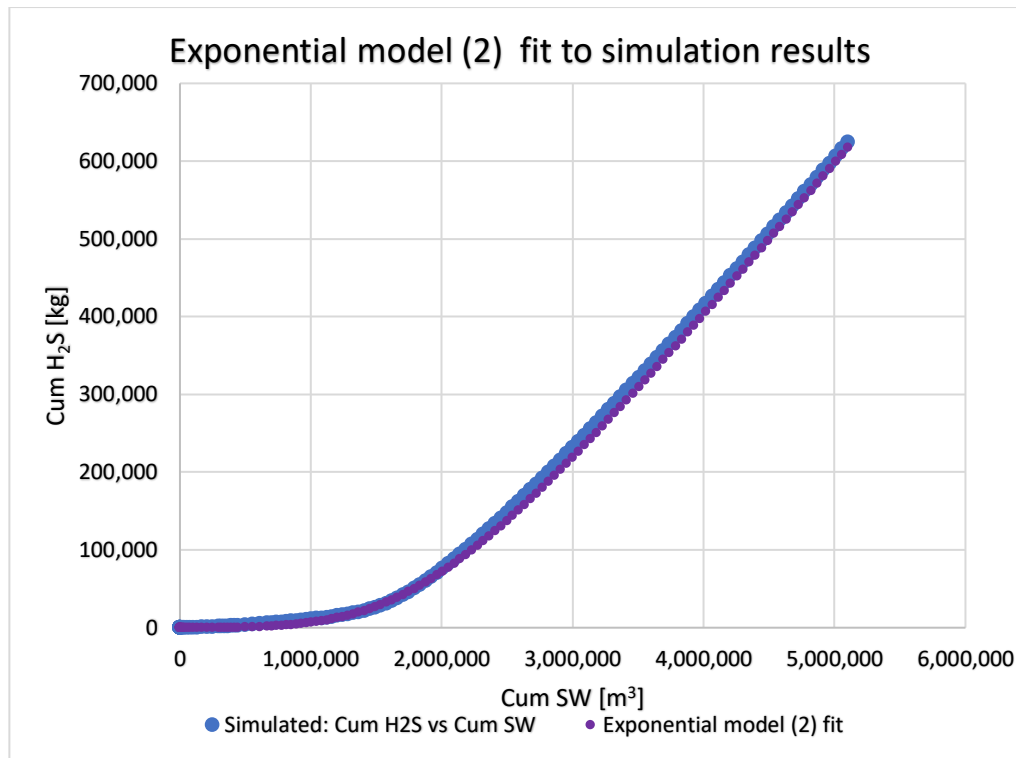
Figure 4.5: Exponential model (2) fit

Having fitted the model to the observed data it could be noted that the mathematical expression used in the model, equation 4.11, gave a reasonably good fit. The squared correlation coefficient R^2 of this correlation was 0.9998.

4.3.1.2 Exponential model comparison
The results of the regression analysis on the two exponential models is summarized in Table 4.4:

Table 4.4: Summary of results from exponential models

Model	# parameters	SSR	SST	R^2
Eq. 4.8	6	1.42E+08	5.38E+12	0.9999
Eq. 4.11	5	8.34E+08	5.38E+12	0.9998

Where:
- SSR: residual sum of squares
- SST: sum of square total
- $R^2 = 1 - \dfrac{SSR}{SST}$

Based on the regression analysis of the exponential models, Table 4.4 they seem to predict the cumulative H₂S production equally well. To be able to choose one over the other, the user should consider the number of parameters used in the models. Equation 4.11, exponential

model (2) contains less parameters and gives more or less similar results. As a result, this model was chosen for application to the field data later in this thesis.

4.3.2 Piecewise linear model

Piecewise linear regression is a form of regression that allows multiple linear models to be fit to the data for different ranges of x. Breakpoints are the values of x where the slope of the linear function changes. The value of the breakpoint is estimated after observing the data. The regression function at the breakpoint may be discontinuous, but a model can be written in such a way that the function is continuous at all points including the breakpoints.

Observing the nature of cumulative H2S production in Figure 4.3, the function should be continuous. When there is a breakpoint, at $x = c$, the model can be written as:

$$y = a_1 + b_1 x \qquad for \ x \leq c \qquad\qquad [4.12]$$

$$y = a_2 + b_2 x \qquad for \ x > c \qquad\qquad [4.13]$$

Where:

a1: intercept of the linear fit to data below the estimated breakpoint.

b1: slope of the linear fit to data below the estimated breakpoint.

b2: slope of the linear fit to data above the estimated breakpoint.

c: estimated breakpoint.

To make the regression function continuous at the breakpoint, the two equations for y need to be equal at the breakpoint (when x= c):

$$a_1 + b_1 c = a_2 + b_2 c \qquad\qquad [4.14]$$

Rearrange the equation to solve for one of the parameters:

$$a_2 = a_1 + c(b_1 - b_2) \qquad\qquad [4.15]$$

Replace a_2 in equation 4.13 with the equation 4.15, the result is a piecewise regression model that is continuous at x= c:

$$y = a_1 + b_1 x \qquad for\ x \le c \qquad\qquad\qquad [4.16]$$

$$y = [a_1 + c(b_1 - b_2)] + b_2 x \qquad for\ x > c \qquad\qquad [4.17]$$

4.3.2.1 Piecewise linear model verification and evaluation

Table 4.5 summarizes the list of parameters used for fitting the cumulative H₂S production curve using the linear piecewise model. The breakpoint, c, was estimated to be the point between the lag and exponential phase i.e. between phase 1 and phase 2 in Figure 4.3.

Table 4.5: Piecewise linear model input parameters

Parameter	Value
a1	-891.86
b1	0.0215
b2	0.166
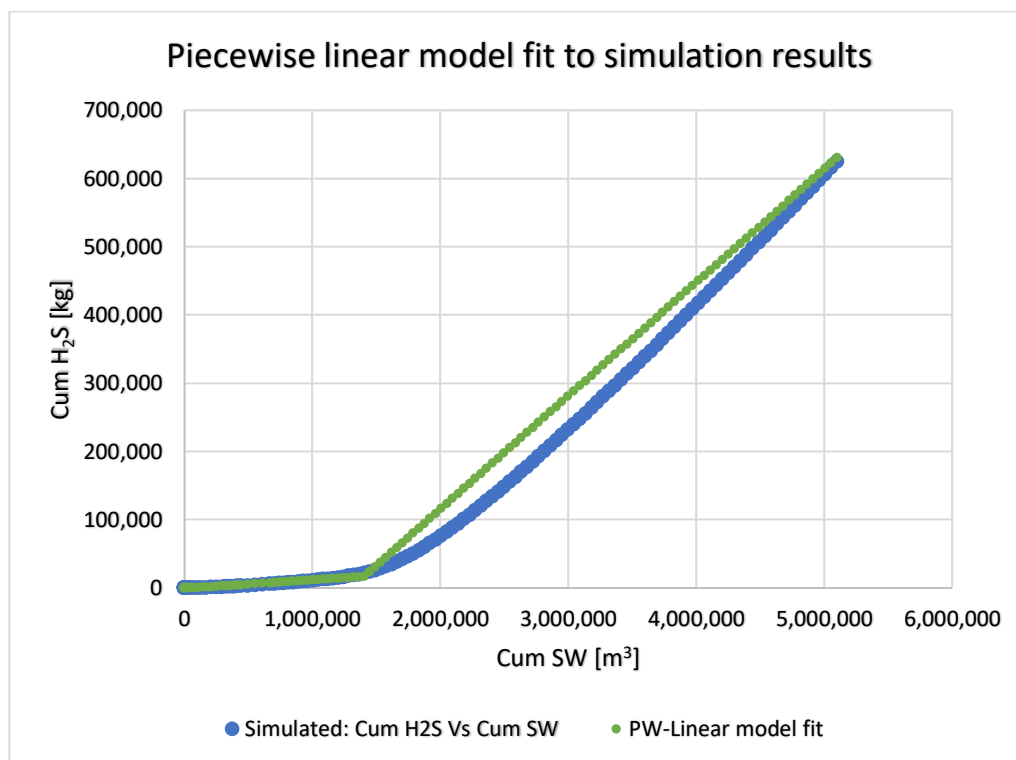
Figure 4.6: Piecewise linear model fit

Having fitted the model to the observed data it could be noted that the mathematical expression used in the model, equations 4.16 and 4.17, gave a reasonably good fit. The squared correlation coefficient R^2 of this correlation was 0.9925.

4.3.3 Results summary: Mathematical model performance on synthetic reservoir model

Two exponential mathematical expressions were tested. A developed exponential correlation, equation 4.8 (Exponential model 1) was tested first. From regression analysis which gave a square correlation coefficient (R^2) of 0.9999, and Figure 4.4, it can be concluded that equation 4.8 gave a good representation of the observed data from the simulated synthetic model. A second exponential correlation, equation 4.11 (Exponential model 2) was also tested. From the regression analysis which gave an R^2 value of 0.9998, and Figure 4.5, it can be concluded that equation 4.11 gave an equally good representation of the observed data from the simulated synthetic model. However, because Exponential model 2 contained fewer parameters and gave similarly good results, it was the chosen exponential model for field application.

A piecewise linear model was also tested, equations 4.16 and 4.17. From regression analysis which gave a R^2 value of 0.9925 and Figure 4.6, it can be concluded that the model also gave a good representation of the observed data from the simulated synthetic model in Eclipse.

Chapter 5 : Well Modelling of H$_2$S Production

Now that the models have been tested on the simulation data, they are applied to the field data on a souring field in the North Sea. Can the models fit the historical cumulative H$_2$S production on a variety of wellbores and give a reasonable prediction for H$_2$S production in the seawater fraction? This chapter attempts to answer that question.

5.1 Data Description and Methodology

H$_2$S Measurement in Gas Phase [ppm]			
H$_2$S Calculator (Historical Data)			
Calculation of H$_2$S in the different phases [kg/d]	Calculation of total H$_2$S [kg]	Calculation of seawater cut [m^3]	Calculation of H$_2$S production rate in seawater [g/m^3]
Model Fitting and Comparison (Future Prediction)			
Exponential model		Piecewise Linear Model	
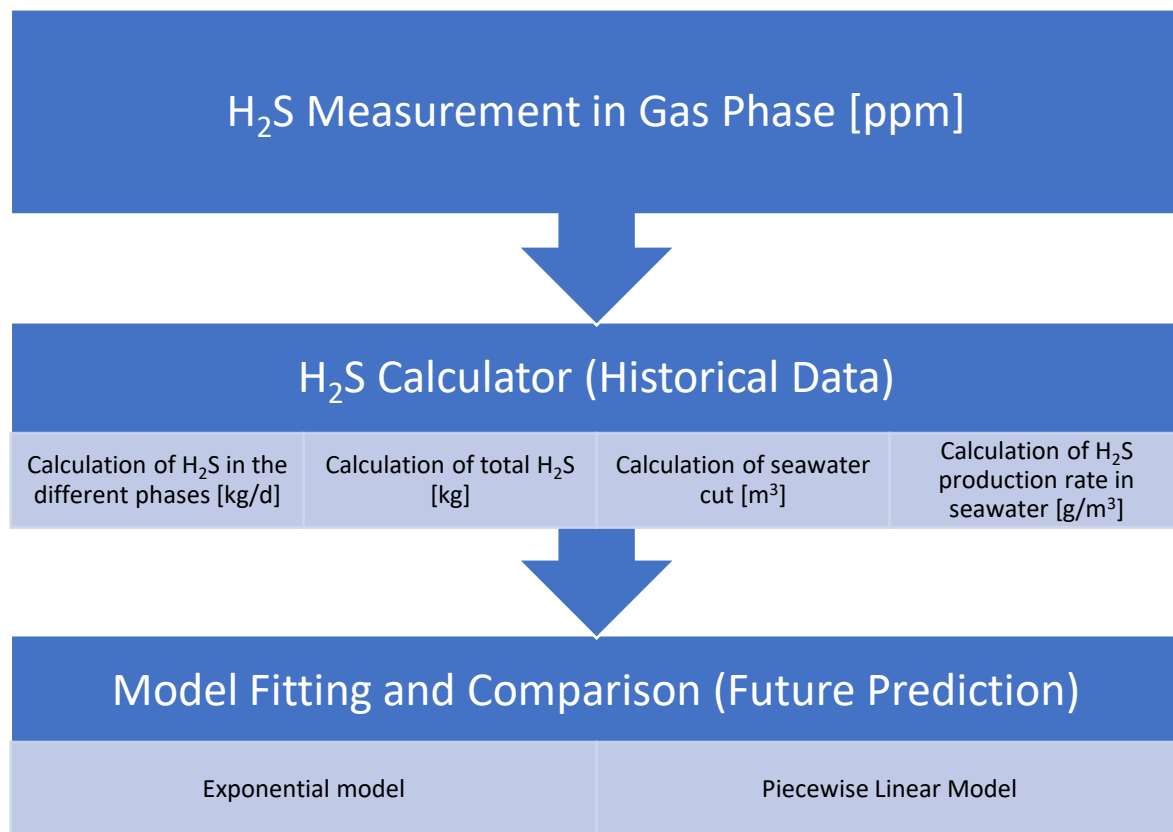
5.1.1 H$_2$S measurement in the gas phase

Measurement of H$_2$S from the wells on field A are done in the gas phase at the test separator. The level of H$_2$S in the separator gas is measured using a Dräger Tube. This method determines H$_2$S concentration from change in colour of the test tube as H$_2$S reacts with iron, forming iron sulphide. The major problem with the measurement of H$_2$S at low concentrations is the chemisorption effect. Loss of just a few ppmv H$_2$S at a concentration of 10-20 ppmv can give a significant error. As H$_2$S is transported to the surface, it is adsorbed to the pipe wall until the pipe is fully saturated and the H$_2$S level in the gas phase stabilizes. It takes about 10 hours, or even longer when the flowrates and/or concentrations are low, before the concentration of H$_2$S

is stabilized and the Dräger tube test gives representative H2S concentration. These results are then recorded in the well test report of the field.

5.1.2 Calculation of H2S in the reservoir fluids

The H2S data available in the well test reports are separator gas concentrations measured during well tests. The well test data also includes the flowrates for each phase and P-T conditions. These gas concentrations are then used to calculate the concentrations of the total hydrogen sulphide in the different phases in the reservoir. Given the long production history of field A, there exists a significant source of historic data. To present this data in a consistent manner that aided the engineers understanding of the factors that affect the rate and degree of souring, a H2S calculator was developed. The reliability of the partitioning calculator to calculate the mass of H2S in each phase depends on the accuracy of the test data. The calculation of H2S in each of the phases is represented in equations 5.1, 5.2 and 5.3:

$$H_2S_{gas}\left[\frac{kg}{d}\right] = \frac{H_2S\ [ppm]}{10^6} * \frac{p_{sc}\ MW_{H2S}}{R\ T_{sc}} * q_g \qquad [5.1]$$

$$H_2S_{oil}\left[\frac{kg}{d}\right] = \frac{H_2S\ [ppm]}{10^6} * p_{sep}k_{og} * q_o \qquad [5.2]$$

$$H_2S_{water}\left[\frac{kg}{d}\right] = \frac{H_2S\ [ppm]}{10^6} * p_{sep}MW_{H2S} * q_w * \gamma_{gas} \qquad [5.3]$$

5.1.3 Calculation of the seawater cut

Another important calculation done by the partitioning calculator is the seawater (SW) fraction of the total produced water (PW). In order to relate the amount of H2S to the seawater fraction, an ion analysis is required to determine the amount of injected water in the PW. An ion analysis is carried out to calculate the percentage of SW in the PW. This aided by the different ion compositions present in the formation and injected waters such as listed in Table 2.1

The concentration of the ions found in the injected seawater can be affected by the chemical reactions with the matrix or the reservoir formation water. Some of the ions in the as shown by Huseby et al. (2005), behaved almost as ideal water tracers, i.e. without sorption to the matrix, ion exchange with the matrix or scale formation. Of the natural tracers that were studied, cross-plots of the ion concentrations in the produced water showed revealed that SO_4^{2-} and Mg^{2+} were the best suited seawater tracers in the investigated case [28]. For the two ions to be ideal, the seawater fraction estimated from one ion should be equal to the fraction estimated for the

other ion, also a cross-plot of the fraction should yield a straight line [28]. Additionally, the sulphate and magnesium content in the formation water is much lower compared to that in the seawater, therefore the initial concentrations of the aforementioned ions are assumed to be zero in the formation water.

$$SW\% = \frac{SW\%_{SO_4^{2-}} + SW\%_{Mg^{2+}}}{2} \qquad\qquad\qquad\qquad \textbf{[5.4]}$$

Once the SW fraction has been calculated, the rate of SW production can be calculated using equation 5.5:

$$SW\left[\frac{m^3}{d}\right] = PW\left[\frac{m^3}{d}\right] * SW\% \qquad\qquad\qquad\qquad \textbf{[5.5]}$$

5.1.4 Calculation of H2S production rate in seawater

Calculation of a 'souring index' (SI) involves the back calculation of the total mass of H2S to a concentration in either total produced water or, alternatively, the fraction of injection water (seawater) in the produced water. This method is reliant on the quality of the well test data as is all the calculations carried out in the 'H2S calculator'.

The calculation of the SW souring index (H2S in the SW fraction or SI SW) is carried out in equation 5.6:

$$SI\ SW\left[\frac{g}{m^3}\right] = \frac{H_2S_{water}\left[\frac{kg}{d}\right]*1000}{SW\left[\frac{m^3}{d}\right]} \qquad\qquad\qquad\qquad \textbf{[5.6]}$$

Figure 5.1 summarizes the calculation workflow from measured data (input) to calculated data (output) within the 'H2S calculator'. The souring index of H2S in produced seawater was calculated in g/m^3 instead of mg/l.
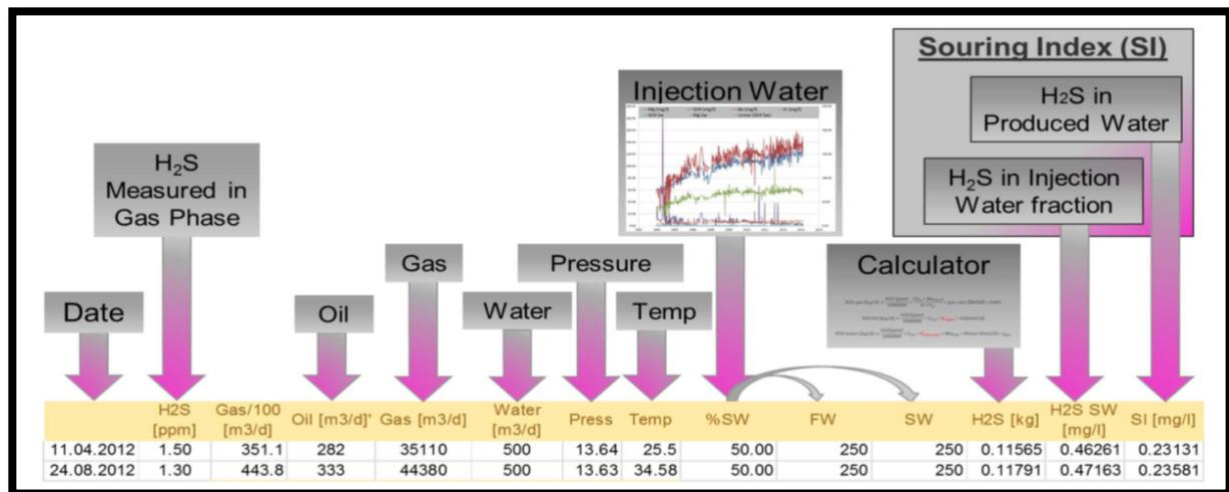
Figure 5.1: Workflow calculation within the H₂S calculator [45]

5.2 Field Case Study: Field A

The work presented in this paper is based on field in the North Sea. The field shall henceforth be referred to as Field A. The field was discovered in the late 1970s and is still in production. The reservoir depth of this field is about 2000 m with a net pay of 127.5 m.

Geological setting: Field A is located in the northern part of the North Sea and was developed with large concrete platforms. The main reservoir lies in the Brent group which contains 73% of the oil in place in moderate to good sands. Because of natural deposition during the Early and Middle Jurassic layers of varying thickness ranging from high quality sandstone to impermeable shale form part of the formation lithology.

Minerology: Fairly clean sandstone consisting of mainly of quartz. Some mica and K-feldspar is also present. Analysis of core samples from the exploration well revealed traces of pyrite in the sandstone.

Petrophysical properties: The main reservoir contains a net pay of 127.5 m. The average porosity is 31.5% and the average water saturation is 15.1%. The permeability varies from 100md to several Darcies. This variation in permeability causes uneven fluid flow, pressure differential and cross flow zones. Field A has reservoir temperatures ranging from 70°C to 80°C.

Water influx from the adjacent aquifer is not enough for maintaining the reservoir pressure above bubble point pressure. Water flooding through water injection is therefore the main form

of recovery. However, H2S content caused by the water circulation created conditions favourable for H2S to generate SRBs close to the injection wells placed in the oil zone of field A. Field A contains 159 production wells that are provided with pressure support from 60 injection wells. Of the 60 injection wells, 11 are gas injectors that are used for water alternating gas (WAG) injection on some areas of the reservoir.

5.2.1 Historical cumulative H₂S production.

The data used in this work is from wellbores in field A. The H2S production history has been calculated on a wellbore basis and presented in a cumulative H2S versus cumulative SW scatter plot. The results are presented in Figure 5.2
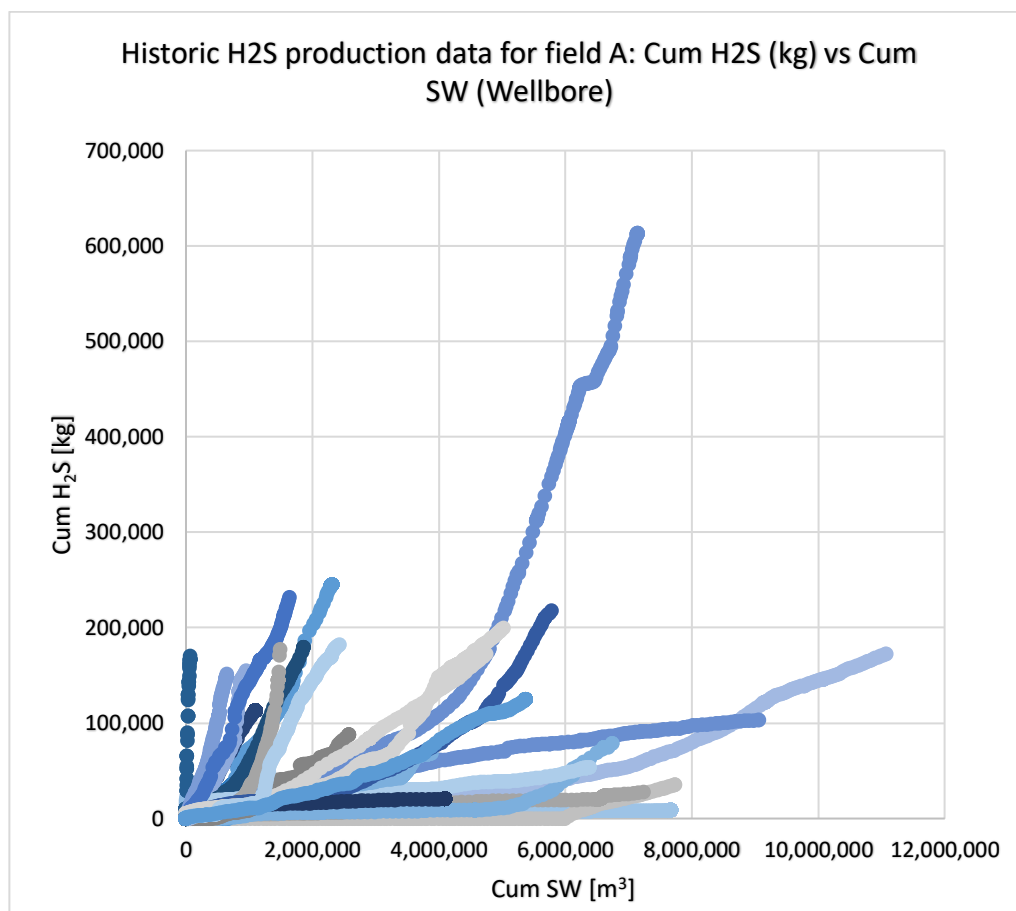

Figure 5.2: Historical cumulative H₂S production data

Based on the development and shape of the cumulative H_2S production profiles, the wellbores on field A can be categorized into three distinct categories:

I. **Type 1**: These are the wellbores that occupy the first third of Figure 5.2. They are characterized by low cumulative seawater volumes ($<2,000,000$ m^3) with a corresponding moderate to high cumulative H_2S production ($100,000$ - $200,000$ kg). The main identifying feature is the early H_2S breakthrough. Possible reasons for early H_2S breakthrough:

    -   This early souring phenomenon may be due to mixing-zone souring generation mechanism in early production wells with VFA in the formation water
    -   Perforation in contaminated reservoir zones
    -   Short distance between the production and injection wells (minor communication routes) that reduces the surface area for adsorption.
    -   No adsorption by formation rock.

II. **Type 2**: These are wellbores that occupy the central part of Figure 5.2 . They are characterized by moderate to high cumulative seawater volumes ($2,000,000$ - $6,000,000$ m^3) with a corresponding moderate to high cumulative H_2S production ($100,000$-$200,000$ kg). One of the wellbores has a cumulative H_2S production of about $600,000$kg. They have three distinct features:

    -   Slow increase in H_2S production: The initial delay in exponential increase of H_2S may be due to longer distances between the injector and producers or the adsorption of H_2S by formation rock (traces of pyrite found in the core samples). The larger the distance, the larger the surface area for adsorption of H_2S. Indicative of the lag phase in microbiological H_2S production
    -   Rapid increase in H_2S production: Indicative of the exponential phase in microbiological H_2S production. This may be due to saturation of mineral scavenging capacity of the formation rock
    -   Constant increase in H_2S production: Indicative of the stationary phase in microbiological H_2S production. This may be due to the lack of increase in nutrient supply

III. **Type 3**: These are wellbores that occupy the last third of Figure 5.2. They are characterized by high cumulative seawater volumes ($4,000,000$ - $11,000,000$ m^3) with low cumulative H_2S production ($8,000$ - $100,000$ kg). The main distinct feature in these wellbores is the extended period of slow H_2S production (lag phase) after H_2S breakthrough. This may be because of long distance between injection and production wells (increasing surface area for adsorption in the reservoir) or low distribution of H_2S in the formation from which the well is producing.

5.2.2 Model fitting and prediction of future H$_2$S production in chosen wellbores

In this section, the mathematical models discussed in chapter 4 will be used to predict the cumulative H$_2$S production in the produced seawater in 6 wellbores producing from field A. The method involves:

- Picking the data of cumulative H$_2$S and SW from the H$_2$S calculator
- Identifying the data where H$_2$S > 0
- Plotting historical data for each of the chosen wellbores by plotting cumulative H$_2$S against cumulative SW
- Fitting the mathematical models: PW-Linear model and exponential model
- Using the average rate of past one year by fitting a linear trendline to predict the rate of H$_2$S produced in SW [g/m^3] one year into the future

5.2.3 Results for individual wellbores

Each subsection below shows the predictions for the future of that wellbore. The first figure shows the historical data of that wellbore and the mathematical model fit curves. The exponential equation input is summarized in Table 5.1 below:

Table 5.1: Exponential model input for field application

Exponential model: Eq.4.17	
Parameter	**Value**
m	0.2 [kg/m^3]
V$_{ref}$	Unique to each wellbore
K1	0.1
K2	5.4E+11
K3	-8.8

The only changing parameter is V$_{ref}$ since the H$_2$S breakthrough is different for each of the wellbores. Since the cumulative H$_2$S production profile for each wellbore is unique, the PW-Linear model has different parameters, a1, b1 and b2. The blue markers represent the historical data of the wellbore, the green markers represent the PW linear model and the purple markers represent the exponential model.

The second figure should be interpreted as follows: The blue data points represent the historical souring index data and the green and purple data points represent the PW-linear model predictions and the exponential model predictions respectively.

Figure 5.3: Well 1 historical data and model fit

Description: Based on the historical data from well 1 (Figure 5.3), the cumulative H₂S production profile matches that described as a type 2 wellbore. This is because it has an initial linear slope indicating a slow increase in cumulative H₂S. This is followed by an exponential phase indicating a rapid increase in cumulative H₂S. After the exponential phase, the increase in cumulative H₂S becomes linear again, however the increase is steeper than the initial linear stage. This is also observed in Figure 5.4 where the degree of souring is delayed after injected sea water breakthrough before a gradual increase in souring later. This could be indicative of the biofilm souring model where H₂S generation is supported by biodegradation of oil components.

Model comparison: Both models are observed to fit the historical data very well. The squared correlation coefficient was 0.9874 for the PW-Linear model and 0.9976 for the exponential model. The exponential model had a superior fit for well 1.

Prediction: Well 1 exhibits a stable souring (constant value) trend for the last 1 year before prediction. The last recorded value is 200.15 g/m^3. Figure 5.4 shows that the PW-Linear model predicts a souring index of 152 g/m^3 whereas the exponential model predicts a souring index of 196.9 g/m^3. Based on the model fit, the exponential model gives a fairly reasonable prediction.

Figure 5.4: One-year prediction for well 1 H₂S production rate [g/m³ of SW]
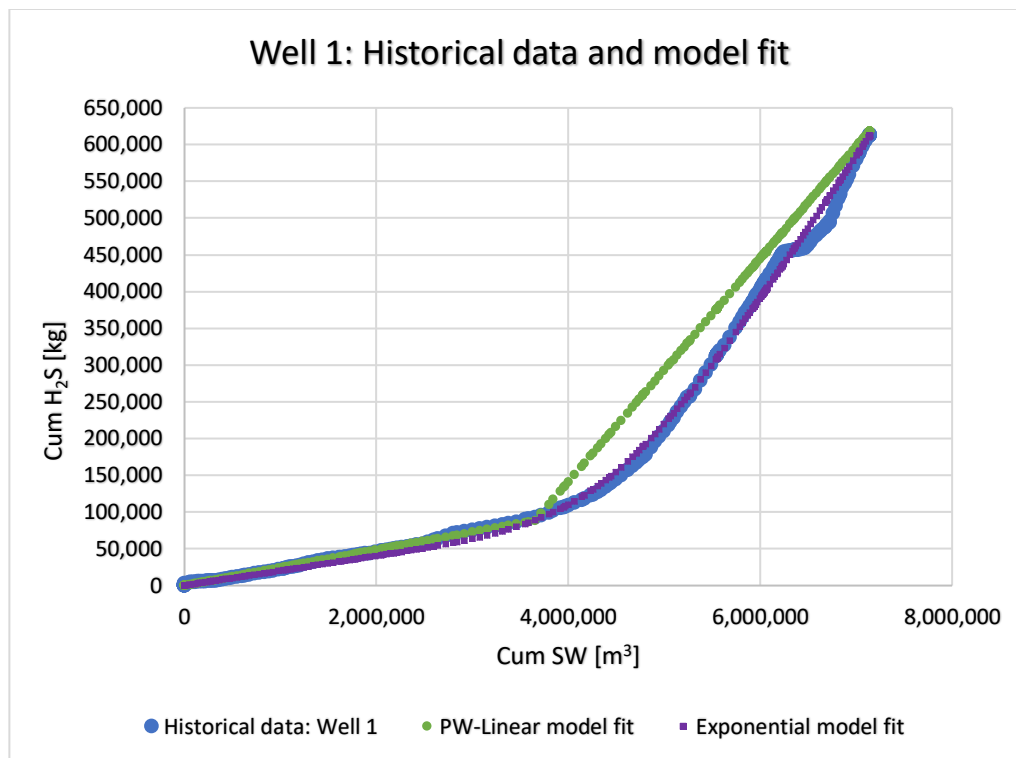
5.2.3.2 Well 2

Figure 5.5: Well 2 historical data and model fit

Description: Based on the historical data from well 2 (Figure 5.5), the cumulative H_2S production profile matches that described as a type 1 wellbore. This is because of the early H_2S breakthrough (H_2S is observed before SW breakthrough).

Model comparison: Both models are observed to fit the historical data very well. The squared correlation coefficient was 0.9935 for the PW-Linear model and 0.9811 for the exponential model. The PW-linear model had a superior fit for well 2.

Prediction: Well 2 exhibits a decreasing souring trend for the last six months. The last recorded value before prediction is 90.17 g/m^3. Figure 5.6 shows that the PW-Linear model predicts a souring index of 89.1 g/m^3 whereas the exponential model predicts a souring index of 157.5 g/m^3. Based on the model fit and the trend before prediction, the PW-Linear model gives a fairly reasonable prediction.

Figure 5.6: One-year prediction for well 2 H₂S production rate [g/m³ of SW]

5.2.3.3 Well 3

Figure 5.7: Well 3 historical data and model fit

Description: Based on the historical data from well 3 (Figure 5.7), the cumulative H_2S production profile matches that described as a type 1 wellbore. This is because of the early H_2S breakthrough (H_2S is observed before SW breakthrough).

Model comparison: Both models are observed to fit the historical data very well. The squared correlation coefficient was 0.9927 for the PW-Linear model and 0.9821 for the exponential model. The PW-linear model had a superior fit for well 3.

Prediction: Well 3 has an unstable souring trend (increasing and decreasing) for the last one year before prediction. However, the last 2 months before show a decreasing trend where the last recorded value is 493.79 g/m^3. Figure 5.8 shows that the PW-Linear model predicts a souring index of 80 g/m^3 whereas the exponential model predicts a souring index of 147.4 g/m^3.
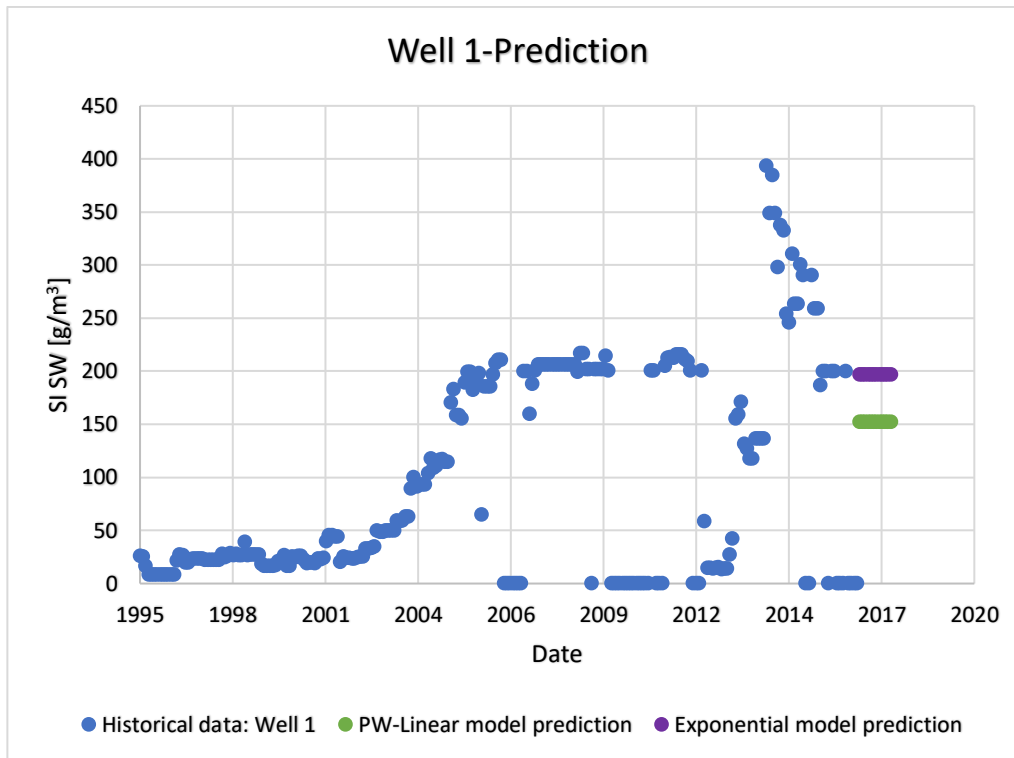
Figure 5.8: One-year prediction for well 3 H₂S production rate [g/m³ of SW]
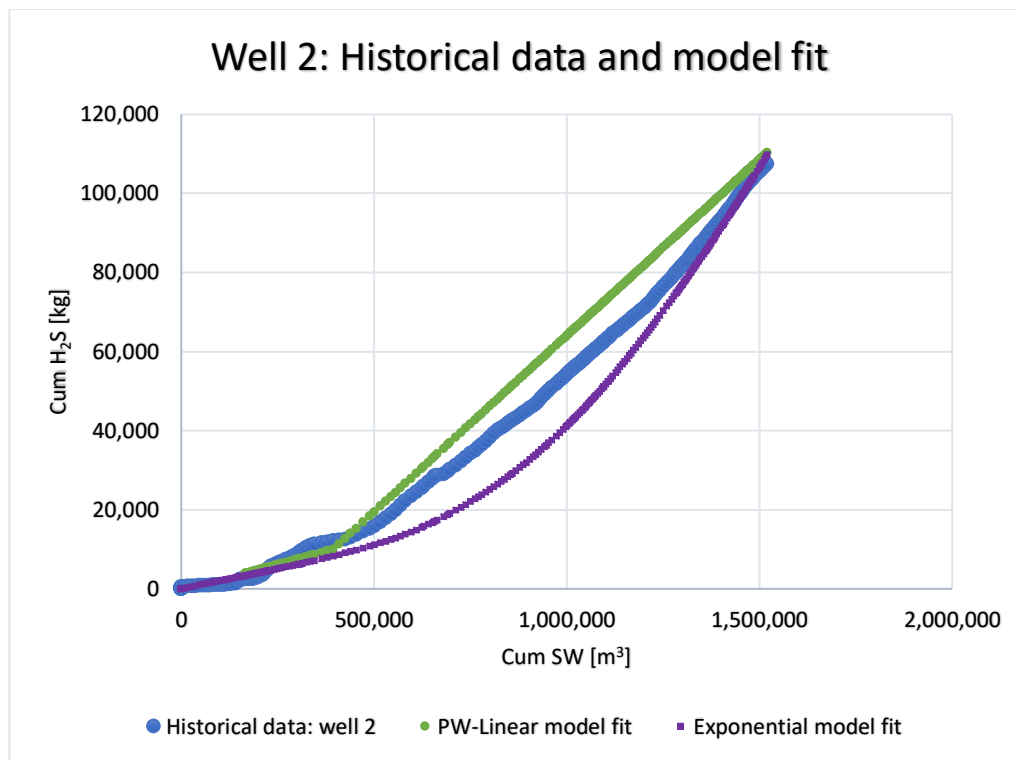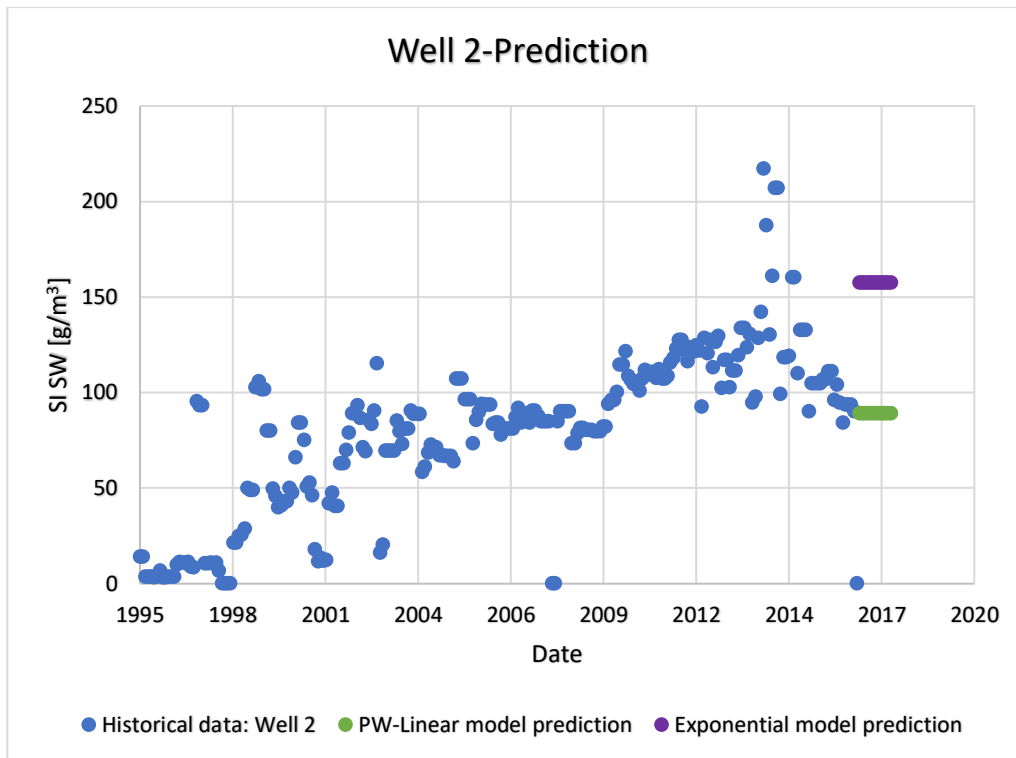
5.2.3.4 Well 4

Figure 5.9: Well 4 historical data and model fit

Description: Based on the historical data from well 4 (Figure 5.9), the cumulative H$_2$S production profile matches that described as a type 1 wellbore. This is because of the early H$_2$S breakthrough. This is also observed in Figure 5.10 where the is a peak in souring index in seawater after H$_2$S breakthrough. This is indicative of the mixing model souring where an initial rise in souring is associated with the initial breakthrough of injected seawater to the producing wells and supported by short chain organic acids or sparingly water-soluble components from the formation water.

Model comparison: Both models are observed to fit the historical data very well. The squared correlation coefficient was 0.9989 for the PW-Linear model and 0.9813 for the exponential model. The PW-linear model had a superior fit for well 4.

Prediction: Well 4 exhibits an unstable souring trend for the last year before prediction. However, the last two months before prediction show a decreasing trend where the last recorded value before prediction was 149.84 g/m^3. Figure 5.10 shows that the PW-Linear model predicts a souring index of 134.1 g/m^3 whereas the exponential model predicts a souring index of 187.2 g/m^3. Based on the model fit and the trend before prediction, PW-Linear model seems to give reasonable prediction.

Figure 5.10: One-year prediction for well 4 H₂S production rate [g/m³ of SW]
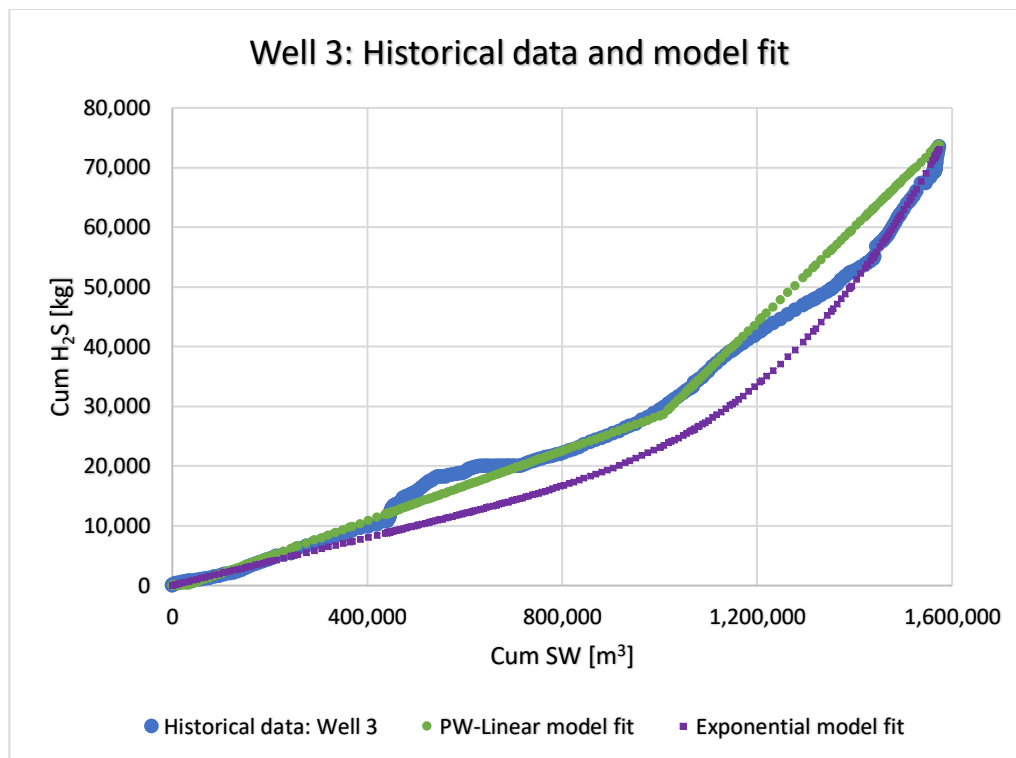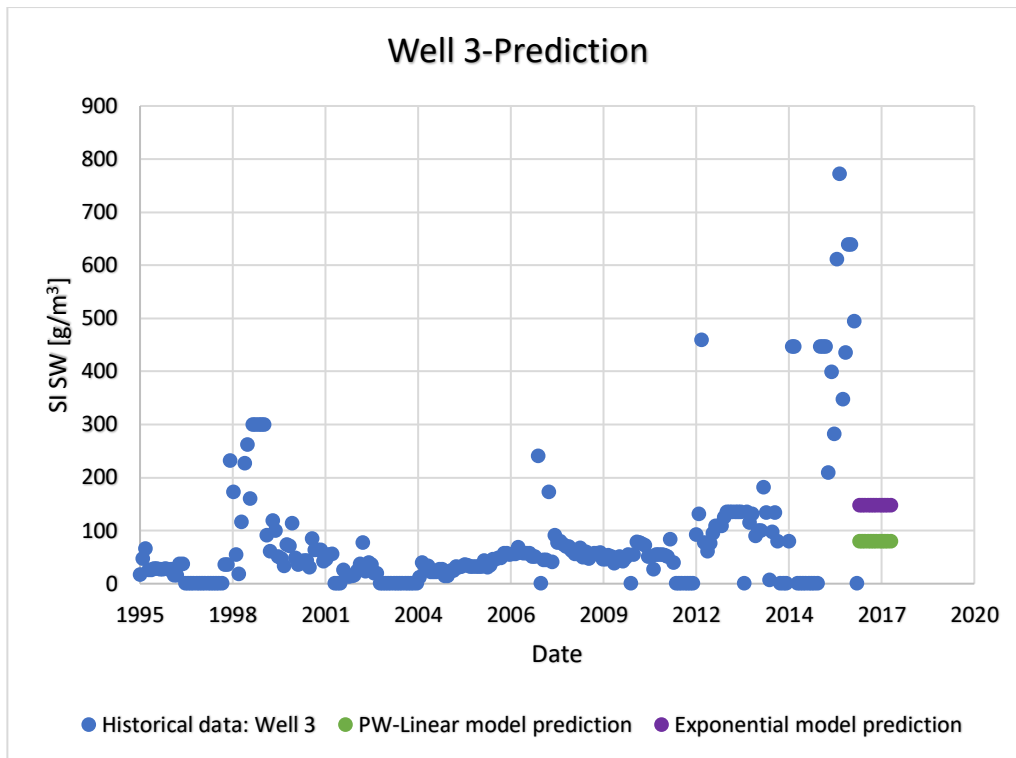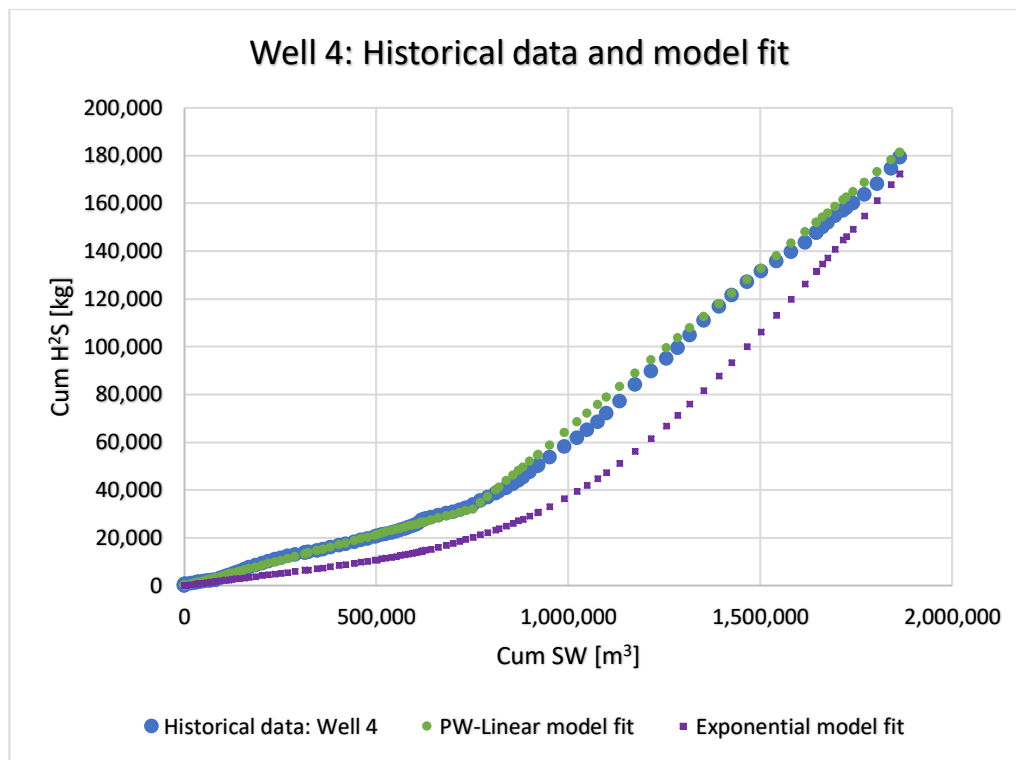
5.2.3.5 Well 5

Figure 5.11: Well 5 historical data and model fit

Description: Based on the historical data from well 5 (Figure 5.11), the cumulative H_2S production profile matches that described as a type 2 wellbore. This is because it has an initial linear slope indicating a slow increase in cumulative H_2S. This is followed by an exponential phase indicating a rapid increase in cumulative H_2S. After the exponential phase, the increase in cumulative H_2S becomes linear again, however the increase is faster than the initial linear stage.

Model comparison: Both models are observed to fit the historical data very well. The squared correlation coefficient was 0.9695 for the PW-Linear model and 0.9965 for the exponential model. The exponential model had a superior fit for well 5.

Prediction: Well 5 exhibits an unstable souring trend the last year before prediction, however the last two months before prediction show a decreasing trend. The last recorded value before prediction was 221.35 g/m^3. Figure 5.12 shows that the PW-Linear model predicts a souring index of 155.6 g/m^3 whereas the exponential model predicts a souring index of 199.1 g/m^3. Based on the model fit and the trend before prediction, the exponential model gives a fairly reasonable prediction.
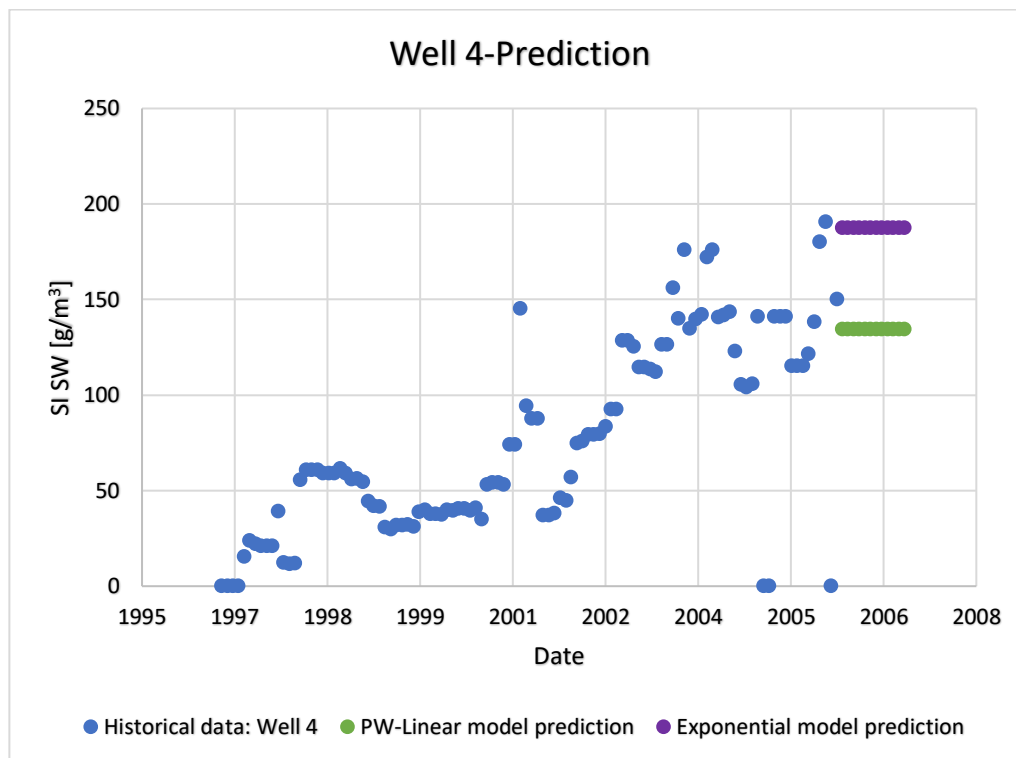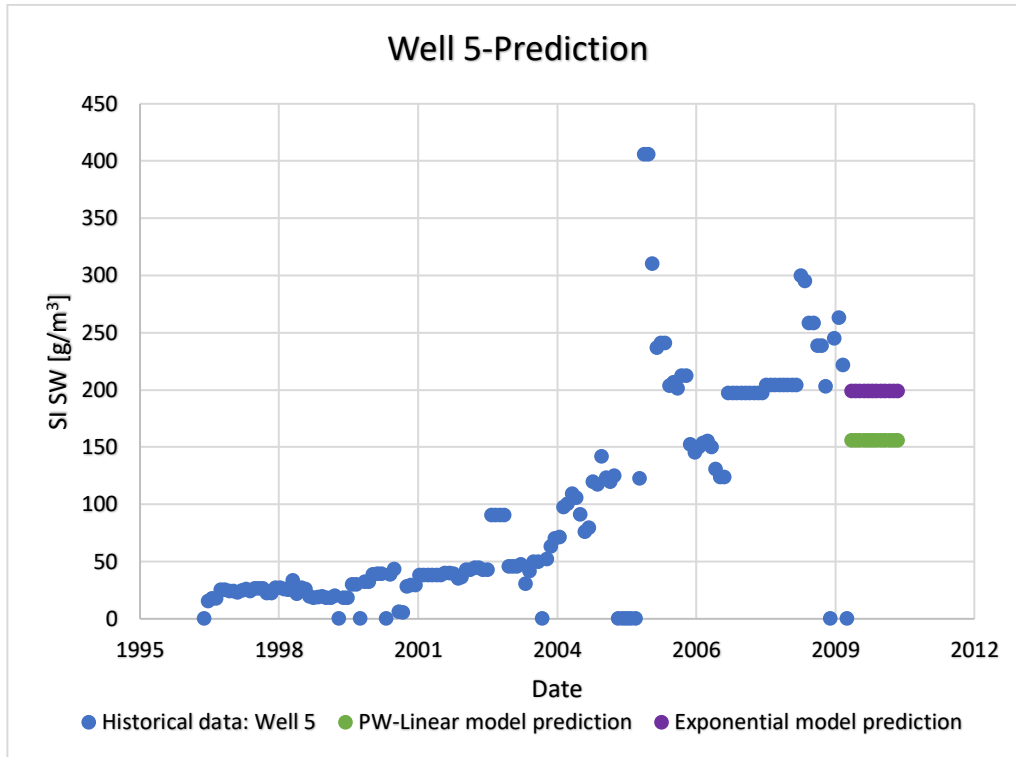
Figure 5.12: One-year prediction for well 5 H₂S production rate [g/m³ of SW]

5.2.3.6 Well 6

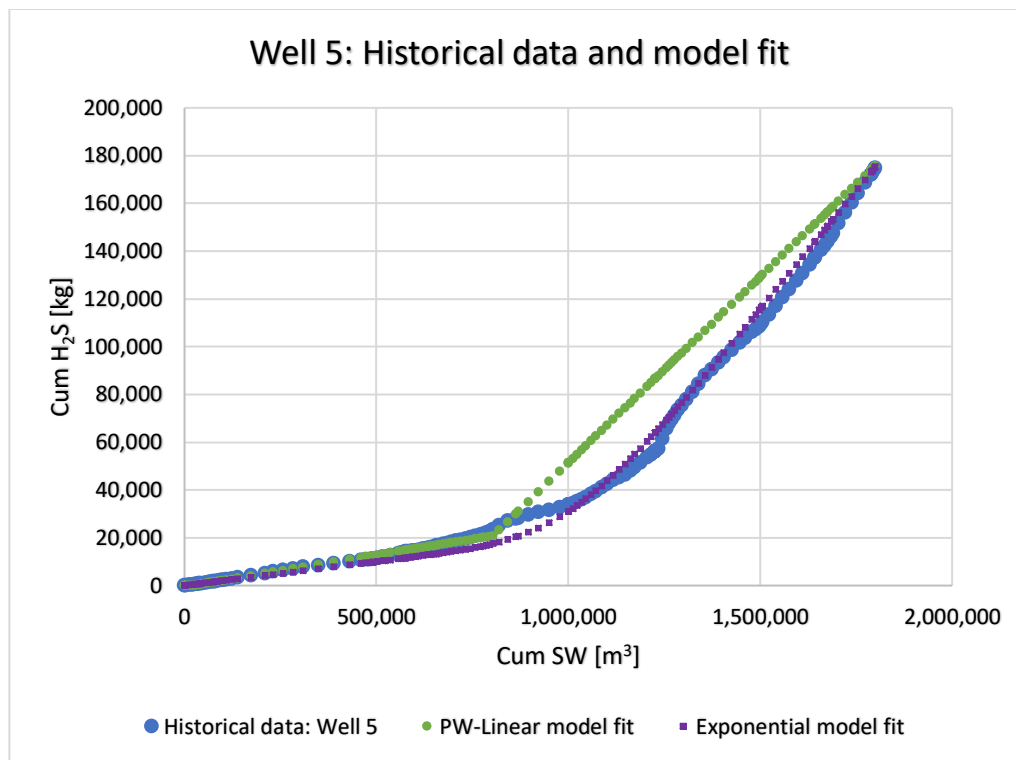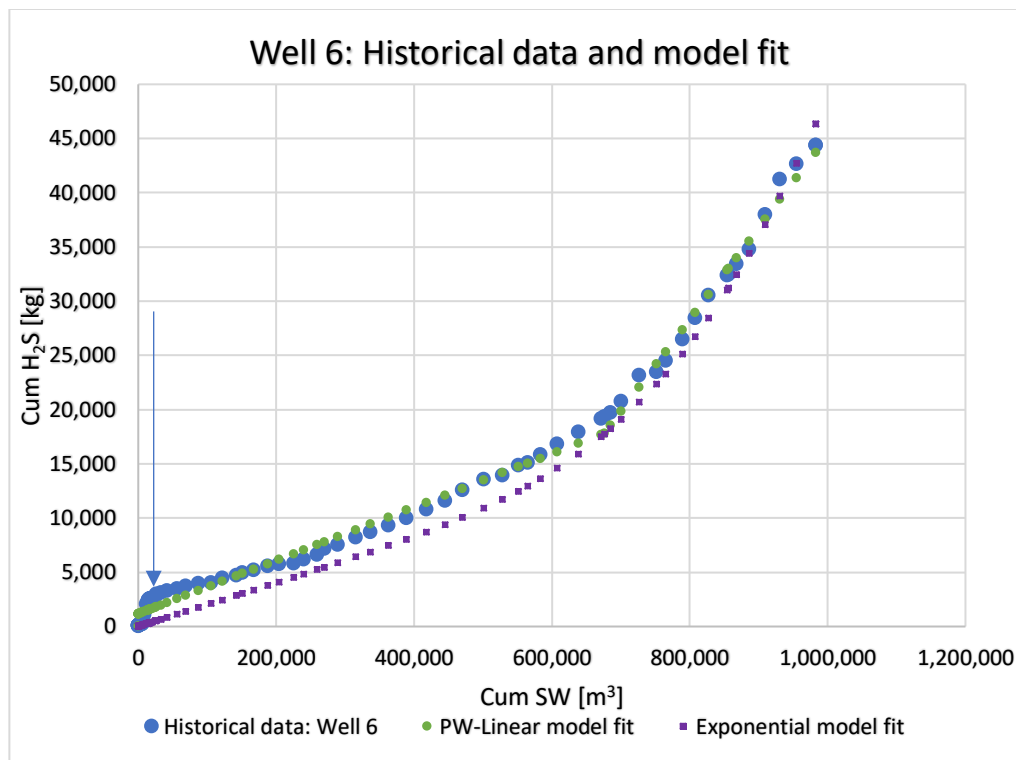*Figure 5.13: Well 6 historical data and model fit*

Description: Based on the historical data from well 6 (Figure 5.13), it is difficult to define the type of wellbore. The initial stages of production show a rapid rise in H₂S production. This may be the effect of the wellbore being perforated in a contaminated region. Additionally, the cumulative H₂S production values are low compared to the other wells, more data is needed for a more comprehensive description of the wellbore. From Figure 5.14 it can be observed that the wellbore undergoes a combination of the mixing model souring and the biofilm model souring. An initial rise in souring associated with the initial breakthrough of injected seawater, followed by a decrease and then a gradual increase.

Model comparison: Both models are observed to fit the historical data very closely. The squared correlation coefficient was 0.9951 for the PW-Linear model and 0.9941 for the exponential model.

Prediction: Well 6 exhibits an unstable souring trend the last year before prediction. The last recorded value before prediction was 53.21 g/m³. Figure 5.14 shows that the PW-Linear model predicts a souring index of 84.6 g/m³ whereas the exponential model predicts a souring index of 108.1 g/m³.
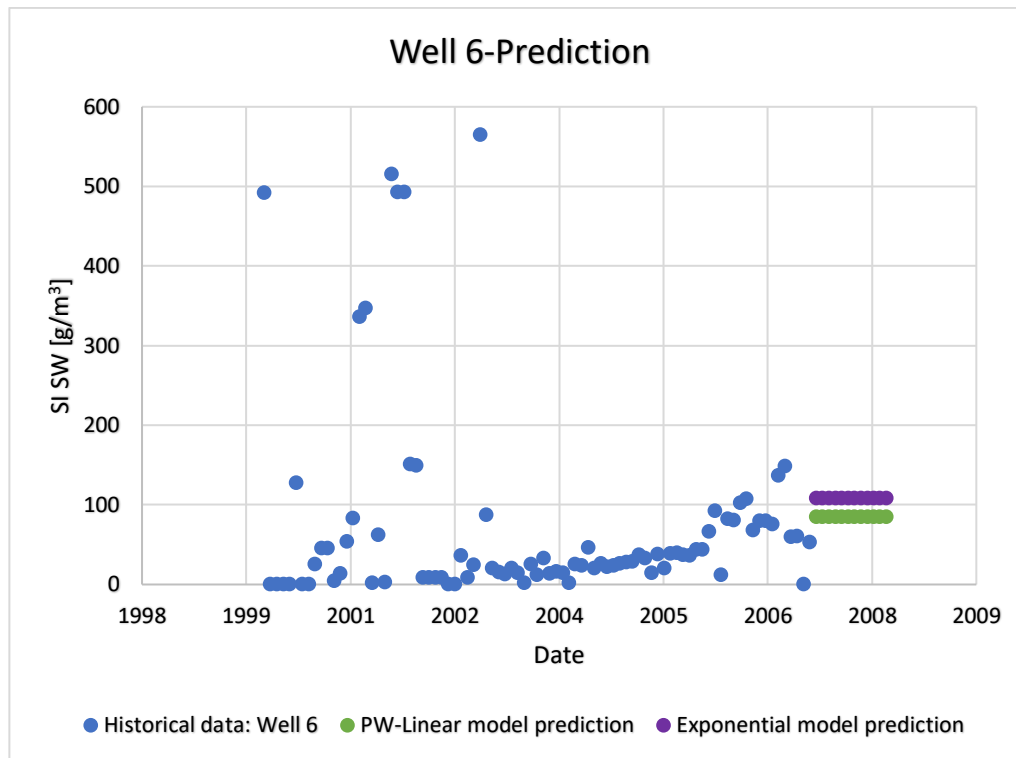
Figure 5.14: One-year prediction for well 6 H₂S production rate [g/m³ of SW]

5.2.4 Results summary: Mathematical models performance on Field A wellbores

Both mathematical models allow a reasonably accurate estimate of the expected production rate of H_2S (g per m^3 of seawater) on wellbores on Field A. For wellbores such as well 2 where the models do not fit the whole historical data curve, fitting the last part of the curve is given priority. This enables extrapolation of the model curve to give predictions of cumulative H_2S production.

The exponential correlation is fairly easy to use. The only parameter that needs to be changed is the V_{ref} which is unique for every wellbore. However, it tends to overestimate the production rate of H_2S in produced seawater in type 1 wells. Type 1 wellbores are observed to start H2S production immediately. For such kinds of wells, $V_{ref} = CumL_{first\_H2S} = 0$. As a result, a minimum reference volume needs to be defined for the exponential model to be able to match the cumulative H_2S production of the wellbores [44]. For wellbore types exhibiting this behaviour in field A, a minimum reference volume of the order of magnitude 100,000 – 200,000 m^3 has been recommended based on the study done by Meisingset [44].

The piecewise model is also very easy to use since the only input data that is used to obtain the cumulative H₂S production is the cumulative seawater. Unlike the other model, no fluid data (cumulative oil and cumulative formation water) is needed. The model tends to underestimate the production rate of H₂S in produced seawater in type 2 wells, but this can be remedied by moving the breakpoint, c, between the linear curves. The summary of these results is given in Table 5.2.

Factors that are considered helpful in reducing uncertainty during model evaluation include: 1) availability of adequate historical data from field A (mature field with a long souring history); 2) accepted theory regarding the microbiological reservoir souring and how this affects the shape of the cumulative H₂S production curve when plotted against cumulative produced seawater; 3) data selection included wellbores with varying production profile e.g. Well 6 which displayed both type 1 and 2 characteristics.

Table 5.2: Summary of results from the PW-Linear and Exponential H₂S prediction models [1]

Wellbore	Type	SST	SSR		R^2	
			PW-Linear	**Exponential**	**PW-Linear**	**Exponential**
Well 1	Type 2	1.19E+13	1.5E+11	2.82E+10	0.9874	0.9976
Well 2	Type 1	4.02E+11	2.61E+09	7.59E+09	0.9935	0.9811
Well 3	Type 1	1.46E+11	1.07E+09	2.61E+09	0.9927	0.9821
Well 4	Type 1	3.25E+11	3.22E+08	6.07E+09	0.9989	0.9813
Well 5	Type 2	4.05E+11	1.23E+10	1.42E+09	0.9695	0.9965
Well 6	Type -	1.28E+10	6.29E+07	7.59E+07	0.9951	0.9941

1

- SSR: Residual sum of squares
- SST: sum of square total
- $R^2 = 1 - \frac{SSR}{SST}$

Chapter 6 : Conclusion and Future Work

6.1 Conclusion

The aim of this thesis was to develop a mathematical model that could be used to predict the amount of H$_2$S produced in seawater. Several tasks were undertaken to achieve this goal. Firstly, a synthetic reservoir model was created using ECLIPSE simulator tracer tracking option to obtain a cumulative H$_2$S production profile by plotting cumulative H$_2$S against cumulative produced seawater.

The reproduced H$_2$S production profile assumed that there exists a biofilm around the injector that generates H$_2$S which is then transported to the producer by the injected seawater. The production profile reproduced had three distinct phases; Phase 1: slow increase in amount of H$_2$S produced in the seawater (linear relationship). Phase 2: rapid increase in amount of H$_2$S produced in seawater (exponential relationship). Phase 3: concentration of H$_2$S produced in biofilm has reached a maximum. This part of the curve shows a linear dependency between the produced cumulative H$_2$S and the produced cumulative seawater.

Secondly, the developed mathematical models were tested on the synthetic reservoir model results. The evaluation of the models was done using the square correlation coefficient R^2. Based on the results of the regression analysis and the model fit, it was concluded that the models gave a good representation of the observed data from the simulated synthetic model.

Thirdly, having tested the mathematical expressions and optimized the parameters, they were then applied to wellbore plots of H$_2$S data from an anonymous field on the North Sea. The summary of the results is given in Table 5.2. The cumulative H$_2$S production profiles observed from the wellbores were categorized into three types. Based on the results from the regression analysis done on the model fit to observed data on each of the wellbores, it can be concluded that the PW-Linear model gave a superior fit of type 1 wellbores whereas the exponential model gave a superior fit of type 2 wells.

Lastly, the mathematical models were used to generate a prediction for the rate of H$_2$S (g/m^3 of produced seawater). The prediction results can be very useful for production management of both producing and new infill wellbores. This includes developing H$_2$S control and

mediation strategies to increase the value of production assets, decrease operational costs and prevent production loss because of shut-in wells.

6.2 Future Work

Due to lack of time and the need for clarity when testing the models, wellbore cumulative H$_2$S prediction was limited to type 1 and type 2 wells. Further experimentation and analysis into the performance of the models has been left to future work. The following ideas could be tested:

1. Further development of the exponential model to fit type 1 and 3 wells: The exponential model can also model type 1 and 3 wellbores more precisely. This would require finding a new set of constants, K1, K2 and K3 for each wellbore type [44].

2. Experimentation of the models on other fields: The historical data of the new fields would have to be plotted to observe the cumulative H$_2$S production profile. Do the profiles display the same shape, i.e. type 1, 2 and 3 as described in chapter 5? If the profiles match, test the exponential model with the same set of parameters assigned to each wellbore type. Does the model give a good fit? It is worth noting that a new value for parameter m, the maximum slope of the Cum H$_2$S versus Cum SW curve (maximum amount of H$_2$S (kg) per m^3 of seawater), needs to be established.

3. Application of the model in Spotfire [2] dashboard: Once the models have been tested, the mathematical expressions that describe the exponential model (equation 4.11) and the PW-Linear model (equations 4.16 and 4.17) can be implemented into the Spotfire dashboard [48]. This would enable reservoir and production engineers to quickly survey the cumulative H$_2$S production of multiple wellbores. This would facilitate better decision making when deciding how to best optimize production from the wellbores. Additionally, Spotfire's intuitive and interactive capabilities enable engineers to analyse data faster.

4. Risk and uncertainty analysis assessment: The main objective of this would be to increase transparency and awareness about the importance and implications of the uncertainty. This uncertainty is in various forms:
   a. Measurement uncertainty: This is the uncertainty in the measured H$_2$S at the test separator. This affects the quality of the field data (historical cumulative

---

[2] Spotfire is an analytics platform that can be used in the upstream oil and gas industry as a tool for production analysis [61].

H$_2$S data). Analysis should be done on the uncertainty in measurement of H$_2$S and the errors should be recorded.

b. Model uncertainty: Uncertainty arising from the mathematical representation of the conceptual model (microbiological souring). This has already been dealt with to some degree in this thesis through the assessment of the performance of alternative models to fit historical data and between model predictions.

c. Scenario uncertainty: This includes uncertainty in the environmental properties. These properties, such as conditions in the reservoir, change from time to time. Predictions in this thesis are made under the assumption that the reservoir conditions will remain constant. However, in reality ecosystems can show resilience and non-linearity. Different scenarios should be assessed to check the reliability of the model.

Nomenclature

1D: One Dimensional

2D: Two Dimensional

3D: Three Dimensional

BHP: Bottom hole Pressure

E&P: Exploration and Production

FA: Fluorescent Antibody

FTPT: Field Tracer Production Total

FW: Formation Water

FWPT: Field Water Production Total

GFA: Gullfaks A

GFB: Gullfaks B

GFC: Gullfaks C

GOR: Gas Oil Ratio

H_2S: Hydrogen sulphide

HSE: Health, Safety and Environment

MIC: Microbiologically Induced Corrosion

MMP: Minimum Miscibility Pressure

NPD: Norwegian Petroleum Directorate

NRB: Nitrate Reducing Bacteria

ppmv: Parts Per Million by Volume

ppmw: Parts Per Million by Weight

PVT: Pressure, Volume and Temperature

PW: Produced water

FWPT: Field Water Production Total

R^2: Squared Correlation Coefficient

SI: Souring Index

SIS: Schlumberger Information Services

SRA: Sulphate Reducing Archaea

SRB: Sulphate Reducing Bacteria

SRP: Sulphate Reducing Prokaryote

SSR: Residual sum of squares

SST: Sum of square total

SW: Sea Water

SWC: Sea Water Cut

TDS: Total Dissolved Solids

THP: Tubing Head Pressure

THPS: TetrakisHydroxymethylPhosphonium Sulphate

TVS: Thermal Viability Shell

US: United States

USD: United States Dollar

VFA: Volatile Fatty Acids

WAG: Water Alternating Gas

WOR: Water Oil Ratio

Sources

1. Ahmed, T. (2001). Reservoir Engineering Handbook (2nd edition), Principles of Waterflooding, Gulf Professional Publishing.

2. Bernardez, L. A.,et al. (2012). A Kinetic Analysis of Microbial Sulphate Reduction in An Upflow PackedBed Anaerobic Bioreactor." Mine Water and the Environment 31.1, 62-68

3. Buckley, S. E., & Leverett, M. C. (1942). Mechanism of Fluid Displacement in Sands. Society of Petroleum Engineers. doi:10.2118/942107-G

4. Burger, D., & Jenneman, E. (2009). Forecasting the Effects of Reservoir Souring from Waterflooding a Formation Containing Siderite. SPE International Symposium on Oilfield Chemistry. Society of Petroleum Engineers.

5. Burger, D., Jenneman, G., & Gao, X. (2013). The Impact of Dissolved Organic-Carbon Type on the Extent of Reservoir Souring. SPE International Symposium on Oilfield Chemistry. Society of Petroleum Engineers.

6. Chen, C. I., Reinsel M. A., & Mueller R. F. (1994). Kinetic Investigation of Microbial Souring in Porous Media Using Microbial Consortia from Oil Reservoirs. Biotechnology and Bioengineering, Vol. 44, No. 3, 263-269.

7. Chen, Ching-I., & Reinsel, M. (1996). Characterization of Microbial Souring in Berea-Sand Porous Medium with a North Sea Oil Field Inoculum. Biofouling 9.3, 175-186.

8. Cohen RRH. (2006). Use of microbes for cost reduction of metal removal from metals and mining industry waste streams. J. of Cleaner Production 14, 1146-1157.

9. Corrin, E., Harless, M., Rodriguez, C., Degner, D. L., & Archibeque, R. (2014). Evaluation of a More Environmentally Sensitive Approach to Microbiological Control Programs for Hydraulic Fracturing Operations in the Marcellus Shale Using a Nitrate-Reducing Bacteria and Nitrate-Based Treatment System. Society of Petroleum Engineers. doi:10.2118/170937-MS.

10. Dake, L. P. (1994). The practice of reservoir engineering. Amsterdam: Elsevier.

11. Davis, R. A., & McElhiney, J. E. (2002). The Advancement of Sulphate Removal from Seawater in Offshore Waterflood Operations. NACE International.

12. De Siqueira, A. G., Araujo, C. H. V., Reksidler, R., & Pereira, M. de C. (2009). Uncertainty Analysis Applied to Biogenic Reservoir Souring Simulation. Society of Petroleum Engineers. doi:10.2118/121175-MS.

13. Eden, B., Laycock, P.J., & Fielder, M. (1993). Oilfield Reservoir Souring. HSE Books.

14. Engelbrektson, Anna, et al. (2014). Inhibition of Microbial Sulphate Reduction in a Flow-Through Column System By (Per) Chlorate Treatment. Frontiers in Microbiology 5, 315

15. Ertekin, T., Kassem, J.H., & King, G. R. (2001). "Introduction" In "Basic Applied Reservoir Simulation" Vol. 7 (SPE Textbook Series), Society of Petroleum Engineers Inc., Richardson, Texas.

16. Evans, P., & Dunsmore, B. (2006). Reservoir Simulation of Sulphate Reducing Bacteria Activity in the Deep Sub-Surface. NACE International.

17. Evans, P., Nederlof, E., & Richmond, W. (2015). Souring Development Associated with PWRI in a North Sea Field. Society of Petroleum Engineers. doi:10.2118/174529-MS

18. Evans, R. (2001). Factors Influencing Sulphide Scale Generation Associated with Waterflood Induced Reservoir Souring. Society of Petroleum Engineers. doi:10.2118/68337-MS

19. Fanchi, R. J. (2006) Chapter 4 - Fluid Displacement, In Principles of Applied Reservoir Simulation (Third Edition), Gulf Professional Publishing, Burlington, Pages 51-64, ISBN 9780750679336.https://doi.org/10.1016/B978-075067933-6/50006-4. (https://www.sciencedirect.com/science/article/pii/B9780750679336500064)

20. Fanchi, R. J. (2006). PRINCIPLES OF APPLIED RESERVOIR SIMULATION, 3rd ed.

21. Gilman, J. R., & Ozgen, C. (2013). Reservoir Simulation: History Matching and Forecasting. Richardson, Texas, SPE.

22. Greene, E. A., et al. (2003). Nitrite Reductase Activity of Sulphate-Reducing Bacteria Prevents their Inhibition by Nitrate-Reducing, Supplied-Oxidizing Bacteria. Environmental Microbiology 5.7, 607-617.

23. Grigoryan, A. A., Cornish, S. L., Buziak, B., Lin, S., Cavallaro, A., Arensdorf, J. J., & Voordouw, G. (2008). Competitive Oxidation of Volatile Fatty Acids by Sulphate- and Nitrate-Reducing Bacteria from an Oil Field in Argentina. Applied and Environmental Microbiology, 74(14), 4324–4335. http://doi.org/10.1128/AEM.00419-08.

24. Guan, L., & Du, Y. (2004). Will Tracer Move the Same Velocity as Its Carrier? Society of Petroleum Engineers. doi:10.2118/89956-MS

25. H. Kleppe., (2007). Reservoir Simulation. University of Stavanger

26. Haghshenas, M., Sepehrnoori, K., Bryant, S. L., & Farhadinia, M. (2012). Modeling and Simulation of Nitrate Injection for Reservoir-Souring Remediation. Society of Petroleum Engineers. doi:10.2118/141590-PA.

27. Håland, K., Barrufet, M. A., Rønningsen, H. P., & Meisingset, K. K. (1999). An Empirical Correlation Between Reservoir Temperature and the Concentration of Hydrogen Sulfide. Society of Petroleum Engineers. doi:10.2118/50763-MS.

28. Huseby, O., Chatzichristos, C., Sagen, J., Muller, J., Kleven, R., Bennett, B., Larter, S.R., Stubos, A.K. & Adler, P.M. (2005). Use of natural geochemical tracers to improve reservoir simulation models. Journal of Petroleum Science and Engineering. 48. 241-253. 10.1016/j.petrol.2005.06.002.

29. Islam, M. R., Mousavizadegan, S., Mustafiz, S., & Abou-Kassem, J. H. (2010). Reservoir Simulation Background. In Advanced Petroleum Reservoir Simulations (eds M. R. Islam, S. Mousavizadegan, S. Mustafiz and J. H. Abou-Kassem). doi:10.1002/9780470650684.ch1

30. Jenneman, G. E., Moffitt, P. D., Baja, G. A., & Webb, R. H. (1997). Field Demonstration of Sulfide Removal in Reservoir Brine by Bacteria Indigenous to a Canadian Reservoir. Society of Petroleum Engineers. doi:10.2118/38768-MS

31. Johnson, R.J., Folwell, B.D., Wirekoh, A., Frenzel, M., & Skovhus, T.L. (2017). Reservoir Souring - Latest developments for application and mitigation. Journal of Biotechnology.

32. Jones, C., Downward, B., Edmunds, S., Hernandez, K., Curtis, T., & Smith, F. (2011). A Novel Approach to Using Thps For Controlling Reservoir Souring. NACE International.

33. Jong T., & Parry, D.L. (2006). Microbial sulphate reduction under sequentially acidic conditions in an upflow anaerobic packed bed bioreactor. Water Research 40, 2561-2571.

34. Jordan, L. C., & Walsh, J. M. (2004). Selection of an Active Souring Management Solution for a Gulf of Mexico Waterflood. NACE International.

35. Kalpakci, B., Magri, N. F., Ravenscroft, P. D., McTeir, M. D. K., & Arf, G. T. (1995). Mitigation of Reservoir Souring—Decision Process. Society of Petroleum Engineers. doi:10.2118/28947-MS.

36. Kleppe, H. (2007) "Reservoir Simulation," University of Stavanger.

37. Koch G., Varney J., Thompson N., Moghissi O., Gould M., & Payer J, (2016). IMPACT (International Measures of Prevention, Application, and Economics of Corrosion Technologies) Study, Report to NACE by DNVGL and APQC

38. Kolmert, Å. (1999). Sulphate-reducing bacteria in bioremediation processes. Licentiate thesis. Lund University. Sweden.

39. Larsen, J. (2002). Downhole Nitrate Applications to Control Sulphate Reducing Bacteria Activity and Reservoir Souring. NACE International.

40. Li, Li, et al. (2009). Mineral Transformation and Biomass Accumulation Associated with Uranium Bioremediation at Rifle, Colorado. Environmental Science & Technology 43.14, 5429-5435.

41. Ligthelm, D. J., de Boer, R. B., Brint, J. F., & Schulte, W. M. (1991). Reservoir Souring: An Analytical Model for H2S Generation and Transportation in an Oil Reservoir Owing to Bacterial Activity. Society of Petroleum Engineers. doi:10.2118/23141-MS.

42. Mattax, C. C., & Dalton, R. L. (1990). Reservoir Simulation, Vol. 13. Richardson, Texas, USA: Monograph Series, SPE.

43. Maxwell, S., & Spark, I. (2005). Souring of Reservoirs by Bacterial Activity During Seawater Waterflooding. Society of Petroleum Engineers. doi:10.2118/93231-MS.

44. Meisingset, K. K. (2017). Well Correlation for cumulative H2S production. Unpublished Study.

45. Mitchell, A. F., Skjevrak, I., & Waage, J. (2017). A Re-Evaluation of Reservoir Souring Patterns and Effect of Mitigation in a Mature North Sea Field. Society of Petroleum Engineers. doi:10.2118/184587-MS.

46. Myhr, S., et al. (2002). Inhibition of Microbial H2S Production in An Oil Reservoir Model Column by Nitrate Injection. Applied Microbiology and Biotechnology 58.3, 400-408.

47. Myoung-Soo, K et al. (2016). Identification of the Microbes Mediating Fe Reduction in a Deep Saline Aquifer and their Influence During Managed Aquifer Recharge. Science of the Total Environment 545, 486-492.

48. Narzulloev, A. (2018). Dashboard for visualization, evaluation and modelling of wellbore and field H2S production. Master thesis, University of Stavanger.

49. Nilsen, R. K., Beeder, J., Torsvik, T & Thorstenson. (1996). Distribution of thermophilic marine sulphate reducers in the North Sea oil field waters and oil reservoirs. Appl. Environ. Microbiol. 62: 1793-1798.

50. Pieiro, G., Paruelo, M Guerschman, P., & Perelman, S. (2008). How to evaluate models: Observed vs. predicted or predicted vs. observed?

51. Porter, K.G & Feig, Y.S. (1980). The use of DAPI for identifying and counting aquatic microflora. Limnol. Oceanogr.25:943-948.

52. Przybylinski, J. L. (2001). Iron Sulfide Scale Deposit Formation and Prevention under Anaerobic Conditions Typically Found in the Oil Field. Society of Petroleum Engineers. doi:10.2118/65030-MS

53. Rajvanshi, A. K., Meyling, R. G., & Heff, D. (2012). Instilling Realism in Production Forecasting: Dos and Don'ts. Paper SPE-155443-MS presented at the SPE Annual Technical Conference and Exhibition, San Antonio, Texas, USA, 8 – 10 October.

54. Reinsel, M. A., et al. (1996). Control of Microbial Souring by Nitrate, Nitrite or Glutaraldehyde Injection in a Sandstone Column. Journal of Industrial Microbiology 17.2, 128-136.

55. Satter, A., Ghulam, I., & Buchwalter, J. (2007). Practical Enhanced Reservoir Engineering.

56. Schlumberger, (2009). "ECLIPSE Reference Manual"

57. Schlumberger, (2014). "ECLIPSE Reference Manual"

58. Sunde, E., Bodtker, G., Lillebo, B.-L., & Thorstenson, T. (2004). H2S Inhibition by Nitrate Injection on the Gullfaks Field. NACE International.

59. Sunde, E., Thorstenson, T., Torsvik, T., Vaag, J. E., & Espedal, M. S. (1993). Field-Related Mathematical Model to Predict and Reduce Reservoir Souring. Society of Petroleum Engineers. doi:10.2118/25197-MS

60. Thorstenson, T., Sunde, E., Bodtker, G., Lillebo, B.L., Torsvik, T., & Beeder, J. (2002). Biocide Replacement by Nitrate in Sea Water Injection Systems. NACE International.

61. TIBCO, (2017). Spotfire® Professional 7.0.2: User's guide. Retrieved from https://docs.tibco.com/products/tibco-spotfire-professional-7-0-2.ZIP.

62. Vallero, M. (2003). Sulphate reducing processes at extreme salinity and temperature: extending its application window. Licentiate thesis Wageningen University, the Netherlands.

63. Vance, I., & Thrasher, D. (2005). Reservoir Souring: Mechanisms and Prevention, p 123-142. *In* Ollivier B, Magot M (ed), *Petroleum Microbiology*. ASM Press, Washington, DC. doi: 10.1128/9781555817589.ch7.

64. Yuan, X., & Voordouw, G. (2015) Control of Microbial Sulfide Production with Biocides and Nitrate in Oil Reservoir Simulating Bioreactors Frontiers in Microbiology 6, 1387

65. Zhao, C., Hobbs, B. E., & Ord, A. (2013). Effects of Medium Permeability Anisotropy on Chemical-Dissolution Front Instability in Fluid-Saturated Porous Media. Transport in Porous Media,99(1), 119-143. doi:10.1007/s11242-013-0177-3.

Appendix A : Reservoir Simulation

Reservoir simulation is a powerful tool that can be applied by reservoir engineers and has become the industry standard for solving reservoir engineering problems. It can be used to predict reservoir performance under a variety of operating strategies through a combination of multiple disciplines such as; physics, mathematics, geology, reservoir engineering and computer programming. Modern reservoir simulators are computer programs designed to model fluid flow in porous media. The reservoir engineer then uses the results of these models to develop and optimize reservoir management strategies. Some advantages and disadvantages are given in the table below:

Table A.1: Advantages and disadvantages of reservoir simulation

Advantages of Reservoir Simulation	**Disadvantages of Reservoir Simulation**
Analytical limitations of simpler methods are overcome.	Modelling requires a significant amount of reasonable data
Data variation within a reservoir can be applied; homogeneity is not a requirement.	Modelling requires a significant amount of knowledgeable manpower and time.
The effect of uncertainty in the reservoir description can be analysed with sensitivity testing.	Results are not unique, i.e. the same answer can be obtained by varying several different parameters.
After matching history, many different methods of operating the reservoir in the future can be investigated and an optimum plan of the reservoir management can be formulated.	Simulation has limitations that a casual user/observer may not fully comprehend.
Continual performance monitoring is available.	Cost of software/hardware required are greater than analytical methods.
Computational burden is reduced for the engineer and the additional time is available for analysing results.	
A common tool is employed in arbitration and unitization decisions.	

A.1 Model Input

To be able to create a model, data must be acquired and evaluated with a focus on its quality and the identification of relevant drive mechanisms. Some of the data that is required can be found from existing reports. Some of the reports that can be reviewed include geophysical,

geological, petrophysical and engineering reports. Table A.2 describes some of the properties needed and how they can be found.

Table A.2: Data required for simulation study [20]

Property	Sources
Permeability	Pressure transient testing, Core analyses, Correlations, Well performance
Porosity and Rock compressibility	Core analyses, Well logs
Relative permeability and capillary pressure	Laboratory core flow test
Saturations	Well logs, Core analyses, Pressure cores, Single well tracer tests
Fluid property (PVT) data	Laboratory analyses of reservoir fluid samples
Faults, boundaries, fluid contacts	Seismic, Pressure transient testing
Aquifers	Seismic, Material balance calculations, Regional exploration studies
Fracture spacing, orientation, connectivity	Core analyses, Well logs, Seismic, Pressure transient tests, Interference testing, Wellbore performance
Rate and pressure data, completion and workover data	Field performance history

Petrophysical data like permeability and porosity exhibit strong heterogeneities. As a result, the reservoir is divided into grid blocks with different properties in order to simulate the variations. Furthermore, the grid is needed for numerical computations.

A.2 Black-Oil Models

The Black-oil model is the simplest and most commonly used model for reservoir simulation. It is a model that describes multiphase flow with mass interchange between the phases in a porous medium. It can predict compressibility and mass transfer effects. This is the model used for the reservoir simulations carried out in this paper. This model is based on some assumptions:

- Three phases are present in the reservoir; oil, gas and water.
- Three components are present; oil, gas and water. The oil components (stock-tank oil) is the residual liquid at the atmospheric pressure left after a differential vaporization while the gas component is the dissolved gas in the oil phase and the free gas in the reservoir. (Figure A.1).
- No phase transfer between water and hydrocarbons takes place.

- Part of the gas component can be dissolved in the oil phase and flow together with the oil component in the oil phase.
- All of the oil component is in the oil phase, i.e. it cannot exist in the gas phase.
- Temperature in the reservoir is constant.
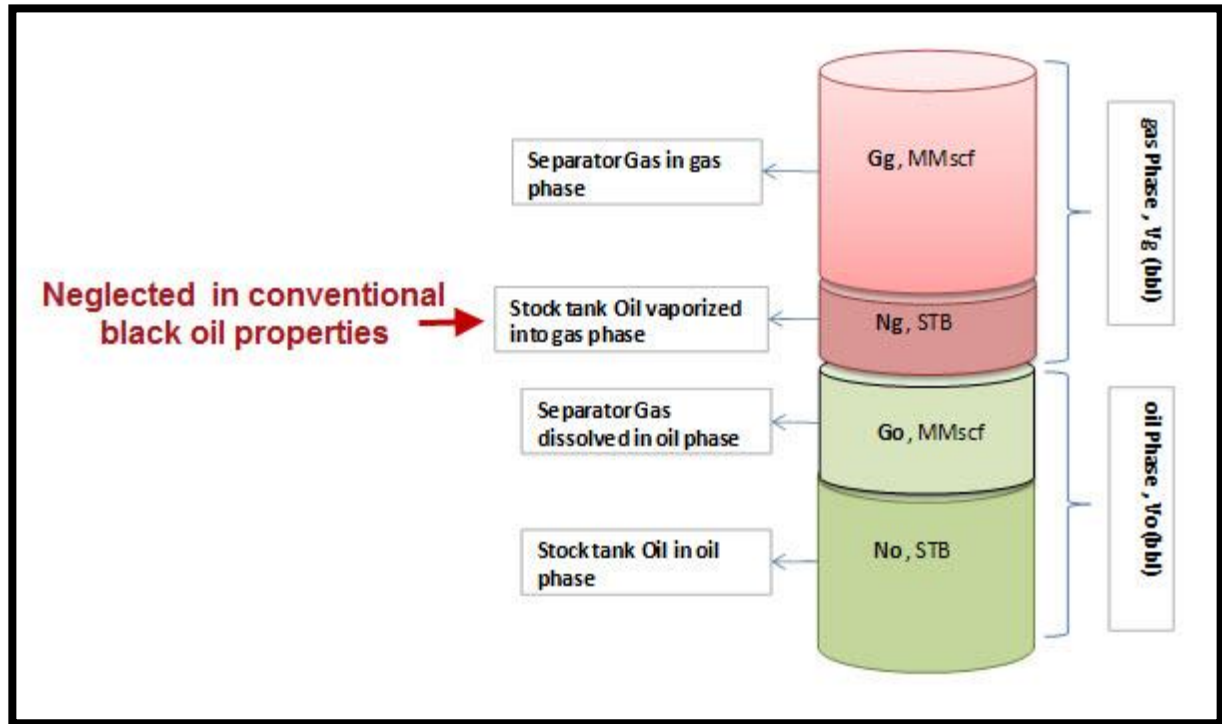
Figure A.1: Fluid at reservoir and surface conditions

From the above assumptions and the three-phase Darcy's law, the Black Oil mass balance equations can be given as follows:

Oil:
$$\nabla \left[\frac{kk_{ro}}{\mu_o B_o} (\nabla p_o - \gamma_o \nabla d) \right] + Q_o = \frac{\partial}{\partial t} (\varphi \frac{S_o}{B_o}) \qquad \text{[A.1]}$$

Water:
$$\nabla \left[\frac{kk_{rw}}{\mu_w B_w} (\nabla p_w - \gamma_w \nabla d) \right] + Q_w = \frac{\partial}{\partial t} (\varphi \frac{S_w}{B_w}) \qquad \text{[A.2]}$$

Gas:
$$\nabla \left[\frac{kk_{rg}}{\mu_g B_g} (\nabla p_g - \gamma_g \nabla d) \right] + \left[\frac{kk_{ro} R_s}{\mu_o B_o} (\nabla p_o - \gamma_o \nabla d) \right] + Q_g = \frac{\partial}{\partial t} (\varphi \frac{S_g}{B_g} + \varphi \frac{R_s S_o}{B_o}) \qquad \text{[A.3]}$$

Where:

k: permeability.

Kr: relative permeability.

μ : viscosity.

B: volume factor.

P: phase pressure.

γ : g*ρ, where ρ is the phase density.

d: Vertical distance for a reference level to a point.

Q: q/ρ^s, where q is the flow rate and ρ^s is the density at standard conditions.

φ : porosity.

S: saturation.

o, w, g: oil, water and gas phases respectively.

In equations A.1, A.2 and A.3 the phase pressures and the saturations are the unknowns that need to be determined from simulation. They are determined based on position and time. Once the pressures and saturations are determined, the flow parameters can be found from using the three mass balance equations and equations A.4, A.5 and A.6 given below:

Capillary pressure oil/water:

$$\boldsymbol{P_{cow}S_w = \; p_o - \; p_w} \hspace{5cm} \textbf{[A.4]}$$

Capillary pressure gas/water:

$$\boldsymbol{P_{cgo}S_g = \; p_g - \; p_o} \hspace{5cm} \textbf{[A.5]}$$

Saturation equation:

$$\boldsymbol{S_w + S_o + \; S_g = 1} \hspace{5.5cm} \textbf{[A.6]}$$

There are now six unknowns and six equations. Two pressures and one saturation are eliminated by the three constraint equations. The three mass balance equations can then be used to determine the remaining unknowns [29].

A.3 History Matching

The principal objective of history matching reservoir models is to improve reservoir understanding, validate the reservoir simulation model, reduce uncertainty and enhance the accuracy of predictions of the reservoir performance. Essentially, if a reservoir model can replicate past reservoir performance it can be used to predict the future. A history match is

therefore performed to make the numerical data fit the observed historical field data. The main goal of the history matching process is to improve forecasting ability of the numerical model and reduce uncertainty in their predictions.

History matching is done by changing uncertain fluid and reservoir parameters to make them better fit the field of interest. A history math is not unique since different strategies can be used to come up with representable solution. One fundamental aspect of the matching process is the availability of a representable geomodel. This geomodel should be derived from evaluation of seismic, well and field data. The geomodel can then be used as a basis for generating a reservoir simulation model that is consistent with observed production data.

There is no well-defined procedure for history matching, but trends can be established during the process. Some of the procedures that can help perform a history match are:

- Define the objectives of the study and the expected product.
- Familiarize the field and well performance.
- Match the overall reservoir energy level.
- Match gas/oil ratio, water-cut performance and pressure (WFT and BHP) for individual wells.
- Match the bottom hole pressure to assure a smooth transition from history to prediction.

Input parameters frequently adjusted in a history matching procedure are given below in order of decreasing uncertainty [42]:

- Aquifer transmissibility, kh.
- Aquifer storage, φhc_r.
- Reservoir permeability thickness, kh.
- Includes vertical flow barriers and high conductivity streaks
- Permeability anisotropy, k_v/k_h
- Relative permeability and capillary pressure functions.
- Porosity and thickness.
- Structural definition.
- Rock compressibility.
- Oil and gas properties (PVT).
- Fluid contacts, WOC and GOC.
- Water properties.

A.4 Reservoir Performance Forecasting

The ability to predict future reservoir performance is dependent on the ability of the reservoir model to accurately match the history production data. Hence, the objective of history matching is to provide a model capable of predicting future reservoir performance under various operational scenarios to reduce uncertainty and answer the questions related to optimal reservoir management [21].

During the change from history to prediction mode, the model should switch smoothly without marked discontinuities in the well capacities. Possible reasons for discontinuities include: Delay in production start-up, lower peak rates due to overestimated reservoir quality, failure to incorporate important reservoir heterogeneities thus causing early breakthrough, steeper decline in production rate due to idealized assumptions about reservoir connectivity, pressure support and flood conformance and earlier cut-off due to production difficulties [53].

Reservoir forecasting helps visualize future performance of the reservoir for different operating strategies. A variety of scenarios can be explored and the strategy with the most desirable performance can then be chosen. From the prediction runs, types of performance predictions that may be generated include [25].

- Oil production rates.
- WOR and GOR performance.
- Reservoir pressure performance.
- Well pressure performance.
- Position of fluid fronts.
- Recovery efficiency by area.
- Information concerning facility requirements.
- Estimated ultimate recovery.

A.5 Reservoir Simulators

Reservoir simulators are computer programs that are written to solve the fluid flow equations in a reservoir. The reservoir simulator begins with reading the applied input data and then initializing the reservoir. Time dependent data such as well and field control data is then read. An iteration process between calculated flow coefficients and unknown variables is performed, which can improve the material balance. When a satisfactory solution to the iterative process has been established, flow properties are updated, and output files created before the next time

step calculations begin [20]. The simulator can give predictions on future reservoir performance and can therefore be used to find the optimal recovery mechanism or future production.

A.5.1 ECLIPSE

ECLIPSE is a reservoir simulator that solves the mass balance equations by numerical methods for approximating the solutions to the differential equations. The program is owned by Schlumberger Information Solutions (SIS). ECLIPSE software covers all the different reservoir models, specializing in black oil, compositional and thermal reservoir simulation.

Eclipse is available in two versions:

- ECLIPSE 100: Solves black oil model on corner point grids.
- ECLIPSE 300: Solves black oil, compositional and thermal models.

For the purposes of this paper, ECLIPSE 100 is used. It is a fully implicit, three phase, 3D, general purpose black oil simulator with gas condensate options.

A.5.1.1 Structure of ECLIPSE data input file

An ECLIPSE data input file is divided into sections, where each section is introduced by a keyword. The sections must come in a certain order, where some sections are required while some can be optional. An overview of the sections is listed below [56]:

RUNSPEC

This is the first section and it contains the run title, start date, units, number of blocks, wells, tables, flags for phases or the components present and the option switches

GRID

The grid section determines the basic geometry of the simulation grid and various rock properties such as porosity, absolute permeability, net-to-gross ratios, in each grid cell. The grid block pore volumes, mid-point depths and inter-block transmissibility can be calculated using the input data.

EDIT

The edit section contains instructions for modifying the parameters computed in the grid section (optional).

PROPS

The props section of the input data contains pressure and saturation dependent properties of the reservoir fluid rocks.

REGIONS

The regions section is optional and splits the computational grid into regions for calculation of PVT properties, saturation properties, initial conditions and fluids in place. If the section is omitted all grid blocks are put in one region.

SOLUTION

The solution section contains sufficient data to define the initial state (pressure, saturations and compositions) of every grid block in the reservoir.

SUMMARY

The summary section specifies a number of variables that are to be written to summary files after each time step. The results can be plotted graphically.

SCHEDULE

The schedule section specifies the operation to be simulated, like production and injection controls and constraints. Also specifies the times at which output reports are required. Vertical flow performance curves and simulator tuning parameters may also be specified in the schedule section.

A.5.1.2 History Matching in ECLIPSE 100

ECLIPSE 100 is constructed to operate wells in either historical or predictive method. During historical mode wells are constrained by a set of historical data provided and entered in the simulator by the user. When the model runs constrained by given historical performance, remaining phases, pressures and production ratios are calculated by the simulator according to mobility ratios as described in chapter 3. Historical data is entered using keywords WCONHIST and WCONINJH for production and injection wells respectively. Table A.3 lists various types of historical performance data that can be specified to constrain production and injection wells. Even though wells are constrained by only one type of historical performance data ECLIPSE 100 allows the user to enter all available historical performance data. This way, historical production data will be written to the summary file and the available for direct comparison with the calculated reservoir performance of the reservoir simulator when plotted in a post-processing software [57]. The WCONHIST/WCONINJH keyword specifying historical data must be entered in the simulation data-file at every timestep data exist.

Table A.3: Historical performance data compatible with ECLIPSE 100 [57]

Production Wells	Injection Wells
Oil production rate	Oil injection rate
Water production rate	Water injection rate
Gas production rate	Gas injection rate
Liquid production rate	BHP
Reservoir voidage production rate	THP
Bottom hole pressure (BHP)	
Tubing head pressure (THP)	
Artificial lift quantity	

Changes needed to improve match can easily be made to the simulation in ECLIPSE 100 during history matching through direct application in the data-file using ECLIPSE 100 syntax.

Appendix B : Simulation input and results

B.1 ECLIPSE100 INPUT FILE AND RESULTS

```
--ANDREW MBURU
--MSC THESIS 2018
--WATER DISPERSION AND H2S TRACER TRACKING
--2D-HOMOGENOUS MODEL


--
RUNSPEC
TITLE
  MODELLING H2S GENERATION AND TRANSPORT PROCESS

DIMENS
  100  100   1 /

WATER

METRIC

EQLDIMS
   1  100  20   2   2 /

TRACERS
   0   3   0   0 'DIFF ' /

TABDIMS
   1   1  20  20   2  20 /

REGDIMS
   2   1   0   0 /

WELLDIMS
  10  10   1  10 /

START
  1 'JAN' 1986  /

NSTACK
   8 /

UNIFOUT
```

GRID

==

NOGGF

DX
  10000*10.0 /

DY
  10000*10.0 /

DZ
  10000*10.0 /

TOPS
  10000*3300.0 /

PORO
  10000*0.2 /

PERMX
  10000*1000.0 /

PERMY
  10000*1000.0 /

PERMZ
  10000*0.01 /

PROPS

==

PVTW
 0.0 1.0 5.2E-05 0.5 0.0 /

ROCK
 380.0   4.5E-05 /

DENSITY
 0.0000 1000.0000   0.0 /

-- TRACER NAMES AND THEIR ASSOCIATED STOCK TANK PHASES ARE
DEFINED USING THE TRACER KEYWORD

```
TRACER
 'INJ' 'WAT' /
 'H2S' 'WAT' /
 'AQ'  'WAT' /
 /

RPTPROPS
-- Passive Tracer Names
--
  'INJ'   'WAT'
  'H2S'   'WAT'
  'AQ'    'WAT' /


SOLUTION
==============================================================

PRESSURE
 10000*380.0 /

TBLKFINJ
10000*0.0 /

TBLKFH2S
10000*0.0 /

TBLKFAQ
10000*1.0 /

RPTSOL
-- Initialisation Print Output
--
'PRES' 'SOIL' 'SWAT' 'FIP=2' 'AQUCT=1' 'TVDP' 'FIPTR=1' 'TBLK'  /

SUMMARY
==============================================================

FWPR
FWPT

FTPRINJ
FTPTINJ
FTIPTAQ
FTIPTH2S
```

```
FTIPTINJ
FTPRAQ
FTPRH2S
FTPTAQ
FTPTH2S

RUNSUM
SCHEDULE
===========================================================
RPTSCHED
'RESTART=2' 'FIP=2' 'WELLS=2' 'VFPPROD=2' 'SUMMARY=2' 'CPU=2' 'WELSPECS'
'NEWTON=2' 'FIPTR=2' 'TBLK'  /

WELSPECS
'I' 'G' 90 80 3300 'WAT' /
'P' 'G' 20 20 3300 'WAT' /
/

COMPDAT
'I    ' 90 80 1  1 'OPEN'  0 .0  1.0 /
'P    ' 20 20 1  1 'OPEN'  0 .0  1.0 /
/

WCONPROD
'P' 'OPEN' 'WRAT' 1* 800.0 /
/

WCONINJE
'I' 'WAT' 'OPEN' 'RATE' 800.0     /
/


-- DEFINE THE CONCENTRATION OF EACH TRACER IN THE INJECTION
STREAMS. INJECTION TRACER CONCENTRATIONS NOT DEFINED USING THE
WTRACER, KEYWORD ARE ASSUMED TO BE ZERO.

WTRACER
'I' 'INJ' 1.0 /
'I' 'H2S' 0.0 /
/

TSTEP
 200. /

WTRACER
```

'I' 'H2S' 0.005 /
/

TSTEP
 100. /

WTRACER
'I' 'H2S' 0.006 /
/

TSTEP
 100. /

WTRACER
'I' 'H2S' 0.007 /
/

TSTEP
 100. /

WTRACER
'I' 'H2S' 0.008 /
/

TSTEP
 100. /

WTRACER
'I' 'H2S' 0.009 /
/

TSTEP
 100. /

WTRACER
'I' 'H2S' 0.01 /
/

TSTEP
 100. /

WTRACER
'I' 'H2S' 0.011 /
/

```
TSTEP
 100. /

WTRACER
'I' 'H2S' 0.012 /
/

TSTEP
 100. /

WTRACER
'I' 'H2S' 0.013 /
/

TSTEP
 100. /

WTRACER
'I' 'H2S' 0.014 /
/

TSTEP
 100. /

WTRACER
'I' 'H2S' 0.015 /
/

TSTEP
 100. /

WTRACER
'I' 'H2S' 0.016 /
/

TSTEP
 100. /

WTRACER
'I' 'H2S' 0.017 /
/
TSTEP
 100. /
```

```
WTRACER
'I' 'H2S' 0.018 /
/

TSTEP
 100. /

WTRACER
'I' 'H2S' 0.019 /
/

TSTEP
 100. /

WTRACER
'I' 'H2S' 0.02 /
/

TSTEP
 100. /

WTRACER
'I' 'H2S' 0.021 /
/

TSTEP
 100. /

WTRACER
'I' 'H2S' 0.022 /
/

TSTEP
 100. /

WTRACER
'I' 'H2S' 0.023 /
/
TSTEP
 100. /

WTRACER
'I' 'H2S' 0.024 /
/
```

```
TSTEP
 100. /

WTRACER
'I' 'H2S' 0.025 /
/

TSTEP
 50. /

WTRACER
'I' 'H2S' 0.0275 /
/
TSTEP
 50. /

WTRACER
'I' 'H2S' 0.03 /
/

TSTEP
 50. /

WTRACER
'I' 'H2S' 0.0325 /
/
TSTEP
 50. /

WTRACER
'I' 'H2S' 0.035 /
/

TSTEP
 50. /

WTRACER
'I' 'H2S' 0.0375 /
/
TSTEP
 50. /

WTRACER
'I' 'H2S' 0.04 /
```

```
/

TSTEP
 100. /

WTRACER
'I' 'H2S' 0.05 /
/
TSTEP
 100. /

WTRACER
'I' 'H2S' 0.1 /
/

TSTEP
 100. /

WTRACER
'I' 'H2S' 0.15 /
/
TSTEP
 100. /

WTRACER
'I' 'H2S' 0.2 /
/

TSTEP
100*60 /
/

END
```
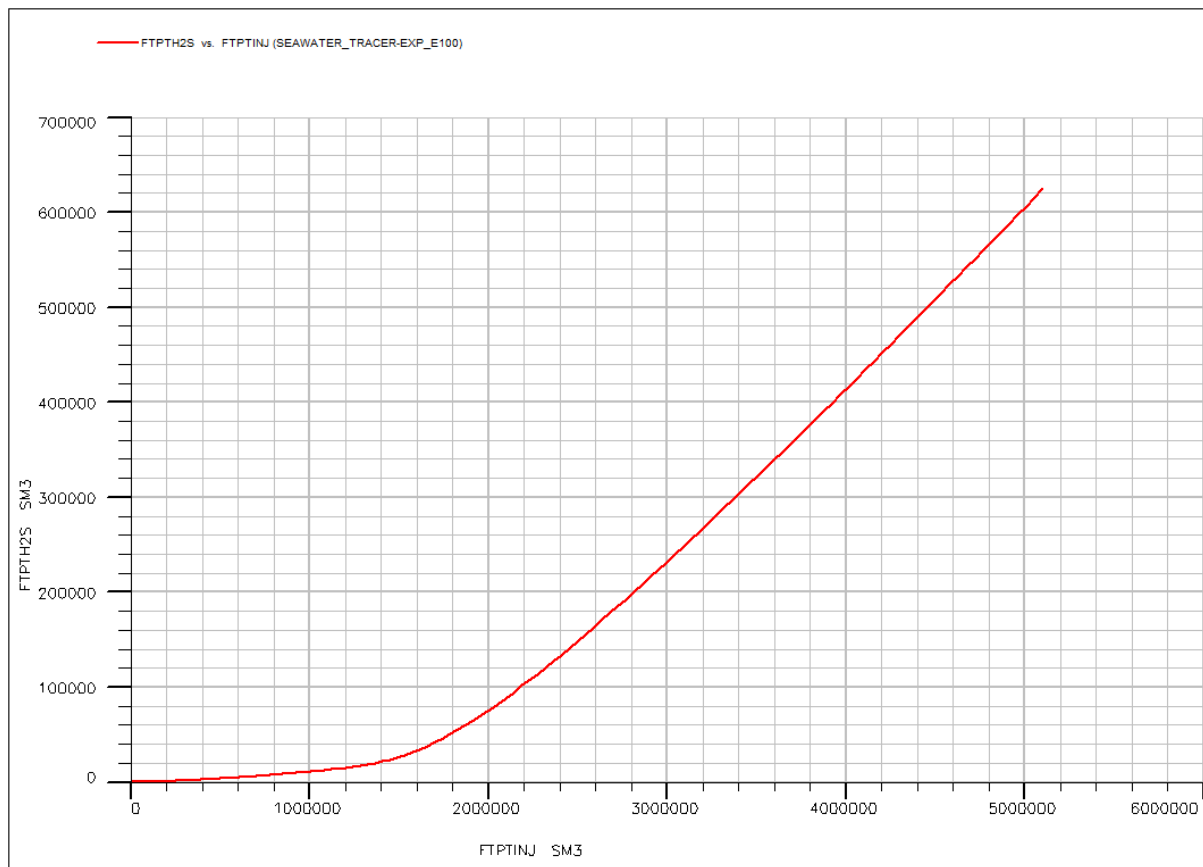
B.2 ECLIPSE100 synthetic model results

Figure B.1: Synthetic model output, FTPTH2S versus FTPTINJ